5. Equatorial waves

- Horizontal (in particular, zonal) homogeneity
  → waves/oscillations (with sufficiently small amplitudes and zero zonal mean)
- Quasi-periodic forcings: solar annual/diurnal cycles, continental distribution (with IMC)
- Small amplitude → Equation linearization
  → Orthonormal (Fourier-Laplace, cylindrical, spherical) expansions
  → Normal (one-dimensional) differential or algebraic equations
  → General (fundamental) solutions and wave dispersion relations (classification)
- Merits of linear wave theory application to atmospheric/oceanic phenomena:
  - Predictability and observation planning
  - Energy/momentum budget

$$\begin{pmatrix} u' \\ v' \\ \phi' \end{pmatrix} \equiv e^{z/2H} \cdot \Re \left[\begin{pmatrix} \tilde{u}(y) \\ \tilde{v}(y) \\ \tilde{\phi}(y) \end{pmatrix} \exp\{i(kx + mz - \omega t)\} \right]$$

Governing equations → Wave solutions
→ Dispersion relations (of frequency & wavenumbers)
Polarization relations (of amplitudes of u, v, w, T, ϕ)

5.1. Classification of waves in geophysical fluids near equator
5.2. Zonal-vertical (Walker) circulation
5.3. Atmosphere-ocean interaction: ENSO (and IOD)
5.4. Wave-mean flow interaction: QBO (and SAO)

Wave equation and solutions

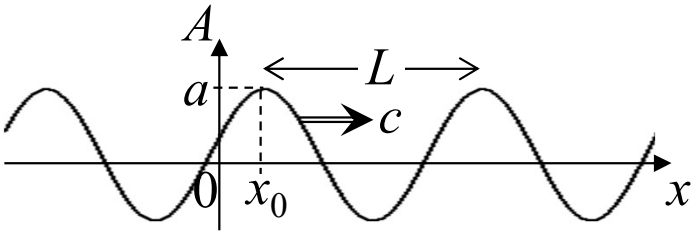

- Wavelike spatial pattern of a quantity A:

$$A(x,t) = a\cos\frac{2\pi(x - x_0 - ct)}{L} = a\cos(kx - \omega t - \delta),$$

where a: amplitude, L: wavelength, $k = 2\pi/L$: wavenumber, c: phase velocity, $T = L/c$: period, $\omega = 2\pi/T = ck$: frequency, x_0: lag, $\delta = kx_0$: phase shift.

- Complex form:

$$A(x,t) = a\,[\cos(kx - \omega t)\cos\delta + \sin(kx - \omega t)\sin\delta] = \mathrm{Re}[\mathcal{A}\exp\{i(kx - \omega t)\}],$$

where $\mathcal{A} = a\,e^{-i\delta}$ is called complex amplitude.

- "Wave equation" which has the wave solution $A(x,t)$:

$$\frac{\partial^2 A}{\partial t^2} = c^2\frac{\partial^2 A}{\partial x^2}$$

- "Dispersion relation" by substituting $A = \mathcal{A}\exp\{i(kx - \omega t)\}$ into the wave equation:

$$\omega^2 = c^2k^2$$

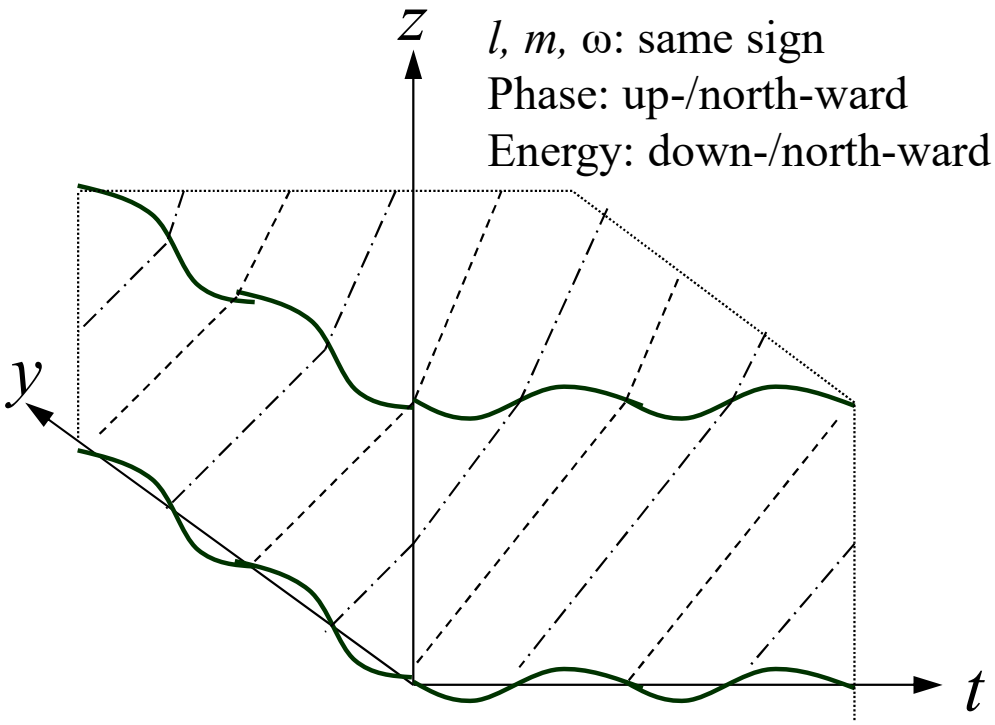

l, m, ω: same sign
Phase: up-/north-ward
Energy: down-/north-ward

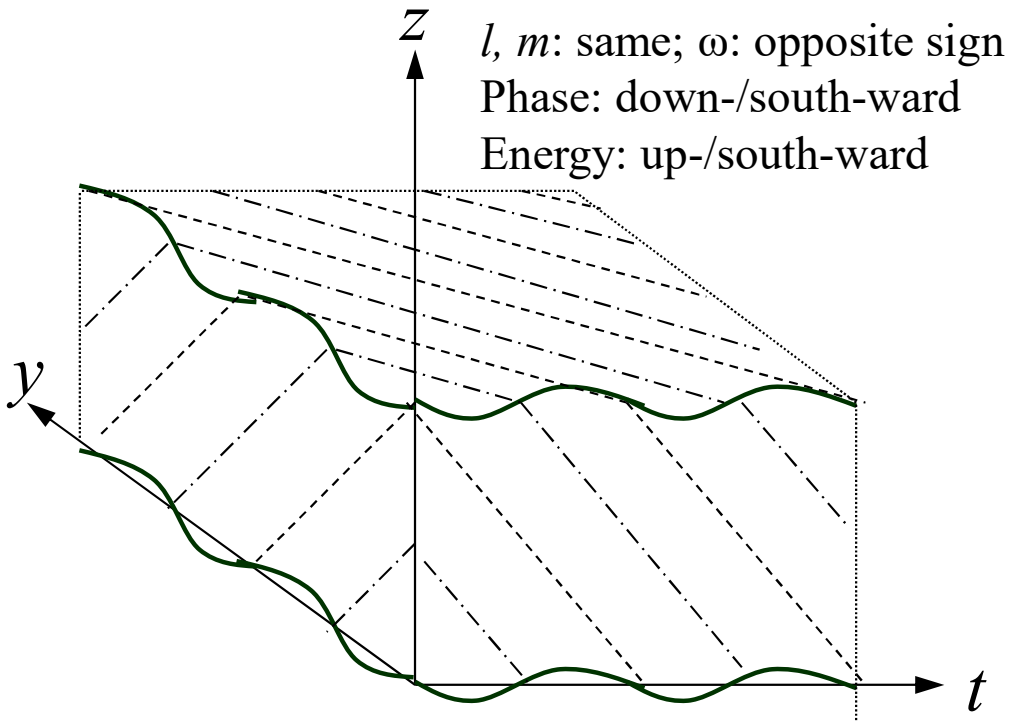

l, m: same; ω: opposite sign
Phase: down-/south-ward
Energy: up-/south-ward

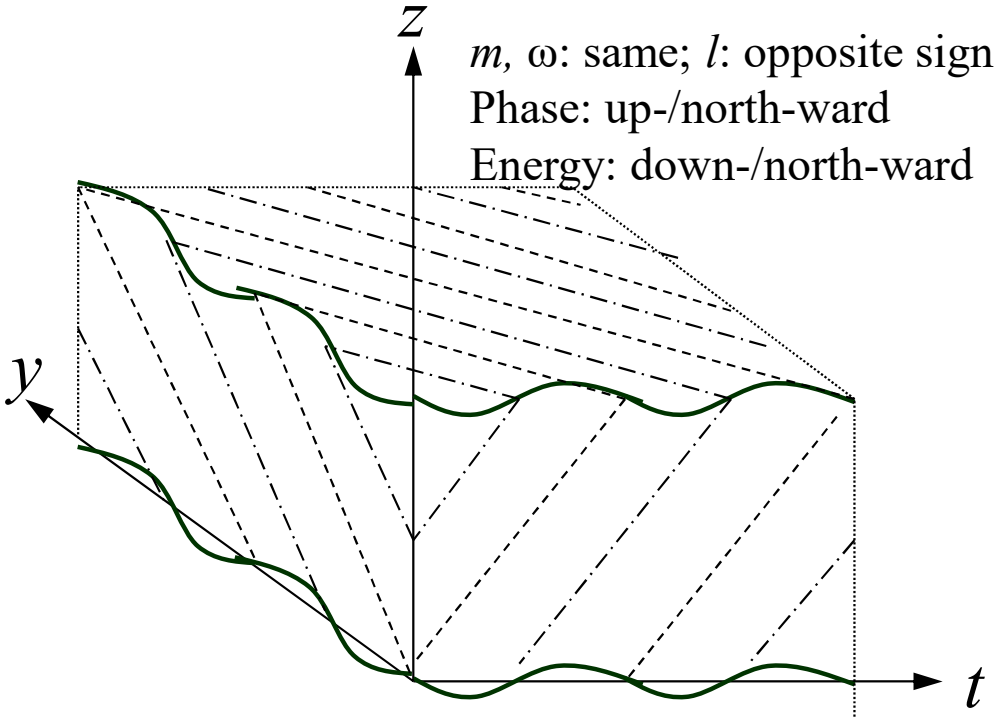

m, ω: same; *l*: opposite sign
Phase: up-/north-ward
Energy: down-/north-ward

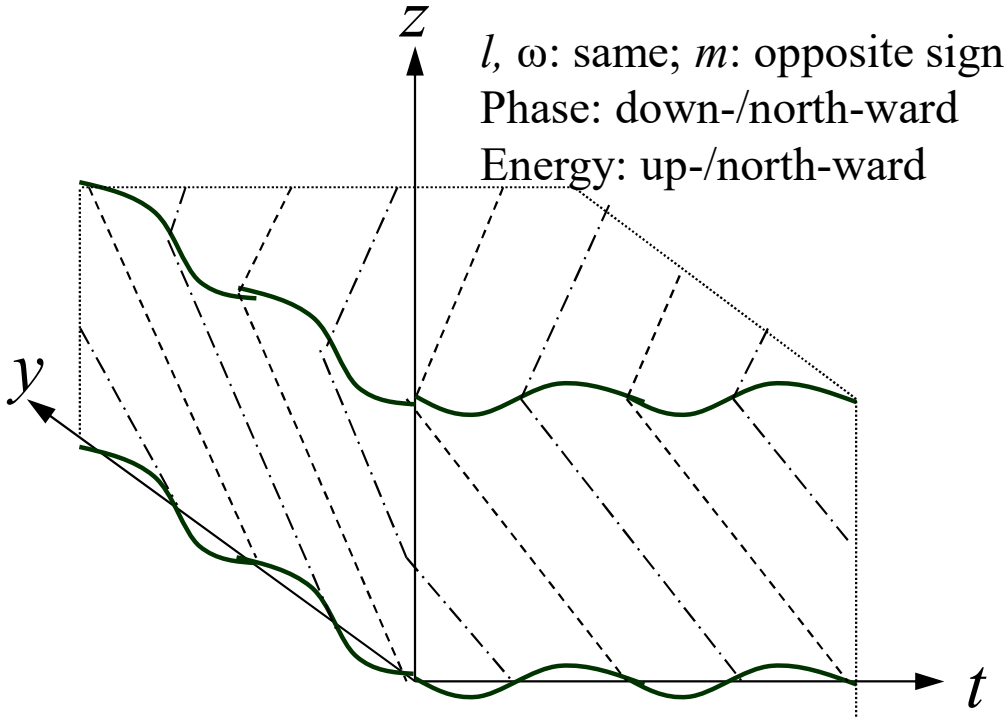

l, ω: same; *m*: opposite sign
Phase: down-/north-ward
Energy: up-/north-ward

Pair of internal waves ＝ Convection

Plain monochromatic wave far/free from boundary

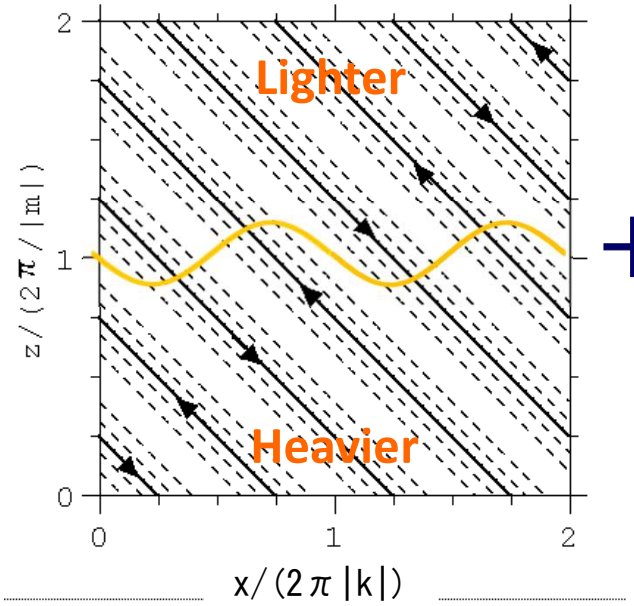

$\psi = \cos(kx+mz)$

＋

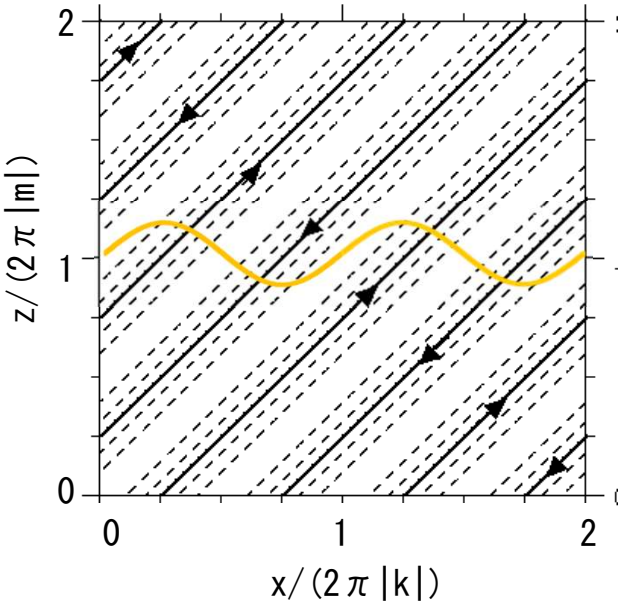

$\psi = \cos(kx-mz)$

＝

On solid boundary ($w = 0$ at $z = 0$)

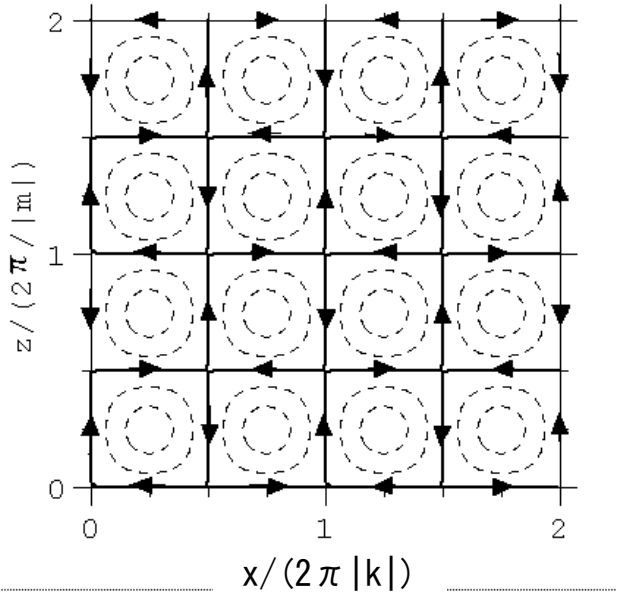

$\Psi = \cos(kx+mz) - \cos(kx-mz)$

$= -2\sin kx \sin mz$

Traveling: [$+x$ direction] $\psi = \cos(kx+mz-\omega t) - \cos(kx+mz-\omega t) = -2\sin(kx-\omega t)\sin mz$

[$-x$ direction] $\psi = \cos(kx+mz+\omega t) - \cos(kx+mz+\omega t) = -2\sin(kx+\omega t)\sin mz$

Wavenumber (k, (l,) m) and frequency (ω) are defined by governing equation (or dispersion relation).

Westward component

$\psi = \cos(kx + mz + \omega t)$

$-\cos(kx + mz + \omega t)$

$= -2 \sin(kx + \omega t) \sin mz$

Stationary convection

(|Westward| = |Eastward|)

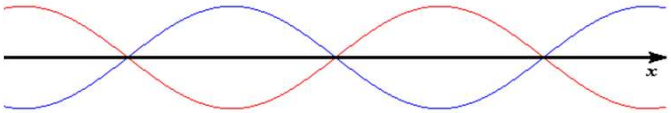

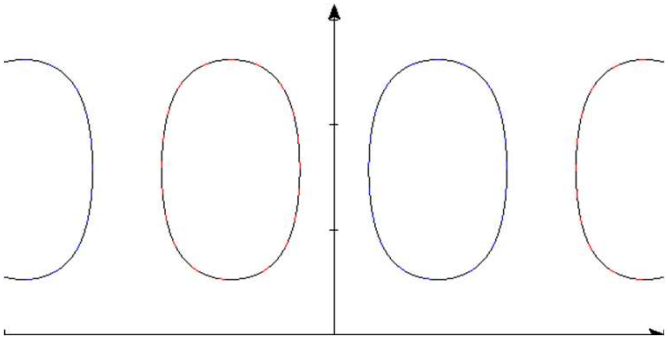

Eastward component

$\psi = \cos(kx + mz - \omega t)$

$-\cos(kx + mz - \omega t)$

$= -2 \sin(kx - \omega t) \sin mz$

Westward traveling convection

(|Wetward| > |Eastward|)

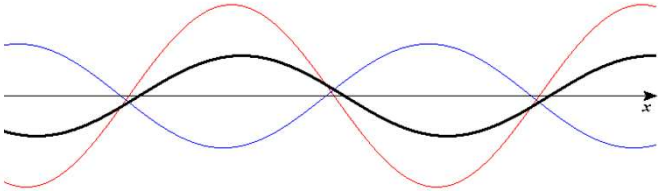

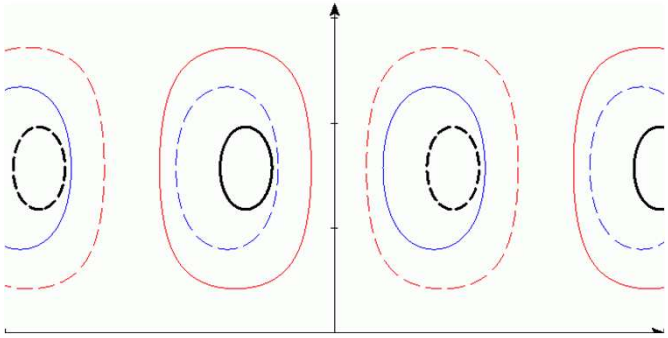

Eastward traveling convection

|Westward| < |Eastward|

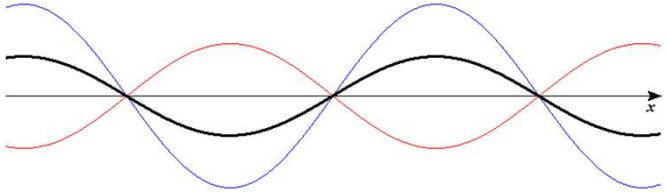

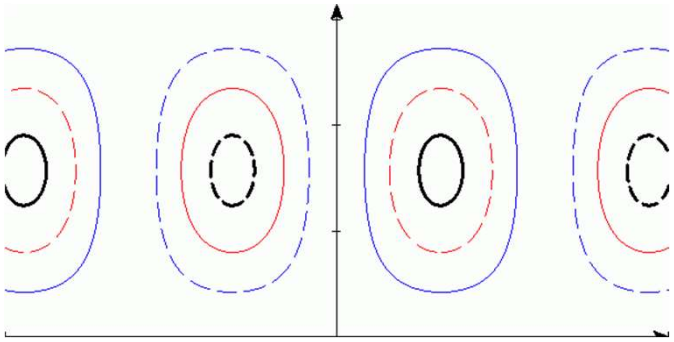

Bernhard Haurwitz (1905 – 1986)

DYNAMIC METEOROLOGY

BY

BERNHARD HAURWITZ, PH.D.

Chairman of the Department of Meteorology
College of Engineering, New York University

FIRST EDITION
SIXTH IMPRESSION

McGRAW-HILL BOOK COMPANY, INC.
NEW YORK AND LONDON
1941

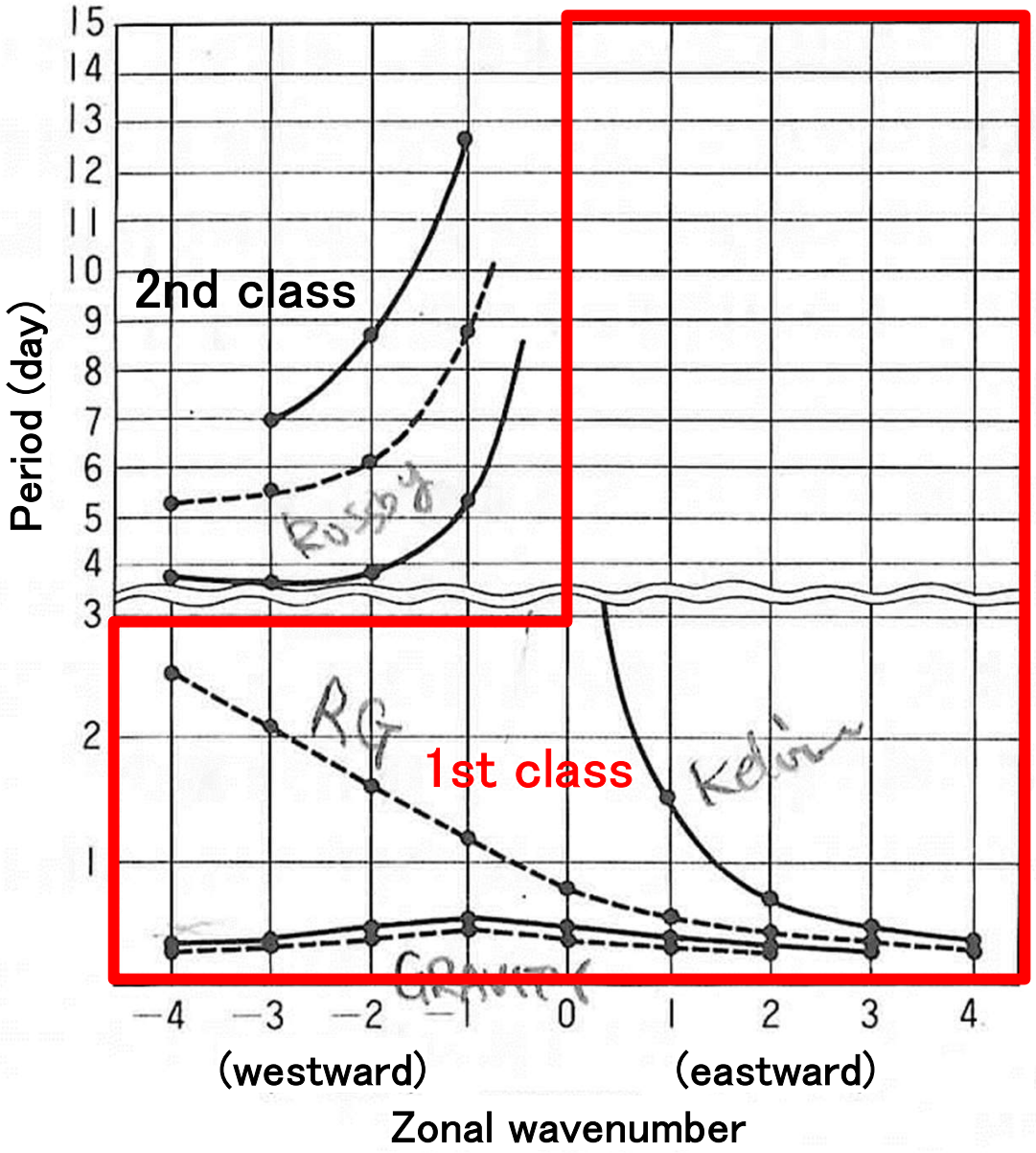

(Haurwitz, 1937; redrawn in Matsuno & Shimazaki, 1981)

Characteristics/Problems of Equatorial Tropics

- Weak annual (seasonal) cycle:
  - Solar radiation: Reverse between hemispheres
  - **Monsoon:** annual but not symmetric
  - **Social** annual cycles (except for Muslims)

    Transmigrations, agricultural, forest burnings, … 、
- Non-annual variations ⇒ **Temporal representability** of observational data
  - Interannual: (Q)BO, **ENSO, IOD**, NAO, AO, …
  - **Semiannual**: Solar radiation, ITCZ (Hadley cell border)
  - **Intraseasonal: Super cloud clusters** (20-60 days)
  - Cloud clusters / Equatorial (trade-wind) waves (3-5 days: Jawanese calender)
  - Strong **diurnal** variations
- Strong localities ⇒ **Spatial representability** of observational data
  - Super cloud clusters: ～ Equatorial deformation radius (～1000 km)
  - Diurnal sea-land / mountain-valley circulations: 10 ~ 1000 km ！
  - Cloud clusters: ～100 km
  - Individual convective clouds: 1～10 km

Quasi-Geostrophic Motions in the Equatorial Area*

By Taroh Matsuno

Geophysical Institute, Tokyo University, Tokyo

(Manuscript received 15 November 1965, in revised form 11 January 1966)

Abstract

Quasi-horizontal wave motions in the equatorial area are discussed. A single layer of homogeneous incompressible fluid with free surface is treated. The Coriolis parameter is assumed to be proportional to the latitude. In general, waves of two different types are obtained as solutions, one being the inertio-gravity wave and the other Rossby wave. They are distinguished from each other by the difference of frequencies and by the relationships between pressure and velocity fields.

For the solutions of the lowest mode (waves confined near the equator), however, the distinction between the Rossby and the inertio-gravity waves is not clear. The wave moves westward and the frequency of this wave is compared to that of the gravity wave, if wave length is large. With the increase of the wave number the frequency decreases and approaches to that of the Rossby type wave. The pressure and wind fields of this wave show somewhat mixed character of the two types, and change continuously with the wave number. In this connection it seems impossible to "filter out" gravity waves from large scale motions.

Another interesting feature of the equatorial disturbances is that the low frequency waves are trapped near the equator. It is shown that the both waves of inertio-gravity type and of the Rossby type have appreciable amplitude only near the equator. The characteristic north-south extent of the waves is $(c/\beta)^{1/2}$, where c is the velocity of long gravity waves and β is the Rossby parameter. This expression is identical with that derived by Bretherton (1964) for inertio-gravity oscillations in a meridional plane.

Wave types and characteristics

- Rossby waves are longer period
- Gravity waves are shorter period (filtered out under extratropical quasi-geostrophic approximation)
- Equatorial (Kelvin and Rossby-gravity) waves (mentioned later)
- Sound waves have been filtered from basic equations (Boussinesq or anelastic approximations)

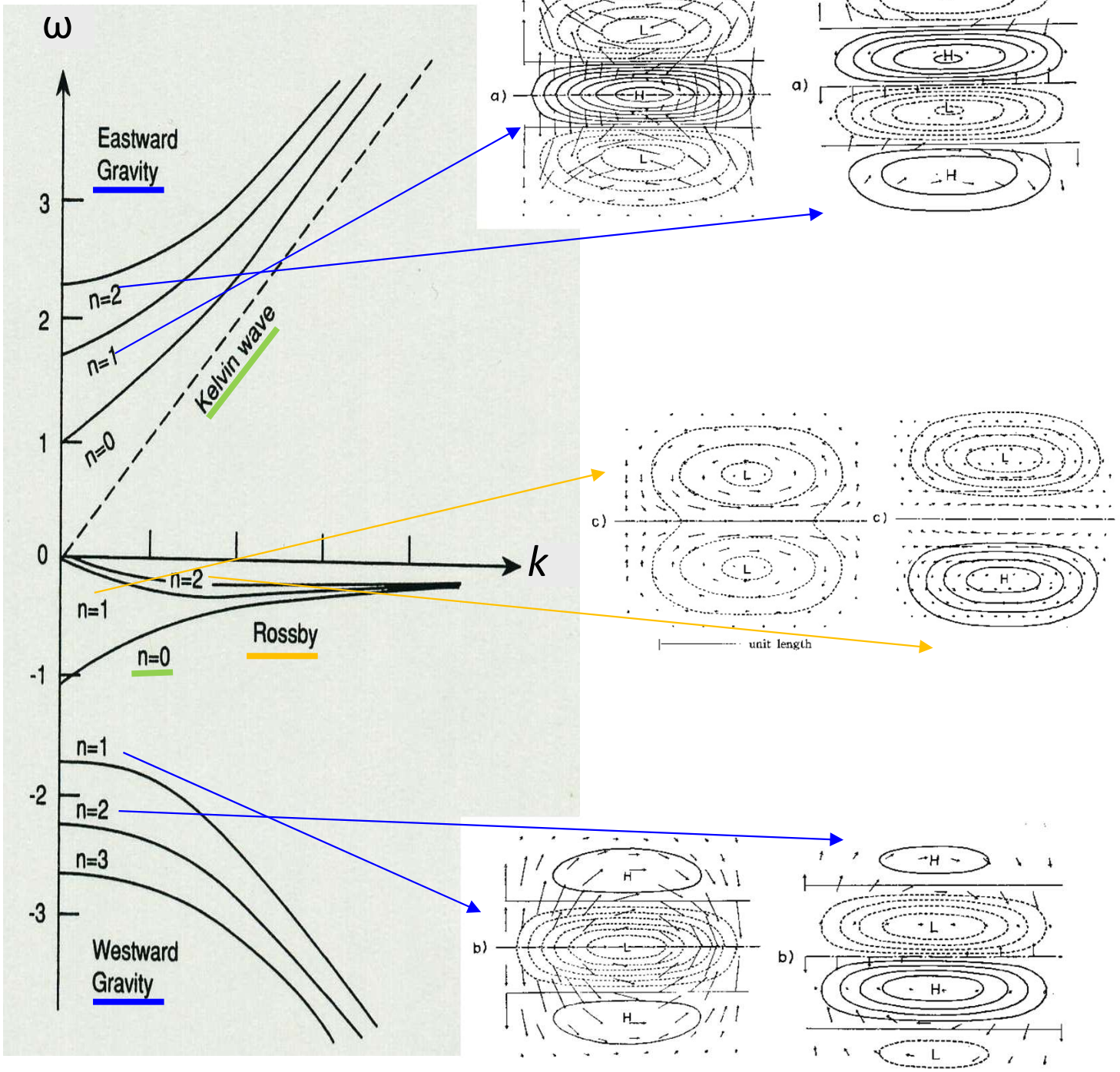

Meaning of waves and special cases near equator

- 3 conservation laws (equations)
  for 3 variables (1 velocity vector: 3 comp. (zonal, meridional, vertical),
  2 thermodynamic variables: pressure, temperature)
  - Mass conservation (Euler's eq. of continuity)
  - Angular momentum vector conservation (Newton's eq. of motion) (3 comp.)
  - Entropy conservation (1st law of thermodynamics)
    (density may be given by an equation of state (ideal gas))

- 5 scaler equations → "in general" 5 roots for a given initial/boundary conditions
  - 2 roots corresponding to sound (elastic) waves
  - 2 roots corresponding to gravity (buoyancy) waves
  - 1 root corresponding to geostrophic mode (planetary (Rossby) waves)

- Shallow water (Boussinesq) approximation:
  Vertical eq. motion → "hydrostatic equilibrium" (no time variation)
  Continuity / thermodynamic equations → 1 equation giving "buoyancy"
  - 2 roots for east-/westward propagating gravity (buoyancy) waves
  - 1 root for geostrophic mode (westward propagating planetary (Rossby) waves)

- Equatorial region (with vanishing Coriolis force):
  - A limiting form for eastward gravity wave → Kelvin wave
  - An intermediate form → Mixed Rossby-gravity (Yanai) wave

History of gravity (buoyancy) wave theories

(Craik, 2004, *Ann. Rev. Fluid. Mech.*; Matsuno, 1982, *Tenki*)

- Newton (1687) , … , Euler (1757, 1761): water waves
- Laplace (1776, 1788), Lagrange (1781, 1786): "shallow" ("long") water waves with phase speed with $\sqrt{gh}$ for gravity acceleration g and depth h
- Cauchy (1815, 1827), Poisson (1818): derived "deep" (or "short") water waves with dispersion relation $\omega^2 = g\sqrt{k^2 + m^2}$ (ω: frequency, (k, m): horizontal & vertical wavenumber)
- Russell (1838): Solitary (nonlinear) waves
- Airy (1841, 1845): Completed linear theory including tides
- von Helmholz (1868, 1888), Thomson (Lord Kelvin)(1871): Shear instability waves
- Thomson (Lord Kelvin)(1879, 1880): Coastal waves
- Thomson (Lord Kelvin)(1882), …, Haurwitz (1937) : Atmospheric tides
- Emden (1907), Väisälä (1925), Brunt (1927): Buoyancy oscillation (high-frequency cut-off)
- Lamb (1908, 1910), Sano (1913), … : Acoustic gravity waves (compressible)
- Benard, Rayleigh, ….., Asai, Ogura : Convection
- Inertial oscillation and inertio-gravity waves
- Scorer (1949), … : Lee (mountain) wave
- Eliassen & Palm (1961): Wave momentum flux
- Matsuno (1966), Longuett-Higgins : Equatorial waves
- Bretherton (1966, 1967, 1969): Critical layer
- Kato (1966), Lindzen (1966): Negative modes (external waves)
- Orlanski (1969), … Lindzen (1981), Matsuno (1982):: Wavebreaking and mean-flow interaction
- McIntyre & Andrews (1976, 1978), Uryu (1978), …: Quasi-Lagrangian theory

Lagrangian motion associated with Eulerian wave

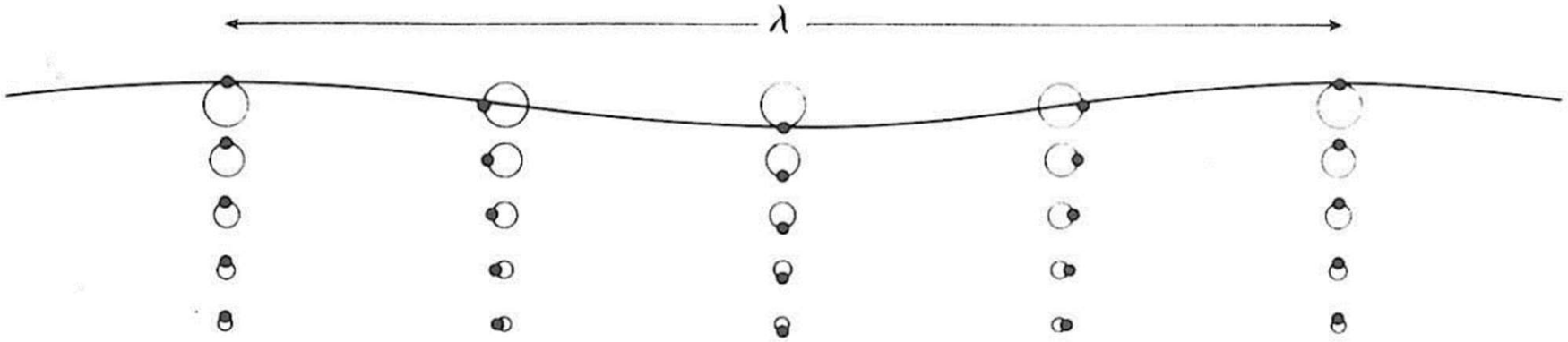

Figure 50. Motion of fluid particles (on linear theory) in a sinusoidal wave of length λ travelling from left to right on deep water. The maximum surface elevation is 0.02λ, and particles on the surface describe circles of this radius. The particles shown at mean depths 0.05λ, 0.1λ, 0.15λ and 0.20λ describe circles of radius 0.0146λ, 0.0106λ, 0.0078λ and 0.0057λ respectively. In each case the particle's instantaneous position on its circular path is shown. (Lighthill, 1978)

Acehnese dance (http://www.tufs.ac.jp/ts/personal/aoyama/courses/studyabroad2005.html)

Kelvin–Helmholtz (shear) Instability and Wavebreaking

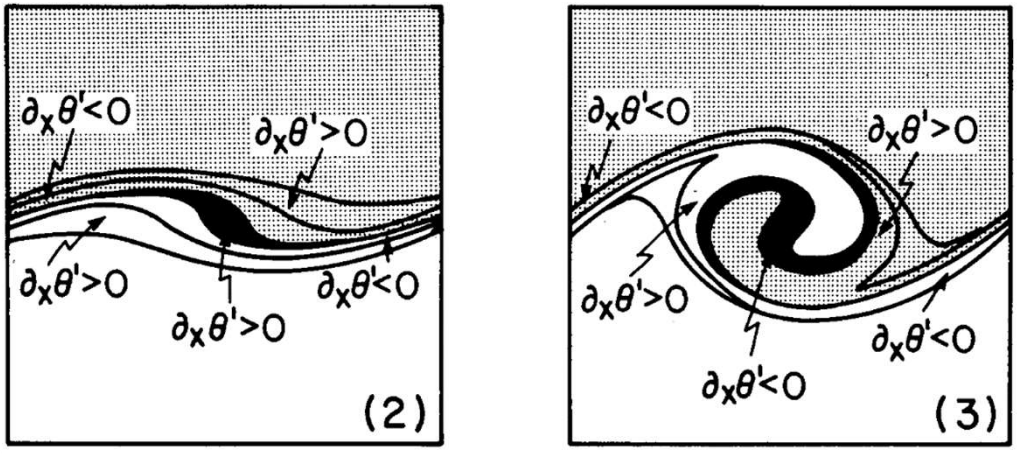

FIG. 4. Sketches of potential temperature field illustrating baroclinic sources and sinks of vorticity for a typical KH wave at key times (2) and (3) in the energy cycle. Median contour interval has been shaded darkly; regions with potential temperatures greater than the median value have been shaded lightly. Regions of baroclinic generation of vorticity ($\partial_x\theta' < 0$) are found in the braids; regions of baroclinic destruction ($\partial_x > 0$) are found at the right and left edges of the core.

(Klaassen and Peltier, 1985)

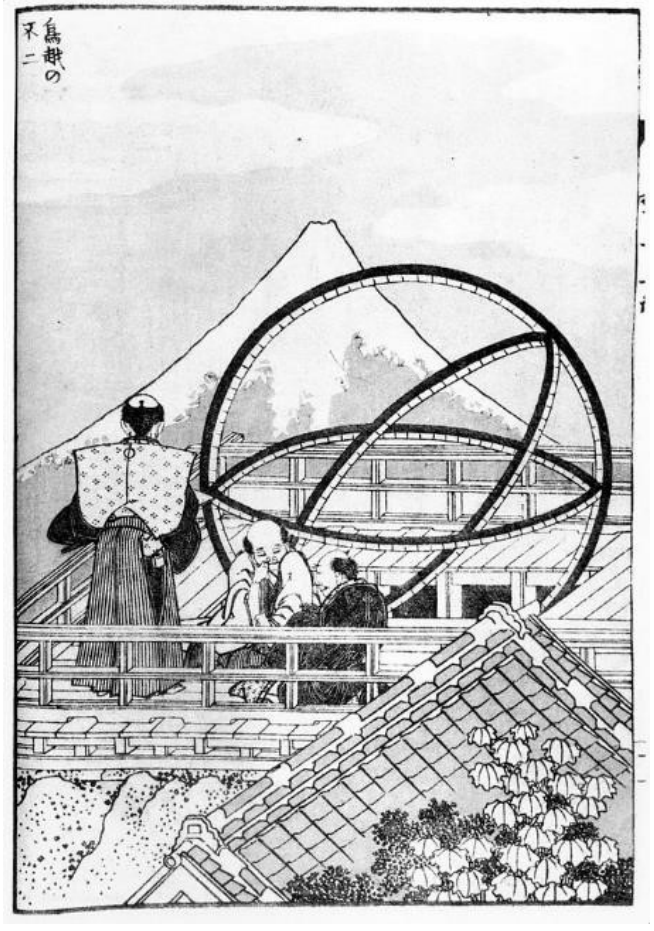

(Hokusai Katsushika, 1833)

Internal Gravity Waves (negligible rotation)

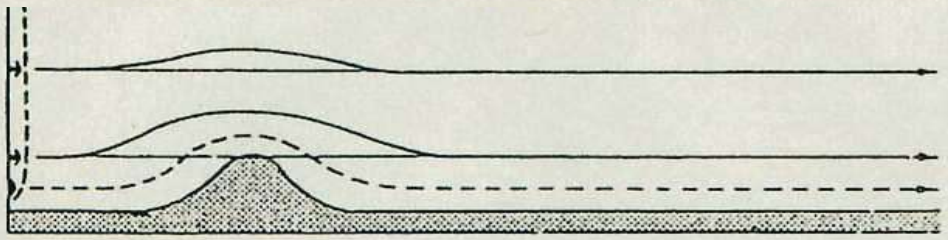

Almost no shear

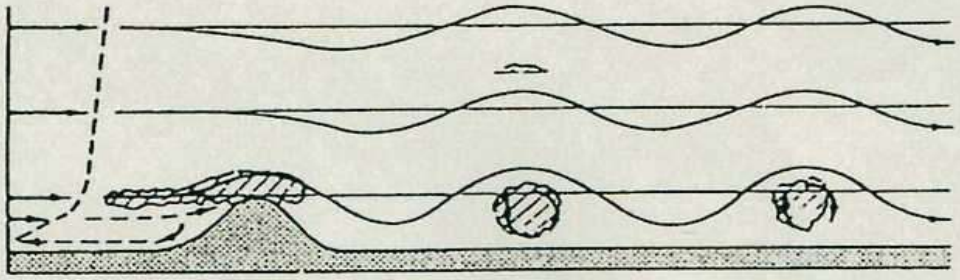

Lee waves and in a shear flow

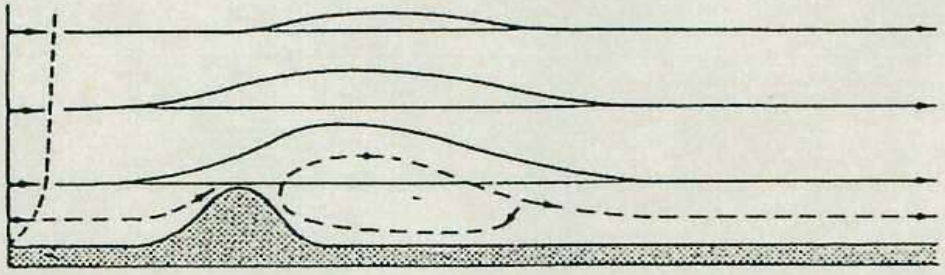

Low-level weak shear

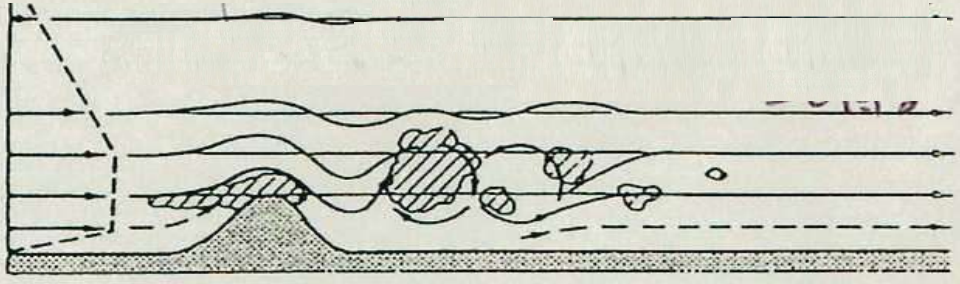

Breaking lee waves and in a low-level jet

(Corby, 1954)

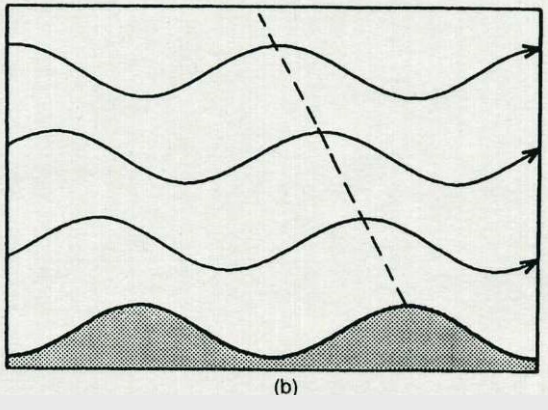

broad ridge case (b). The dashed line in (b) shows the phase of maximum upward displacement. (After Durran, 1990.)

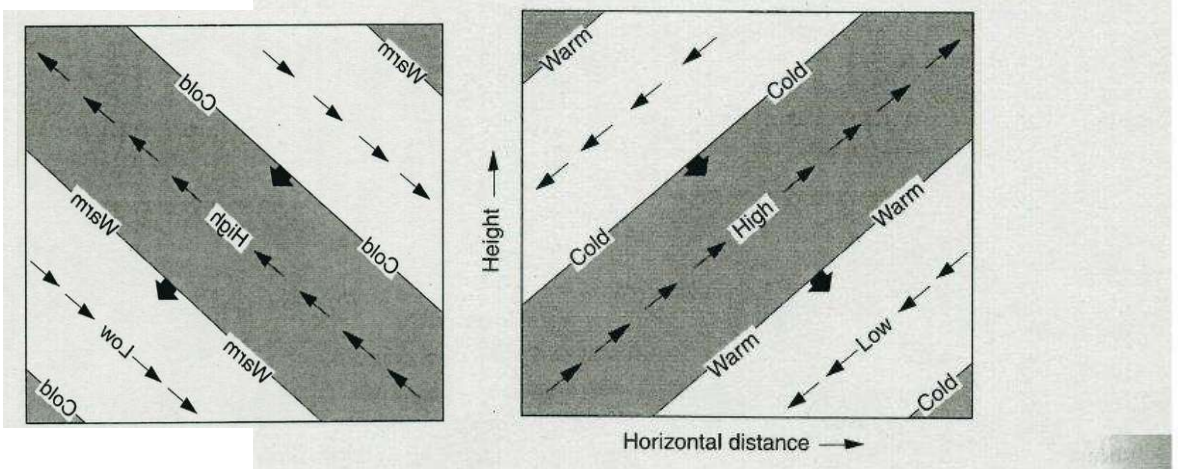

Fig. 7.9 Idealized cross section showing phases of pressure, temperature, and velocity perturbations for an internal gravity wave. Thin arrows indicate the perturbation velocity field, blunt solid arrows the phase velocity. Shading shows regions of upward motion.

"inertio-gravity" waves

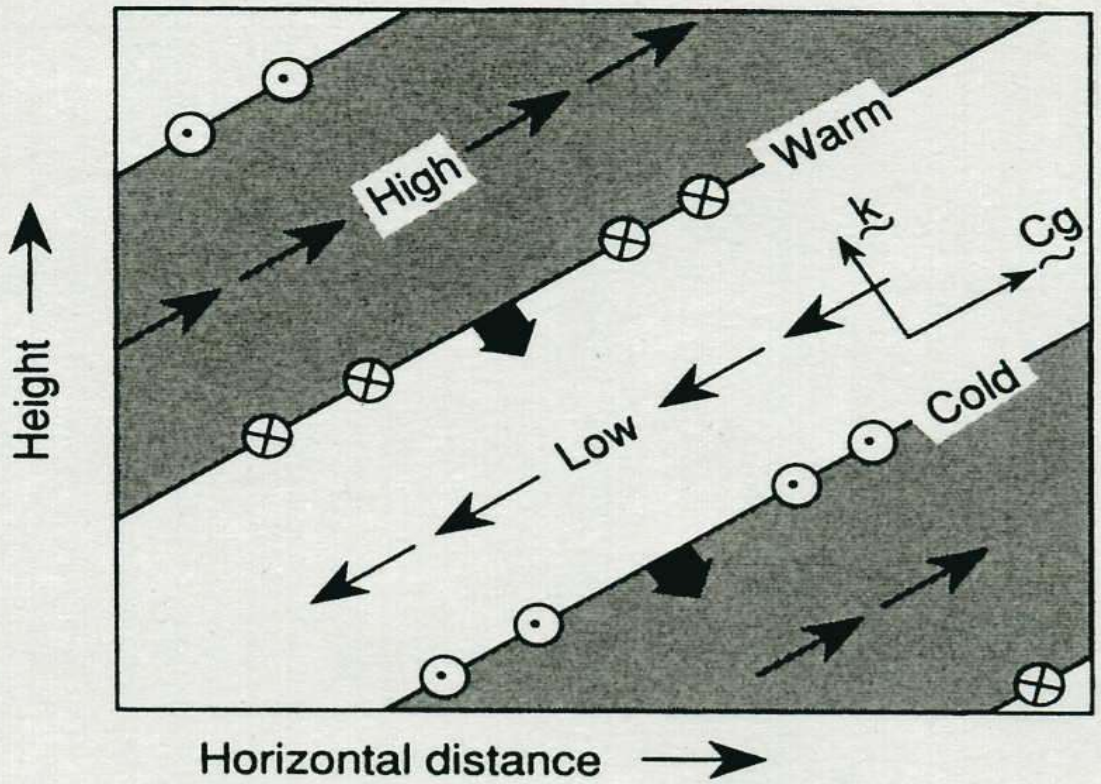

Fig. 7.12 Vertical section in a plane containing the wave vector $\boldsymbol{k}$ showing the phase relationships among velocity, geopotential, and temperature fluctuations in an upward propagating inertia–gravity wave with $m < 0$, $\nu > 0$, and $f > 0$ (Northern Hemisphere). Thin sloping lines denote the surfaces of constant phase (perpendicular to the wave vector), and thick arrows show the direction of phase propagation. Thin arrows show the perturbation zonal and vertical velocity fields. Meridional wind perturbations are shown by arrows pointed into the page (northward) and out of the page (southward). Note that the perturbation wind vector turns clockwise (anticyclonically) with height. (After Andrews et al., 1987.)

Intensive radiosonde observations of internal (inertio-)gravity waves

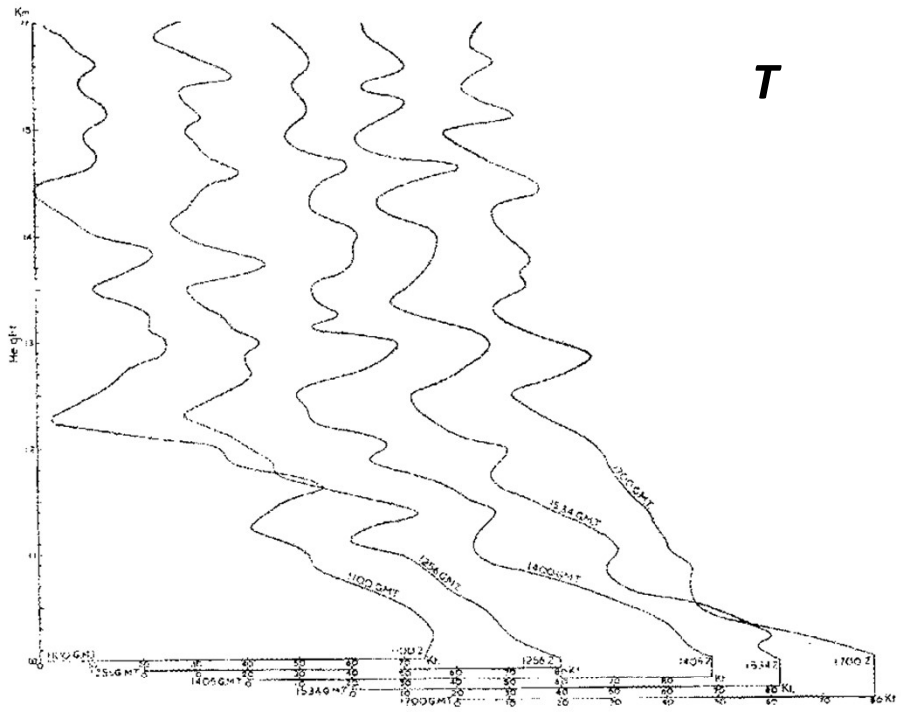

Figure 3. Northward component of velocity on five successive soundings on 24 March 1959.

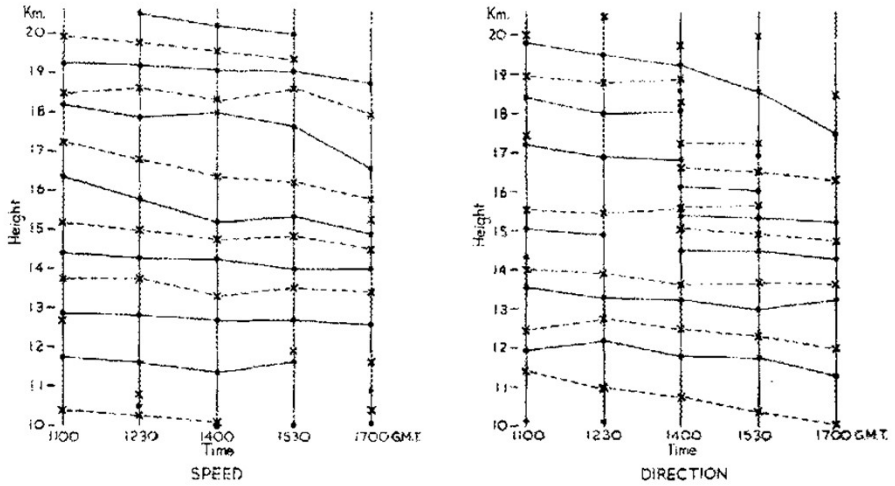

Figure 4. Heights of maxima and minima of wind velocity and extremes of wind direction on five successive soundings on 19 March 1959 (Maxima are indicated by ● and joined by continuous lines where appropriate; minima are indicated by × and joined by broken lines).

(Sawyer, 1961; Crawley, UK; 51.1ºN)

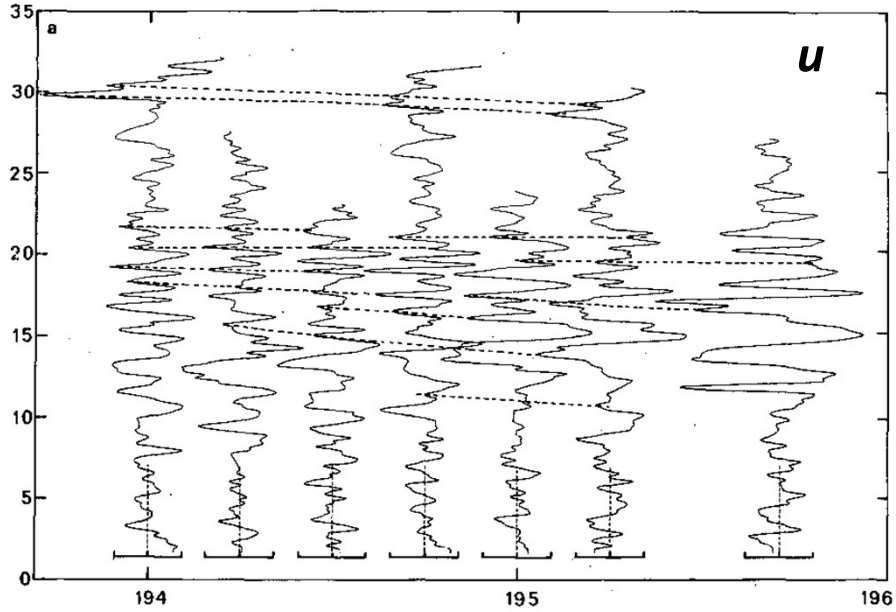

FIG. 8a. Sequence of vertical profiles of the *u* component in the vertical wavelength band 200–1500 m. Phase 1. The abscissa for each time is shifted so that the origin is indicated by vertical dashed lines. Time is in Julian Days.

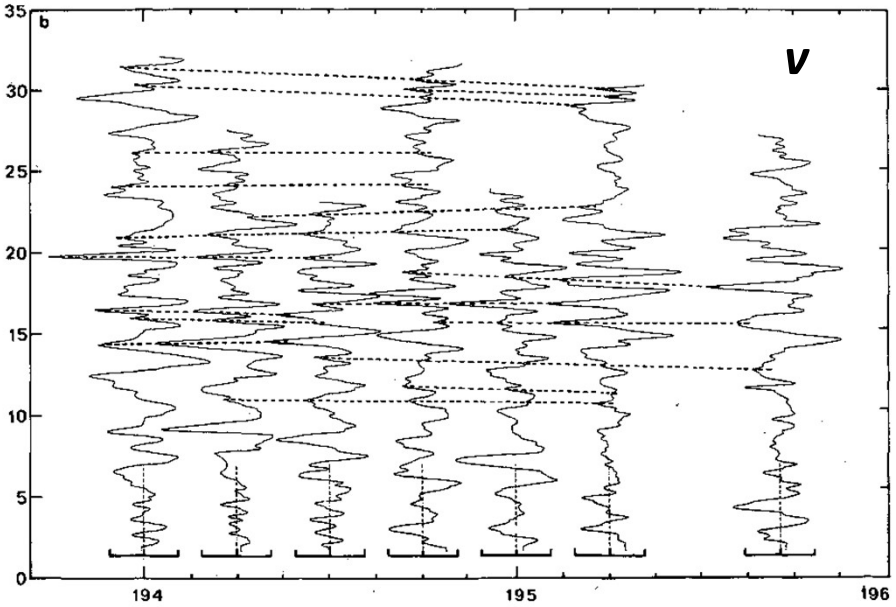

FIG. 8b. Sequence of vertical profiles of the *v* component in the vertical wavelength band 200–1500 m. Phase 1.

(Cadet & Teitelbaum, 1979; USNS-R/V Vanguard at 8.5ºN over the Atlantic)

Example of Inertio-Gravity Waves (2)

Equatorial Pacific rawinsonde obs from res.vessel “Hakuhomaru”

(Ogino et al., 1995)

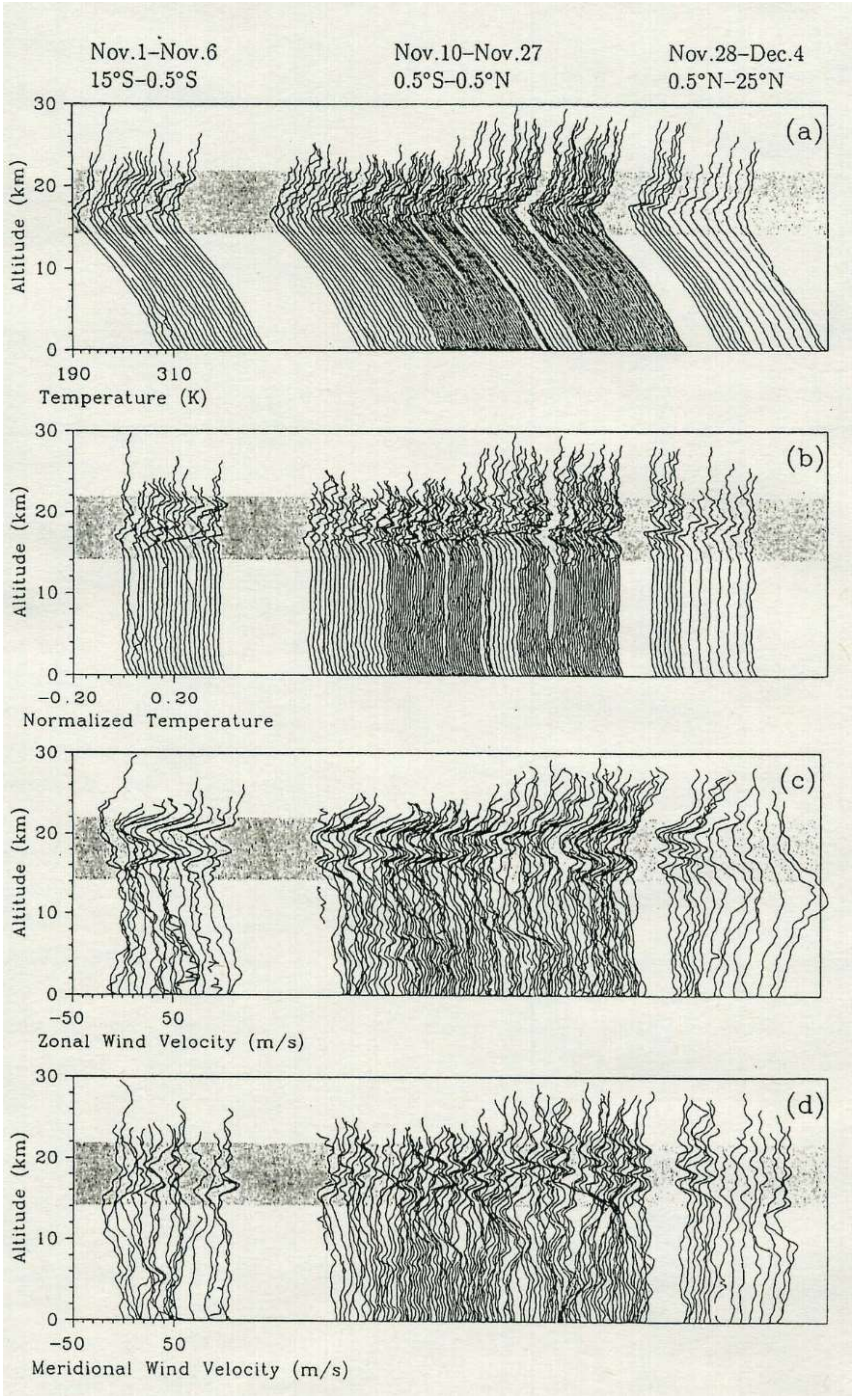

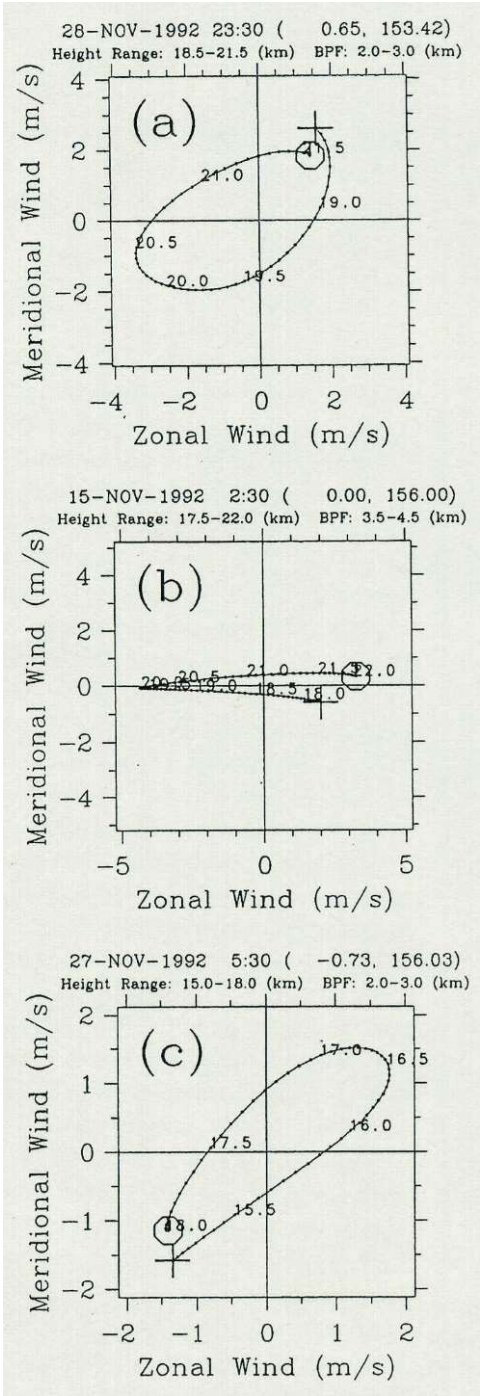

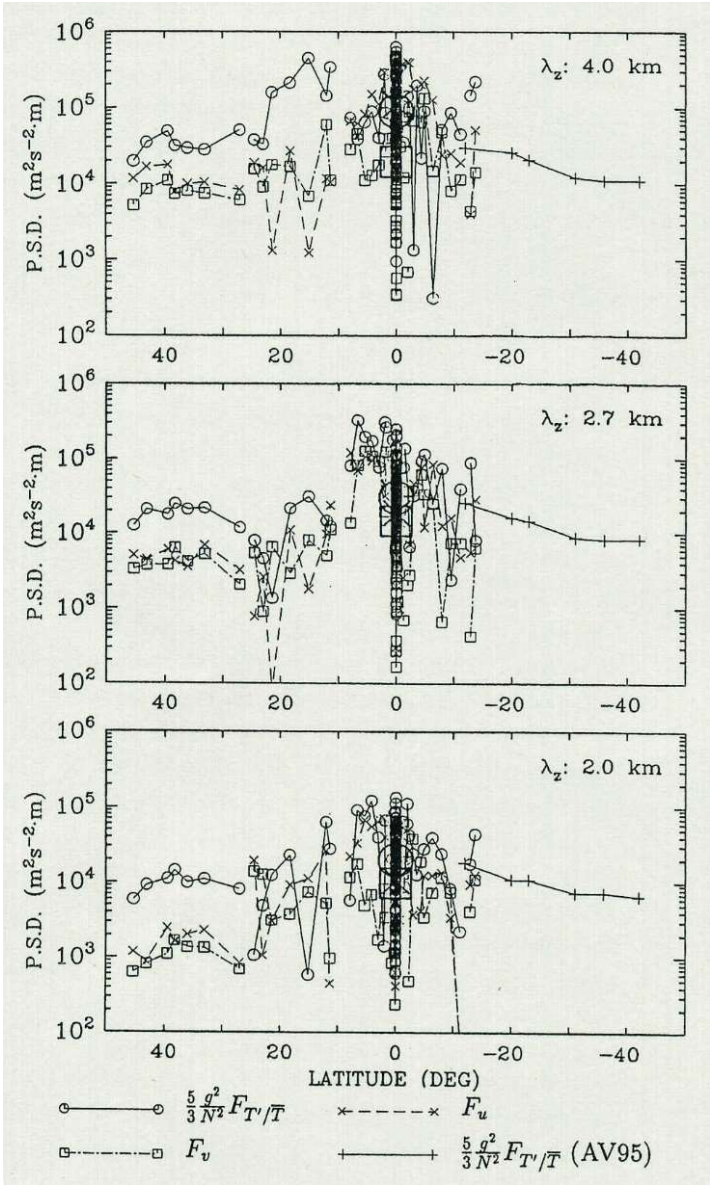

MU radar (1984)

JMA-WINDAS (2000)
33 stations

Serpong MWR/BLR (1992); Kototabang BLR (1998) EAR (2001)
(Kyoto U, BPPT, BMKG, LAPAN)

Profilers vs balloons

- High time resolution, continuity ⇔ High vertical resolution, up to stratopause
- Almost vertical sounding ⇔ Possible quasi-Lagrangian sounding
- RASS Tv, turbulence parameters ⇔ Direct p, T, q; instrumental gondoras
- Almost unmanned operation ⇔ Low cost, transportable

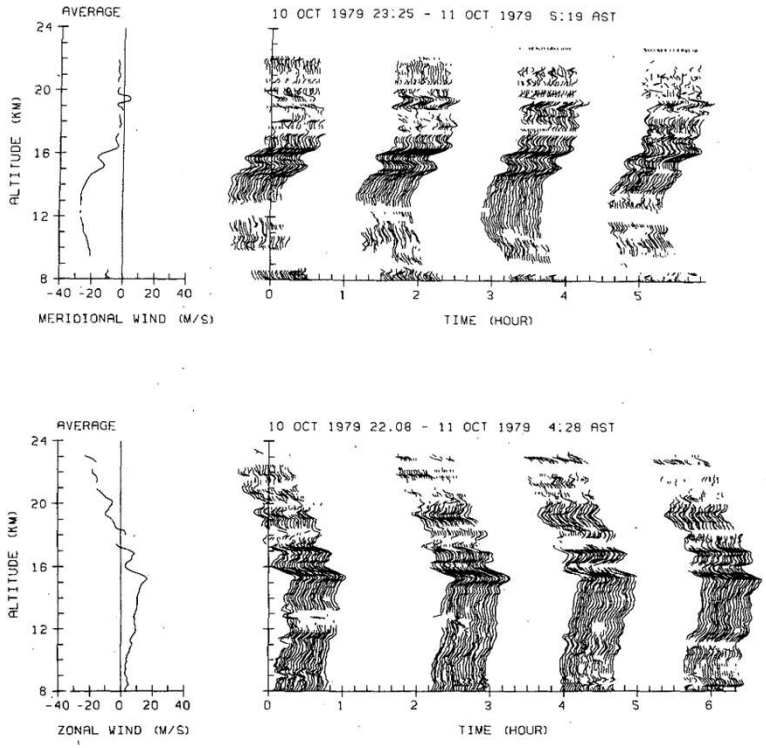

(First gravity wave observations with a UHF (430 MHz) radar at Arecibo, Puerto Rico (18.3ºN) in 1979, analyzed by Sato & Woodman, 1980)

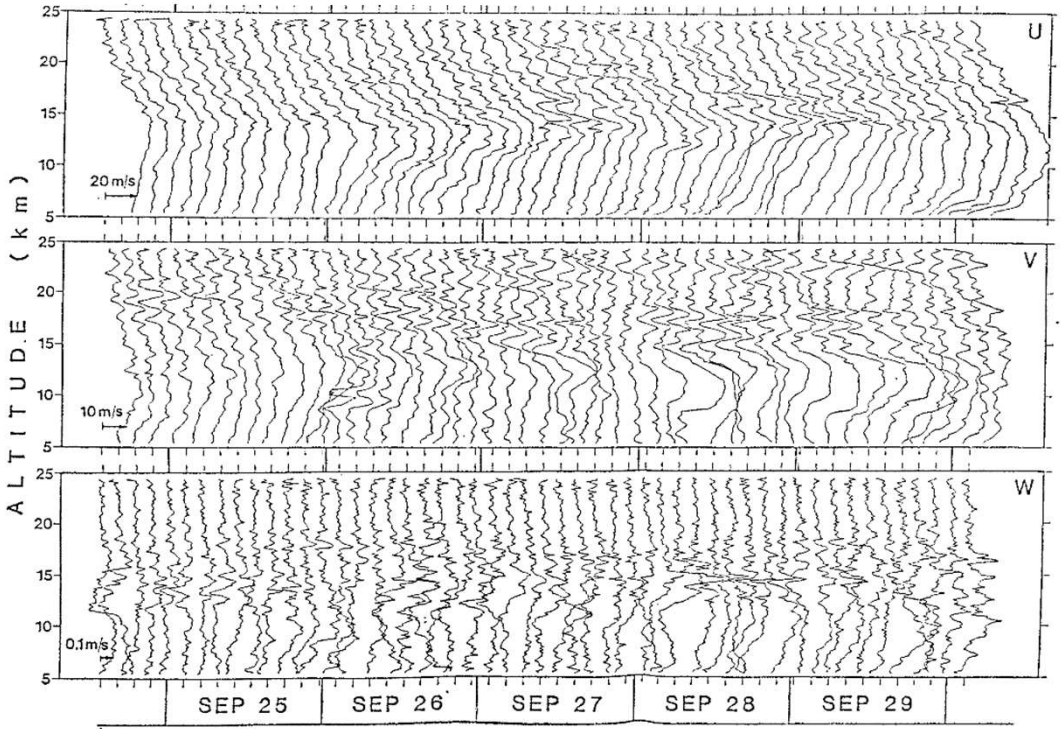

(First one-week continuous operation of Kyoto University's MU radar (VHF, 46.5 MHz) at Shigaraki, Japan (34.9ºN) in 1985 (Yamanaka, 1987), Detailed analysis published finally by Ushimaru & Tanaka, 1990)

Example of Internal Inertio-Gravity Waves (1)

Wind profiler (MUR) obs. in Japan

(Yamanaka et al., 1996)

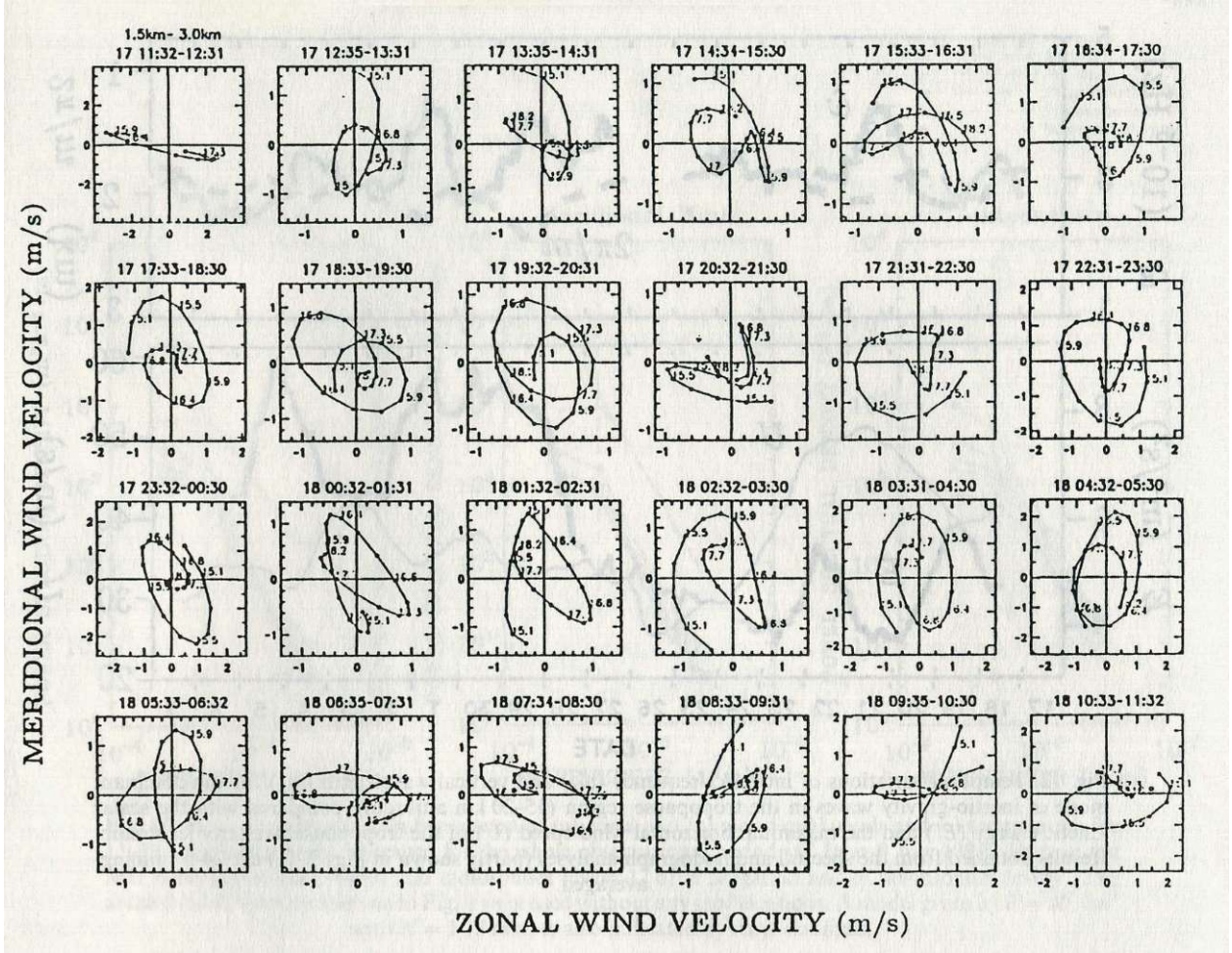

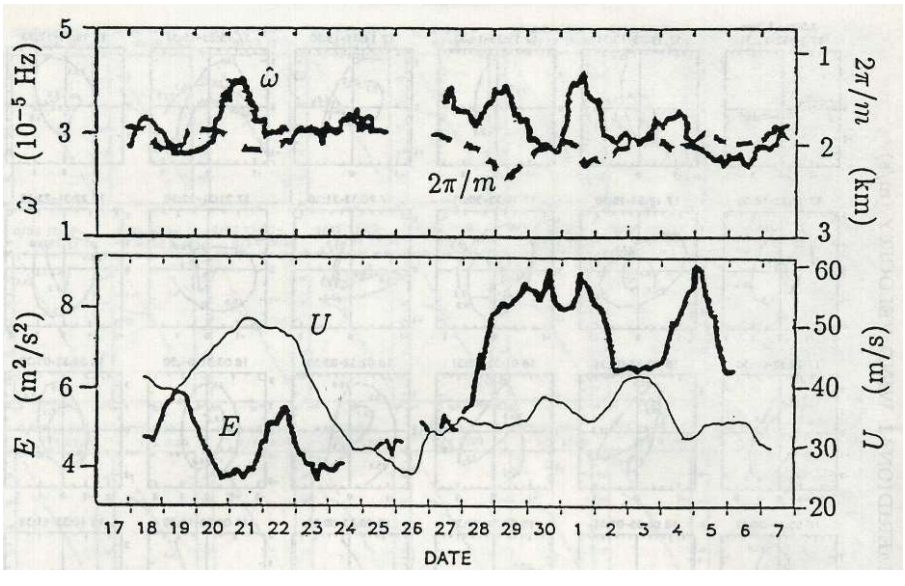

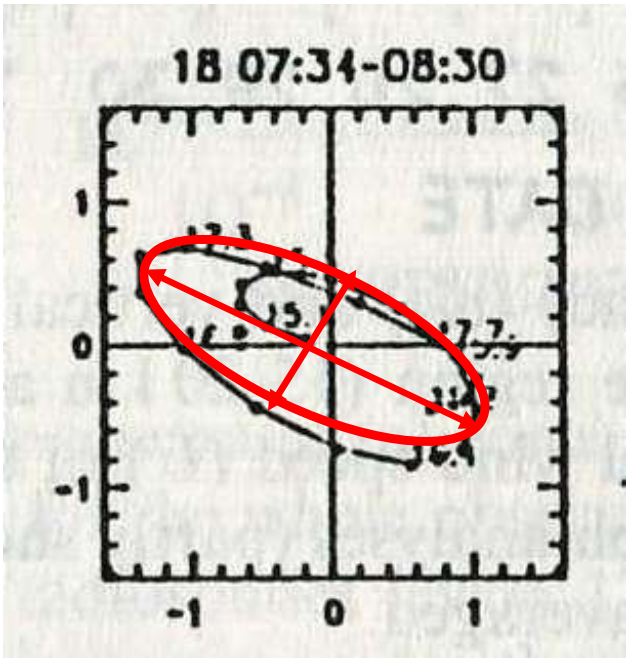

Rossby Waves (Planetary Waves)

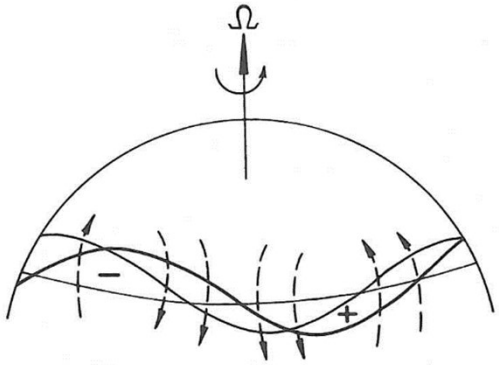

Fig. 7.14 Perturbation vorticity field and induced velocity field (dashed arrows) for a meridionally displaced chain of fluid parcels. Heavy wavy line shows original perturbation position; light line shows westward displacement of the pattern due to advection by the induced velocity.

(Holton's texbook)

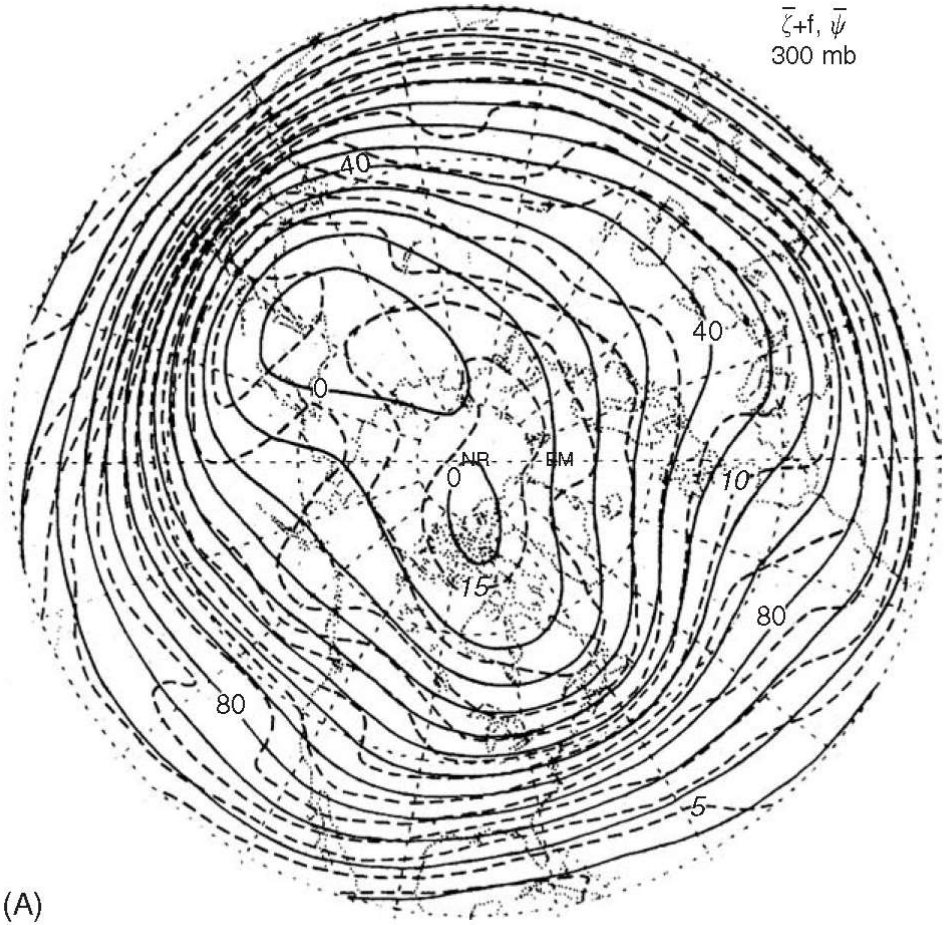

Figure 2 (A) Streamlines (solid) and absolute vorticity, $\xi + f$, averaged at the 300 hPa level in the upper troposphere (figure from Lau NC, *Journal of the Atmospheric Sciences*, 36: 996–1016, 1979). The deviation of the streamlines from circles is a wave pattern analogous to **Figure 1**. If this were simply barotropic Rossby waves, the dashed and full lines would coincide. Continents are shown with dotted curves; North America is at the bottom of the figure.

(Rhines' overview)

Note: In the mid-latitude troposphere, baroclinic instability (extratropical cyclones) is dominant

Planetary (Rossby) waves (equatorially trapped)

Zonal wavenumber = 0
(stationary)

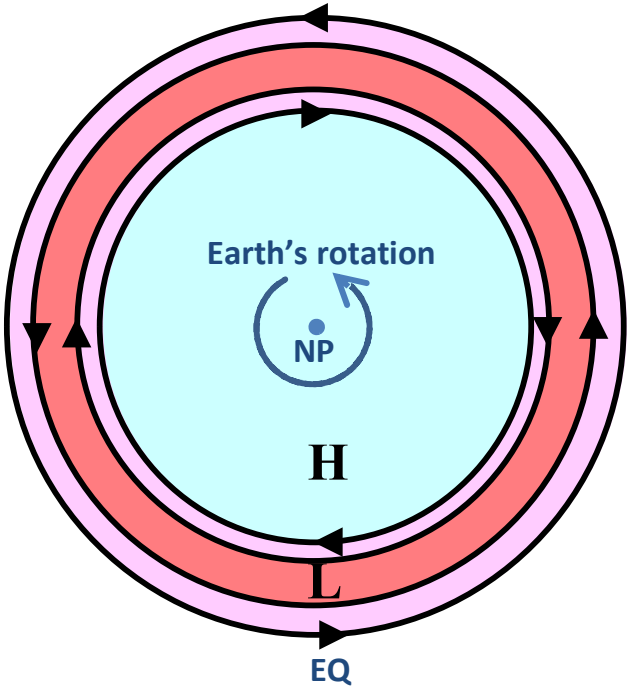

Zonal wavenumber = 1
(westward propagation)

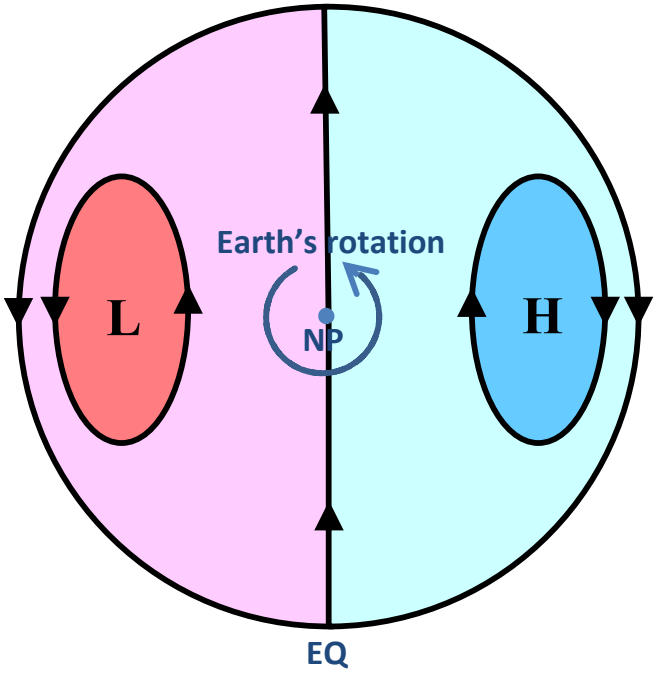

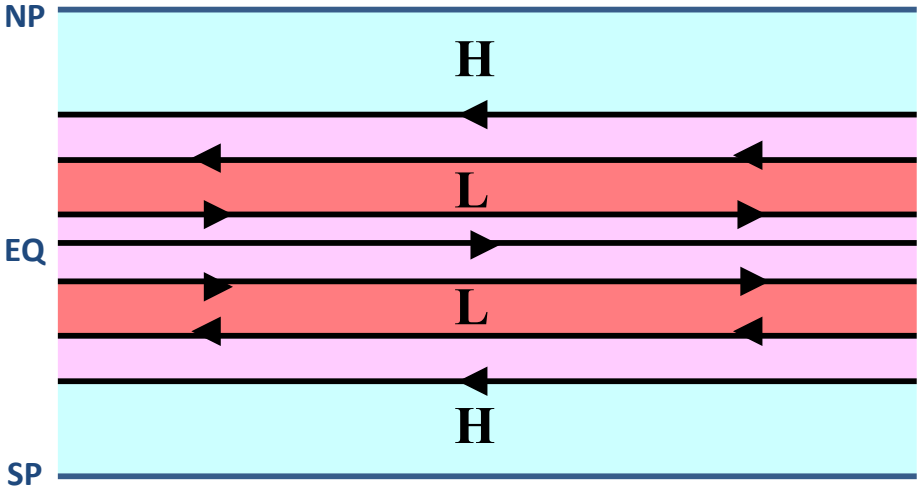

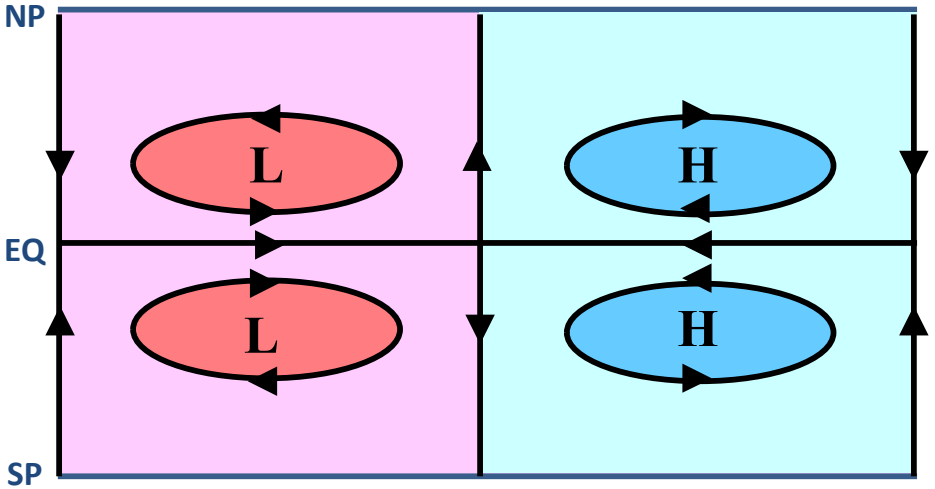

Global abnormal weather due to Rossby wave propagation forced at the equator ("Teleconnection")

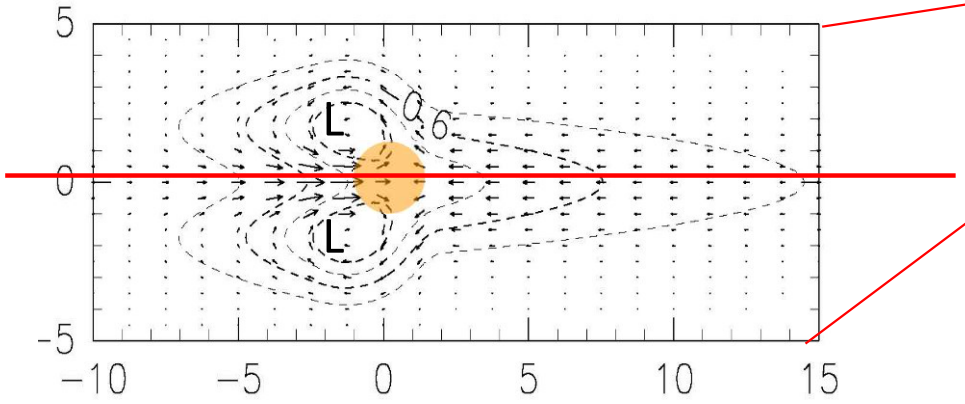

(Gill, 1966)

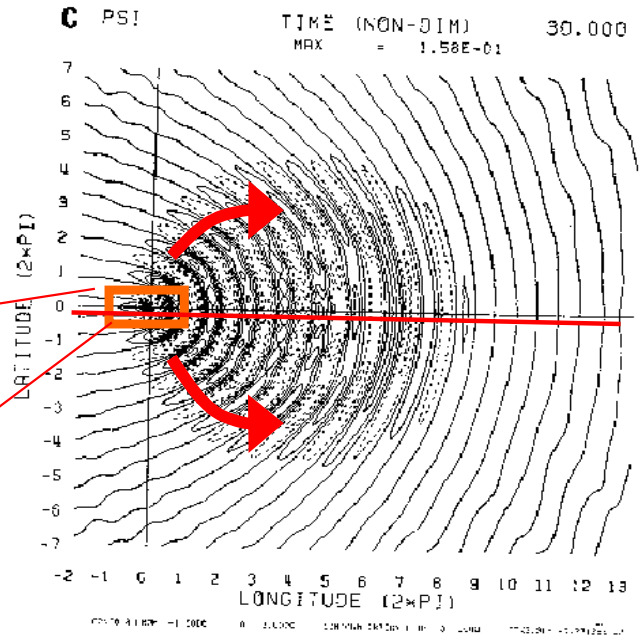

(Hayashi, 1987)

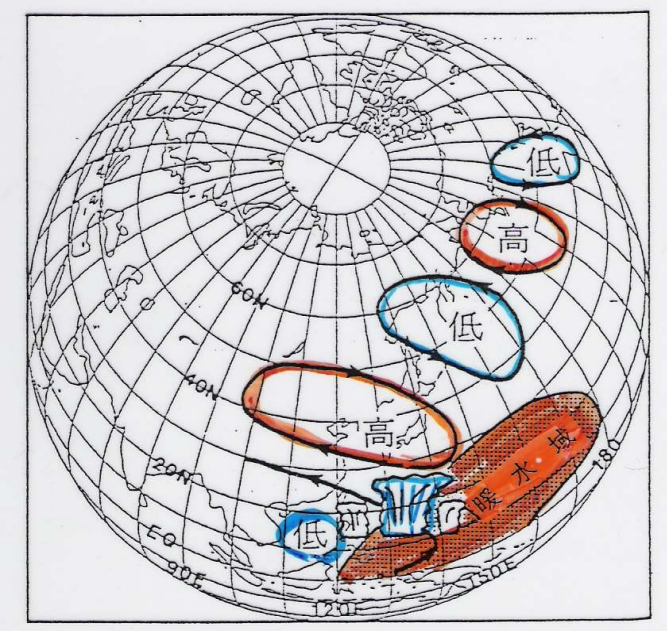

(Nitta, 1987)

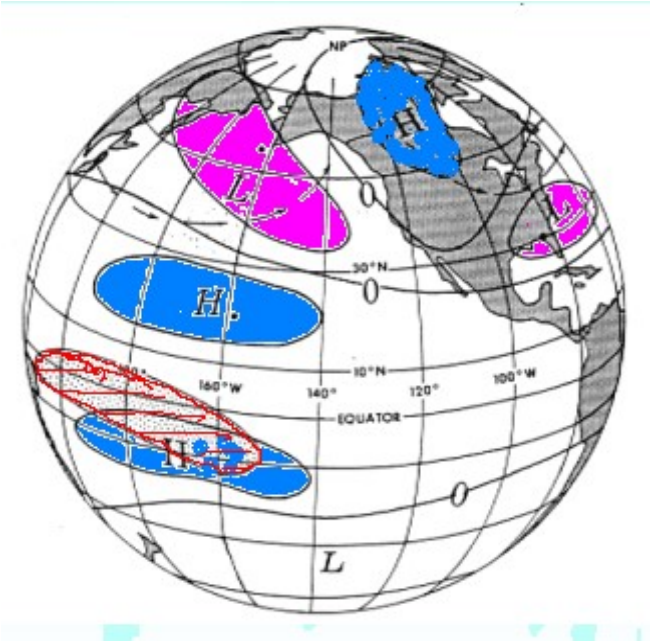

(Wallace, 1981)

Equatorial (Kelvin and Rossby-Gravity) Waves

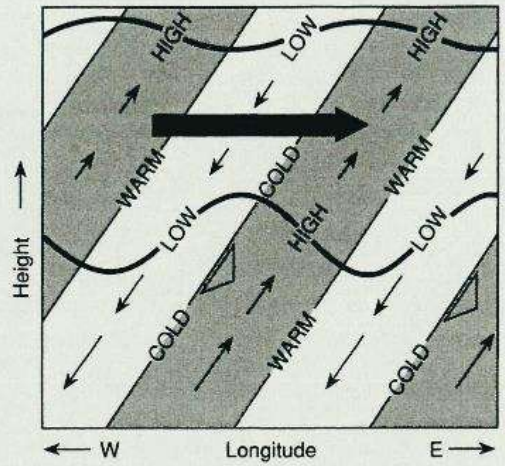

Fig. 12.12 Longitude–height section along the equator showing pressure, temperature, and wind perturbations for a thermally damped Kelvin wave. Heavy wavy lines indicate material lines; short blunt arrows show phase propagation. Areas of high pressure are shaded. Length of the small thin arrows is proportional to the wave amplitude, which decreases with height due to damping. The large shaded arrow indicates the net mean flow acceleration due to the wave stress divergence.

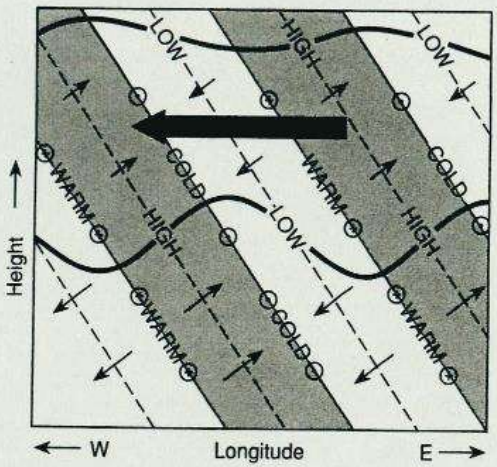

Fig. 12.13 Longitude–height section along a latitude circle north of the equator showing pressure, temperature, and wind perturbations for a thermally damped Rossby–gravity wave. Areas of high pressure are shaded. Small arrows indicate zonal and vertical wind perturbations with length proportional to the wave amplitude. Meridional wind perturbations are shown by arrows pointed into the page (northward) and out of the page (southward). The large shaded arrow indicates the net mean flow acceleration due to the wave stress divergence.

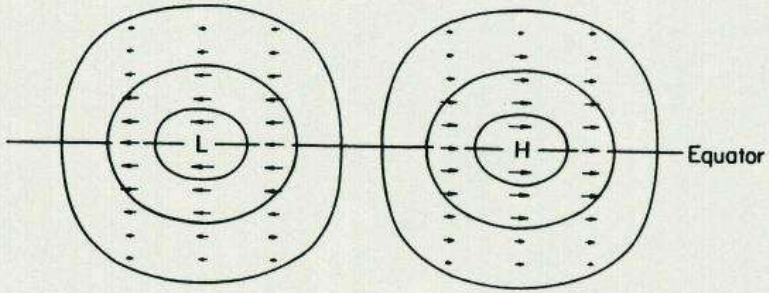

Fig. 11.15 Plan view of horizontal velocity and height perturbations associated with an equatorial Kelvin wave. (Adapted from Matsuno, 1966.)

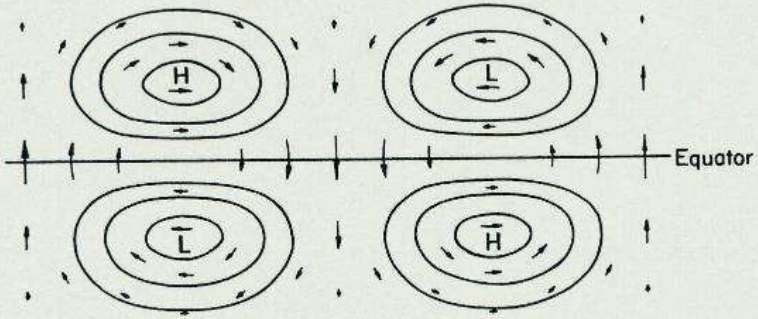

Fig. 11.13 Plan view of horizontal velocity and height perturbations associated with an equatorial Rossby–gravity wave. (Adapted from Matsuno, 1966.)

Coastal Kelvin Waves in oceans, lakes and channels

XVI. *On Gravitational Oscillations of Rotating Water.*
By Sir WILLIAM THOMSON.*

THIS is really Laplace's subject in his Dynamical Theory of the Tides; where it is dealt with in its utmost generality except one important restriction—the motion of each particle to be infinitely nearly horizontal, and the velocity to be always equal for all particles in the same vertical. This implies that the greatest depth must be small in comparison with the distance that has to be travelled to find the deviation from levelness of the water-surface altered by a sensible fraction of its maximum amount. In the present short communication I

* From the Proceedings of the Royal Society of Edinburgh, March 17, 1879. Communicated by the Author. (reprinted in *Philos. Mag.*, 1880)

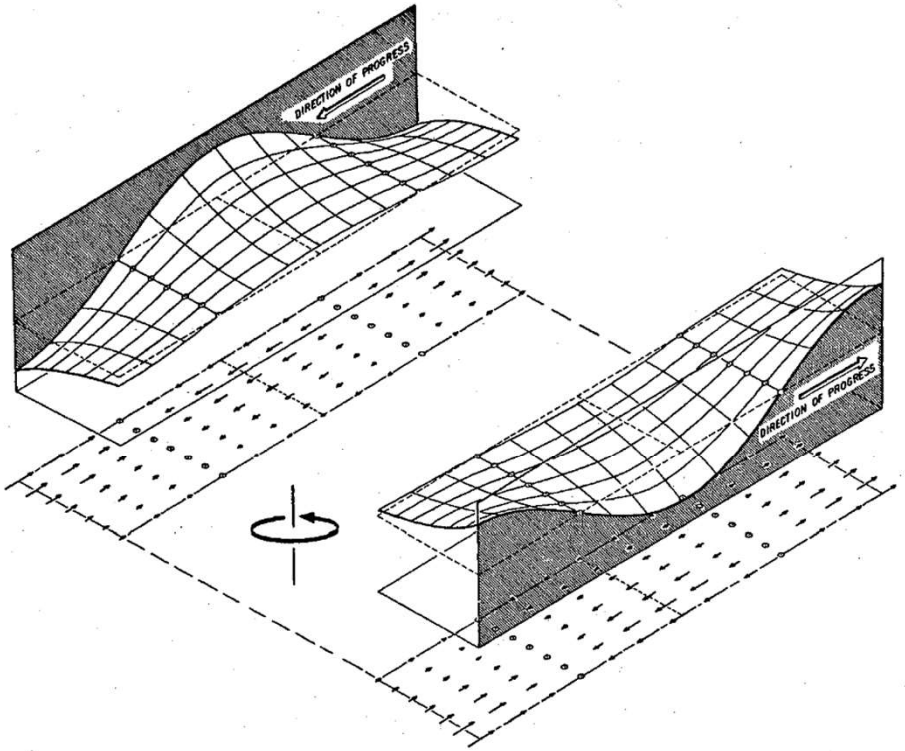

Fig. 10.3. Northern hemisphere Kelvin waves on opposite sides of a channel that is wide compared with the Rossby radius. In each vertical plane parallel to the coast, the currents (shown by arrows) are entirely within the plane and are exactly the same as those for a long gravity wave in a nonrotating channel. However, the surface elevation varies exponentially with distance from the coast in order to give a geostrophic balance. This means Kelvin waves move with the coast on their right in the northern hemisphere and on their left in the southern hemisphere. [From Mortimer (1977).]

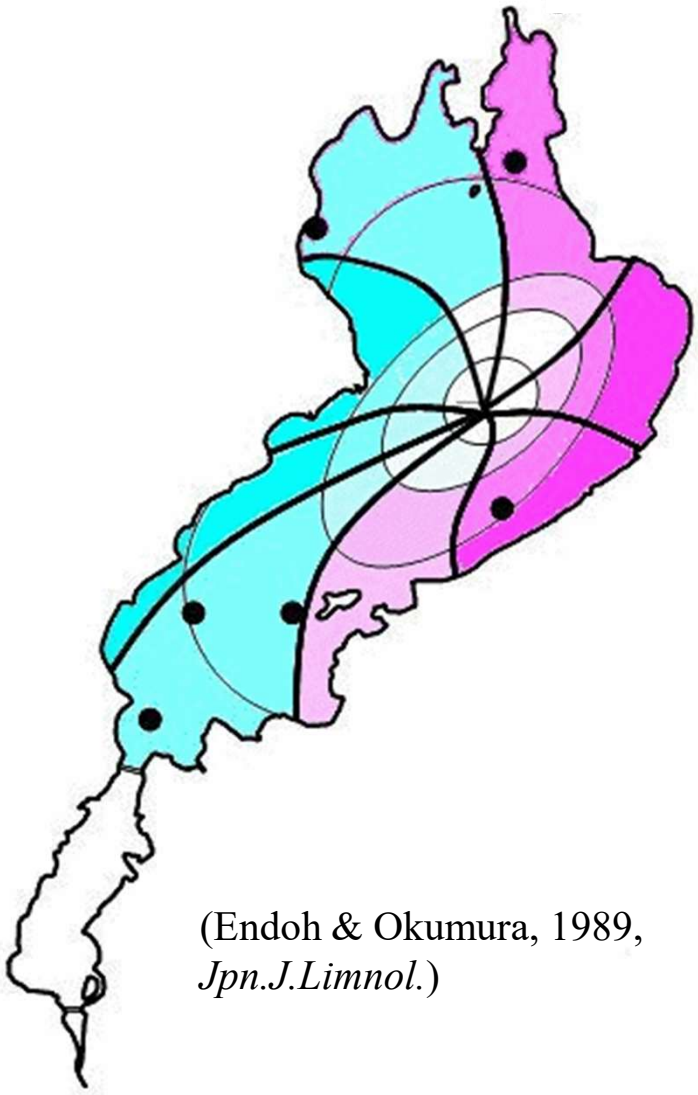

(Endoh & Okumura, 1989, *Jpn.J.Limnol.*)

Kelvin waves: Coastal & Equatorial

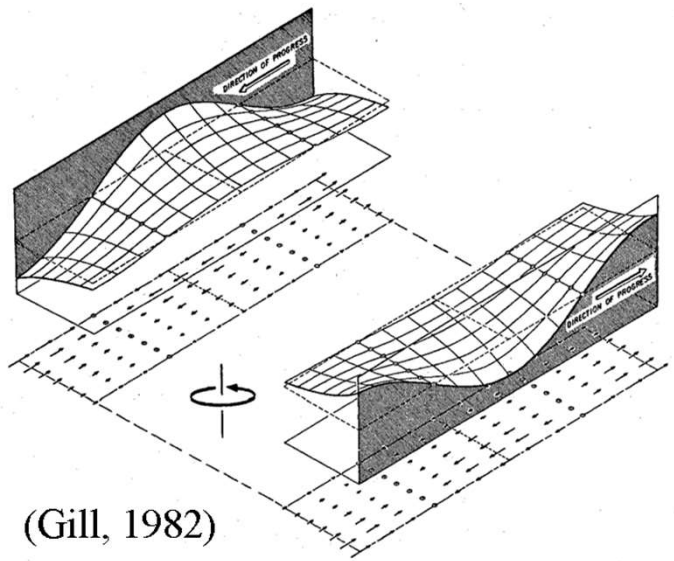

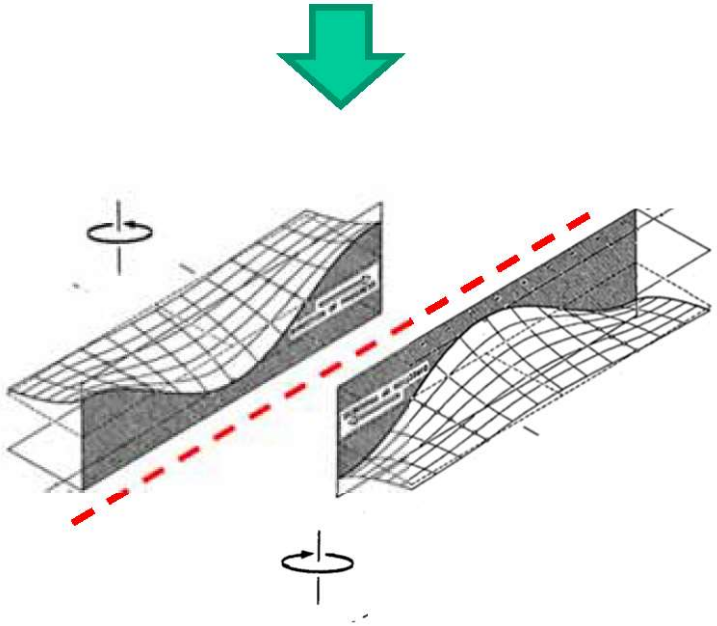

Zonal wavenumber = 1 (eastward propagation)

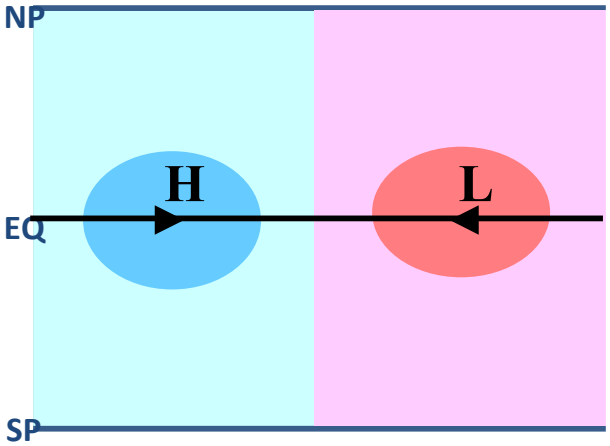

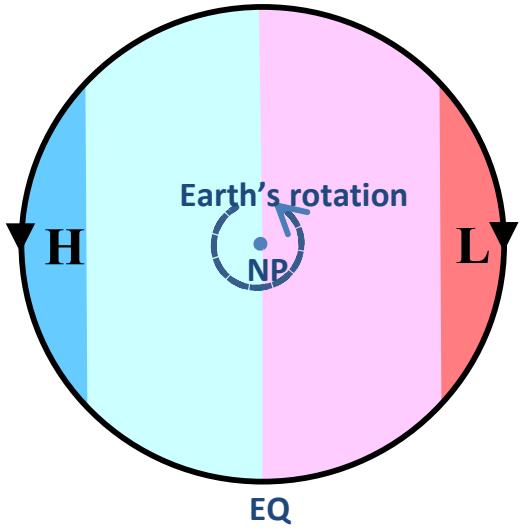

Zonal wavenumber = 0 (stationary)

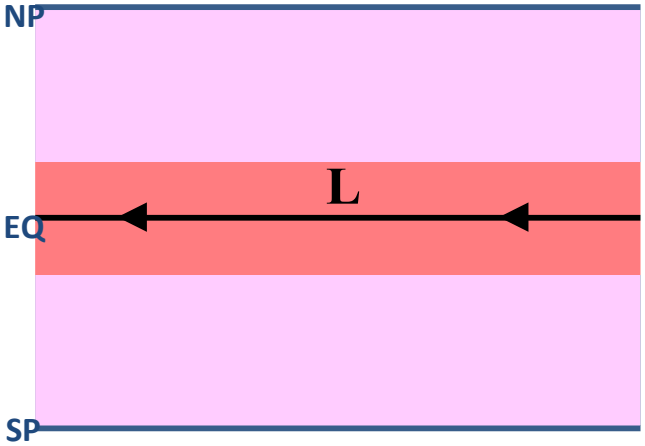

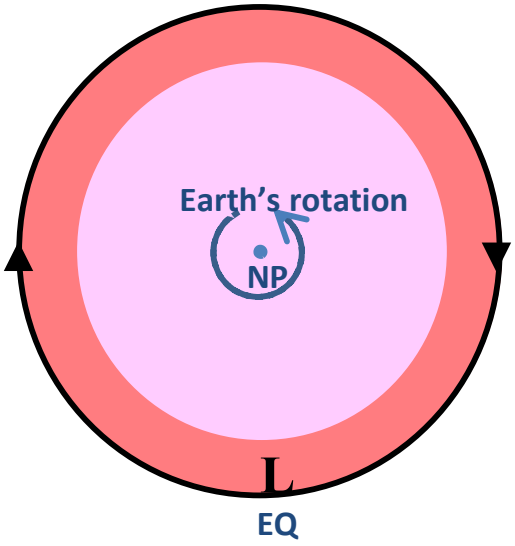

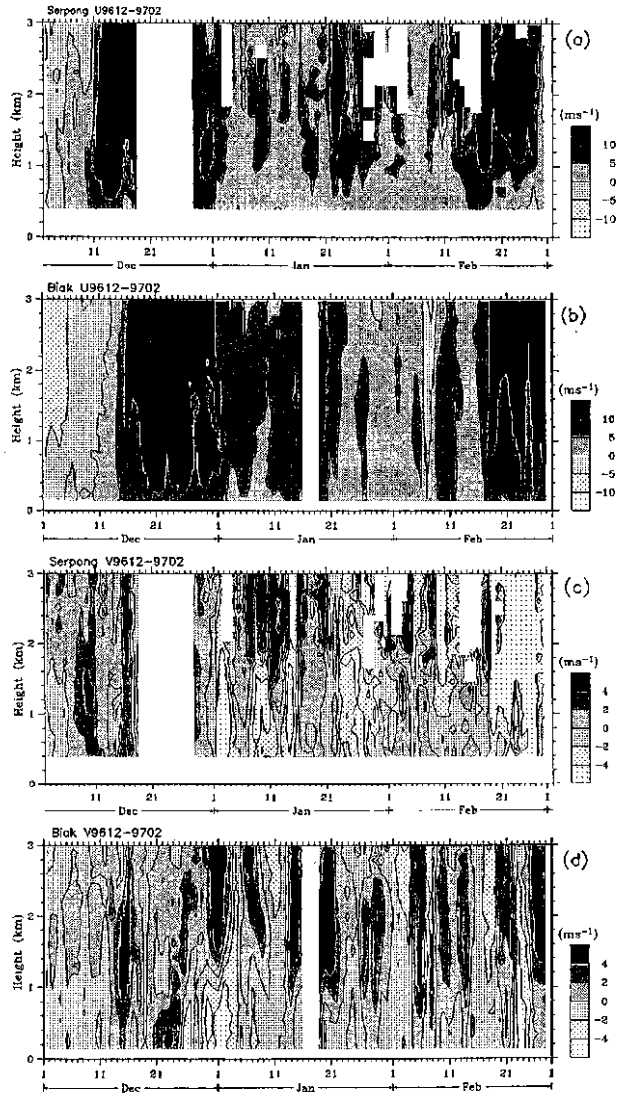

図 1.5: インドネシア東西 2 地点でのプロファイラ高分解能観測による下部対流圏内の西風 (a) (b)・南風 (c) (d) 各成分風速の時間・高度変化。約 3200 km 離れた Serpong (Jakarta 郊外；6°S, 107°E) (a) (c) および Biak (Papua 島の属島；1°S, 136°E) (b) (d) における観測結果。Widiyatmi *et al.* (2001) による。

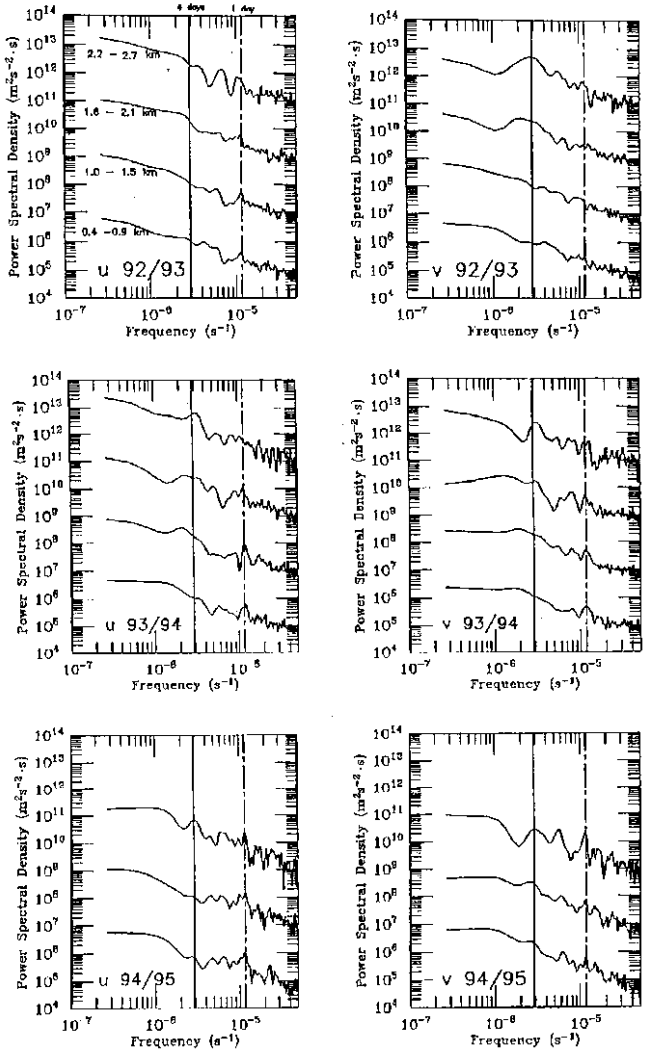

図 1.6: インドネシアの雨季における風速変動の周波数スペクトル。Serpong (6°S, 107°E) における 1992 ～ 93 (上), 93 ～ 94 (中), 94 ～ 95 (下) の 11 ～ 2 月のプロファイラ観測による西風 (左)・南風 (右) 各成分風速データから作成。各図の 4 本の曲線は 0.4 ～ 0.9, 1.0 ～ 1.5, 1.6 ～ 2.1, 2.2 ～ 2.7 km の各高度領域 (100 m ごとの結果を 6 個ずつ平均) における結果を，後 3 者はそれぞれ 10^2, 10^4, 10^6 倍したもの。縦直線は 4 日 (実線) および 1 日 (鎖線) 周期を示す。Widiyatmi *et al.* (1999) による。

Carl-Gustaf Arvid Rossby
(1898 – 1957)

(http://sok.riksarkivet.se/sbl/bilder/6953_7_030_00000575_0.jpg)

Michio Yanai（柳井迪雄）
(1934 – 2010)

(http://web.atmos.ucla.edu/~yanai/)

Equatorial Forcing and Atmospheric Response

- Stationary modes
  - Zonally uniform (k=0 or Zonal mean)
    - Symmetric ⇒zonal **Hadley cells (ITCZ)**
    - Anti-symmetric ⇒ "**Monsoon**"
  - Cyclic/isolated
    - ⇒ Zonal (Walker) circulations
      - (**Matsuno-Gill patterns**)
      - Teleconnections
      - Rossby-wave propagation

- Traveling modes
  - Eastward along equator (Kelvin)
    - ⇒ **IntraSeasonal variations**
      - (Madden-Jullian Oscillation, etc.)

- Regional/Local modes (gravity waves)
  - ⇒ Sea-Land (Mountain-Valley)
    - breeze circulations

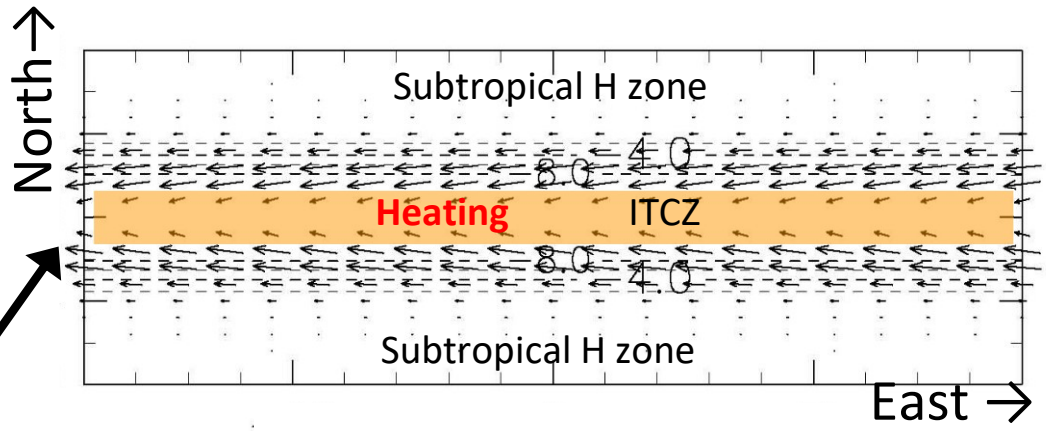

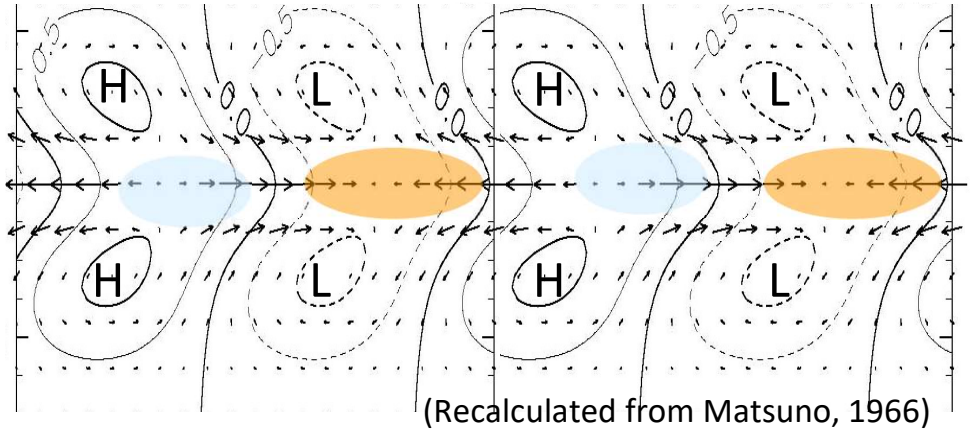

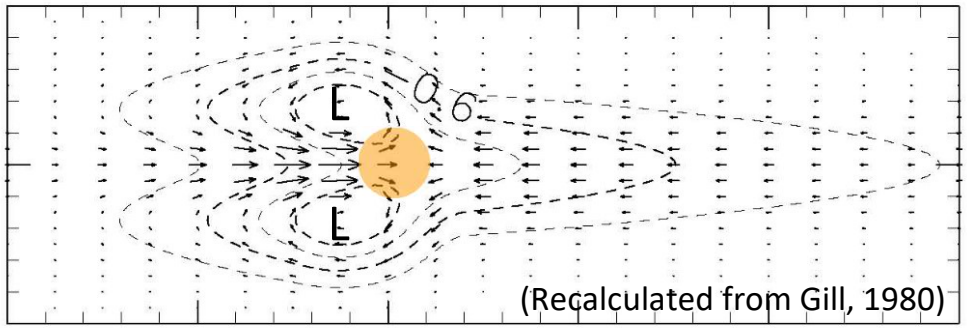

Horizontal convection or waves trapped along equator or coastline

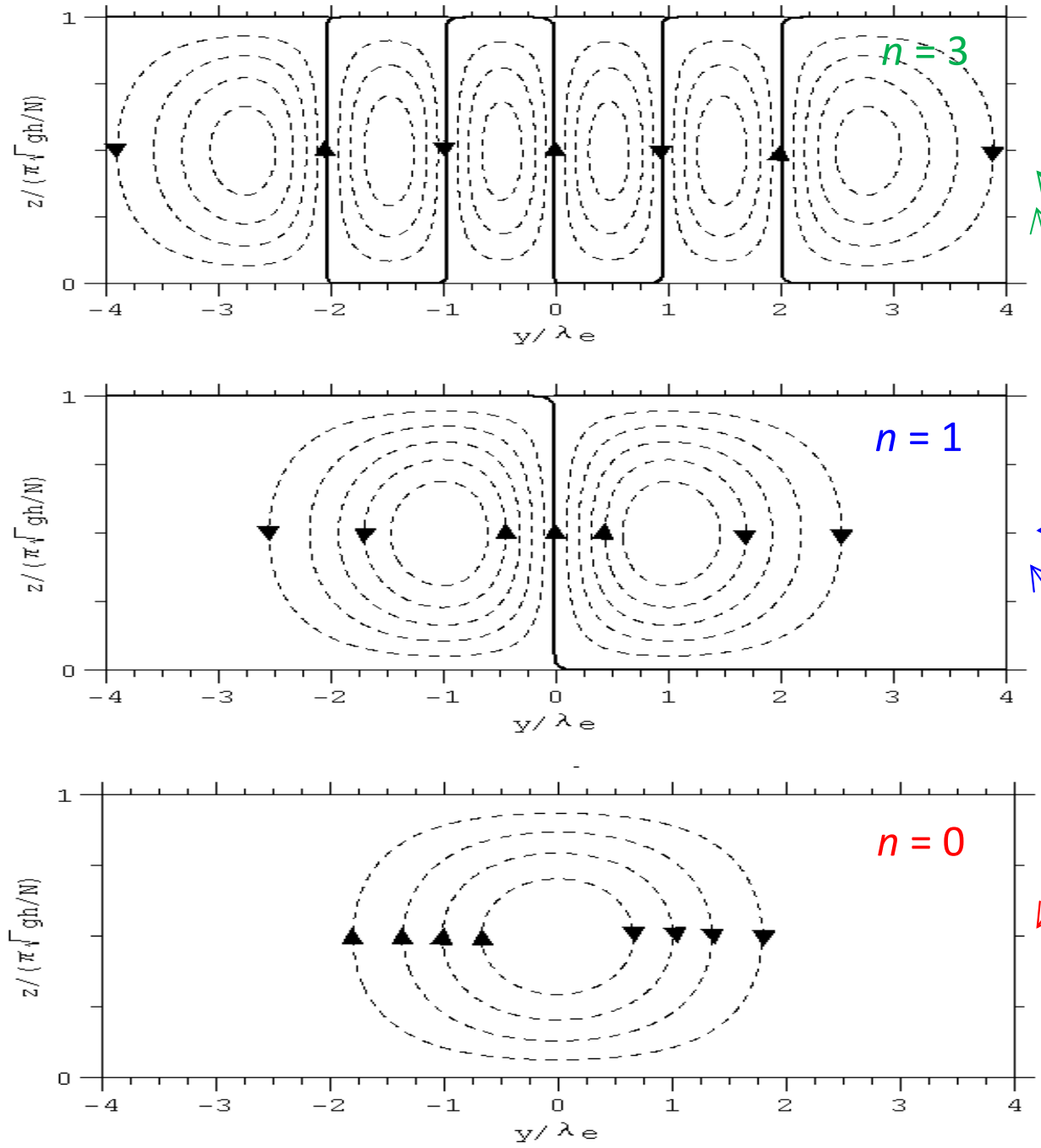

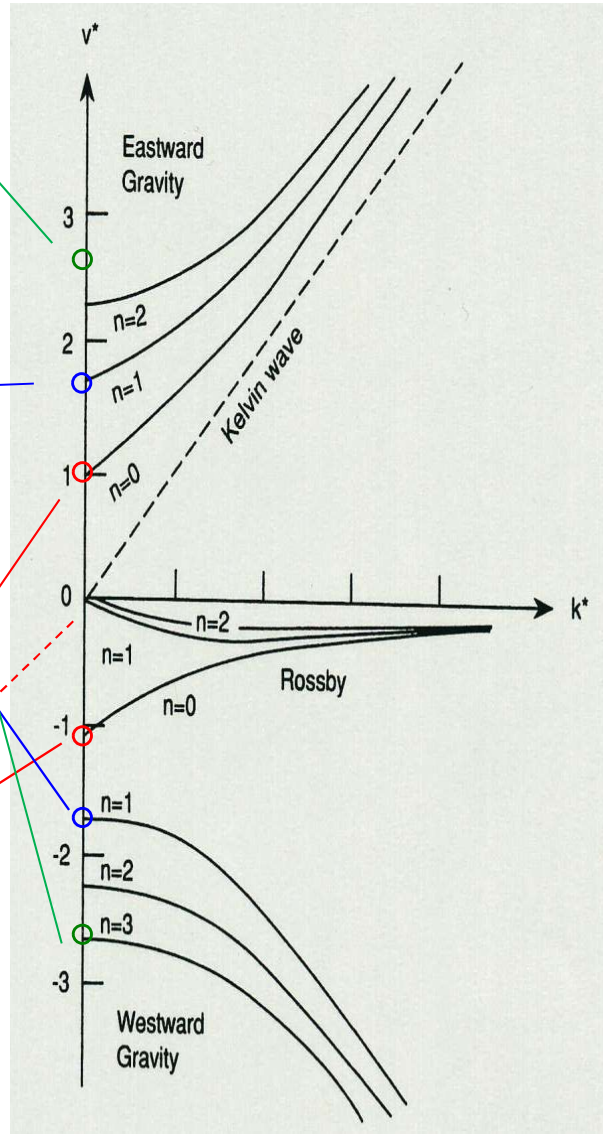

(Matsuno, 1966, for equatorial nonzero zonal wavenumber case)

Hadley cell by zero-zwn Kelvin and Rossby waves

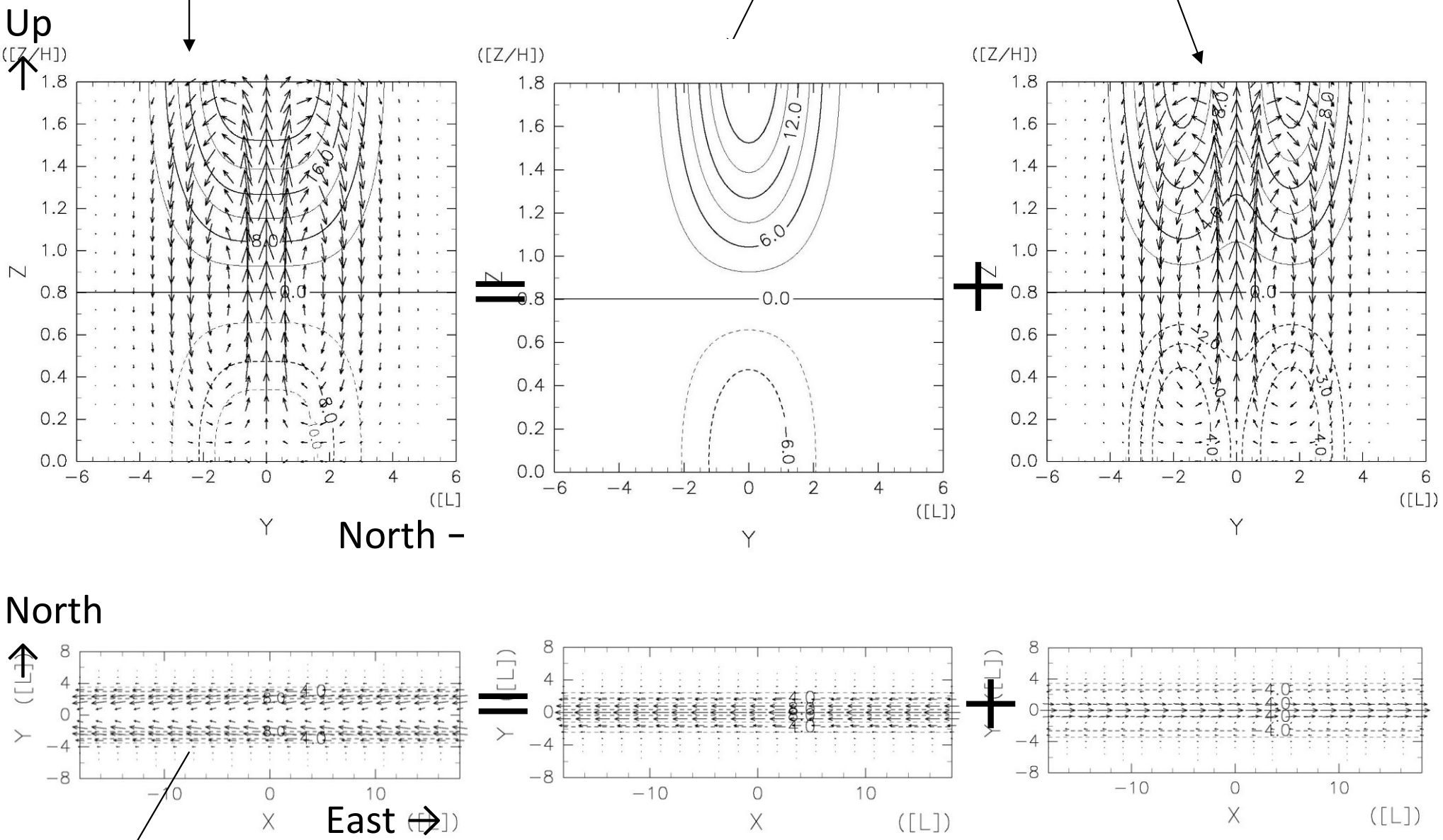

Matsuno-Gill pattern and Hadley-Walker circulations

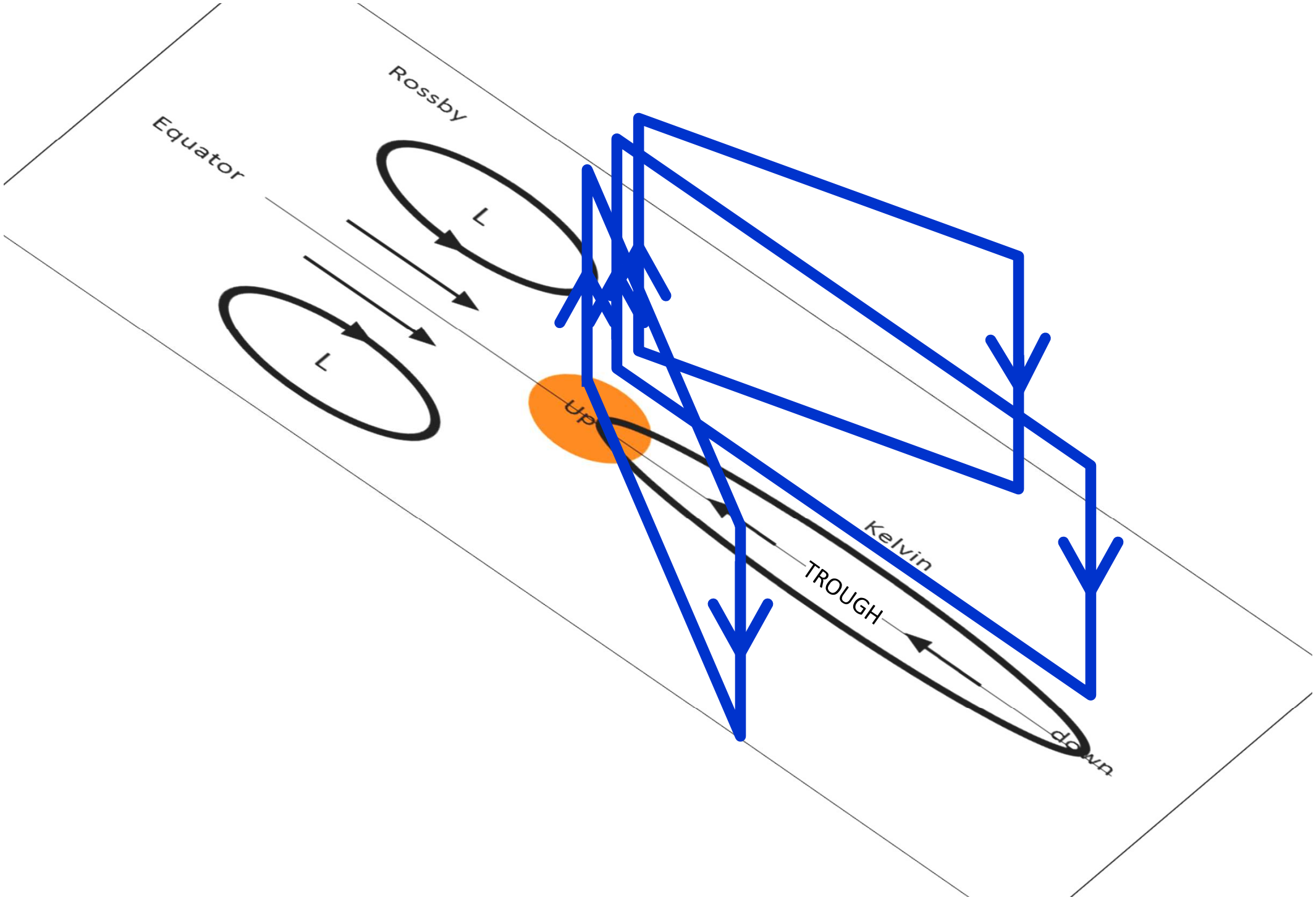

Meridional (Hadley) and Zonal (Walker) Circulations

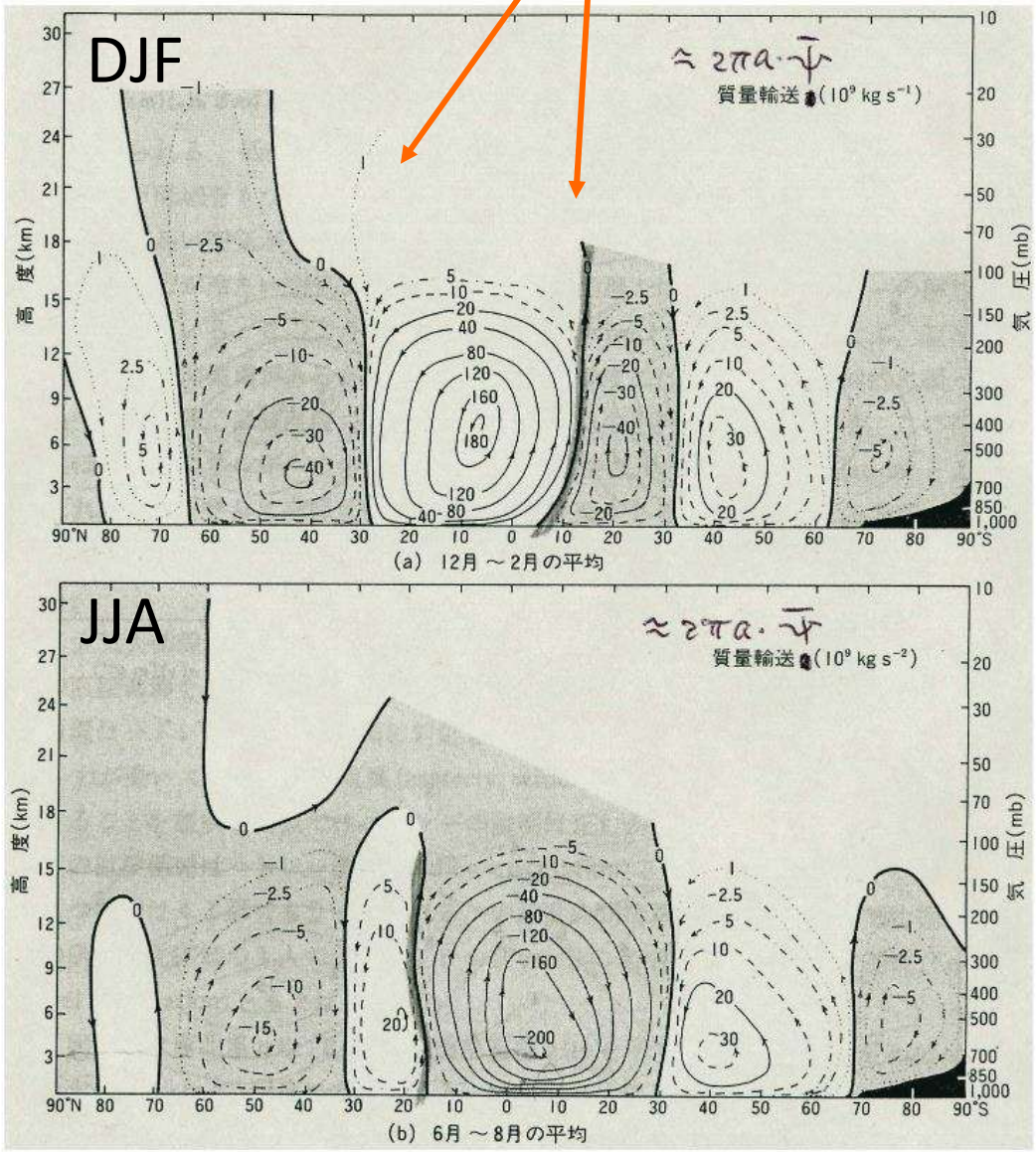

平均子午面循環場 (Newell *et al.*, 1972). 質量輸送量 (単位 10^9 kg s^{-1})

(North-south shift by annual cycle)

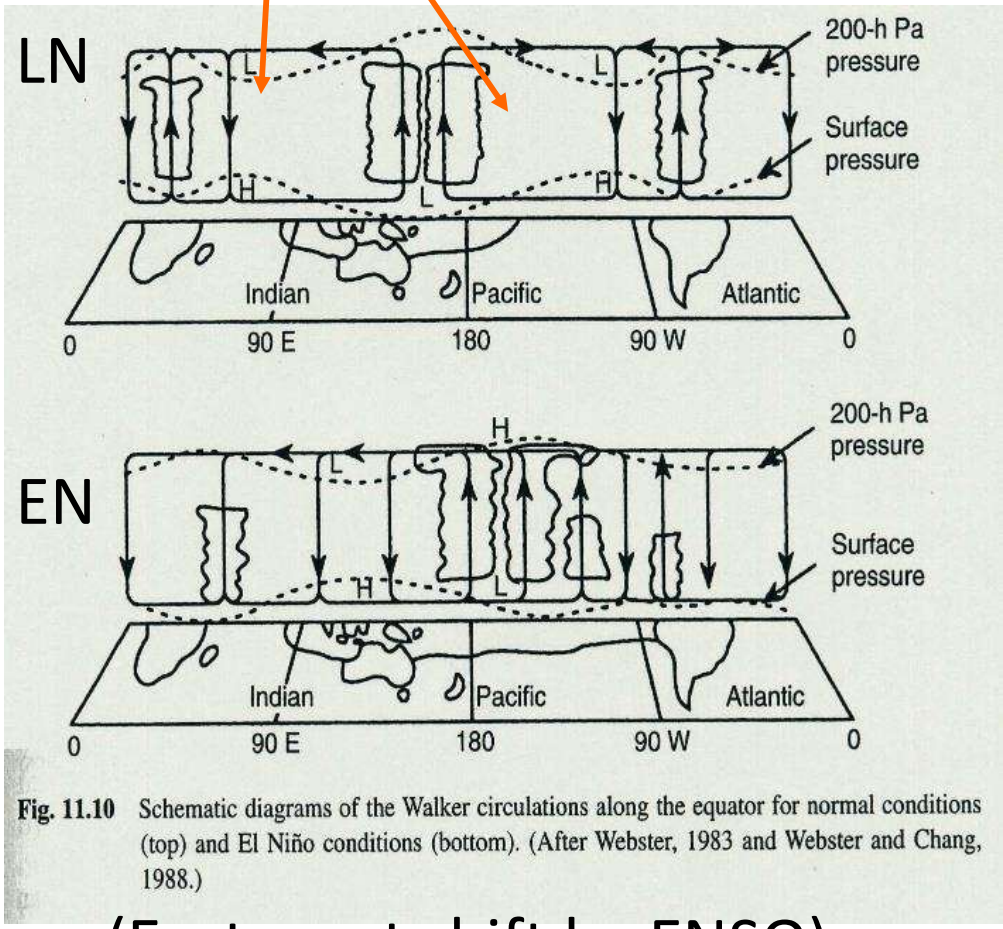

Fig. 11.10 Schematic diagrams of the Walker circulations along the equator for normal conditions (top) and El Niño conditions (bottom). (After Webster, 1983 and Webster and Chang, 1988.)

(East-west shift by ENSO)

5.3. Atmosphere-ocean interaction and El Niño-southern oscillation (ENSO)

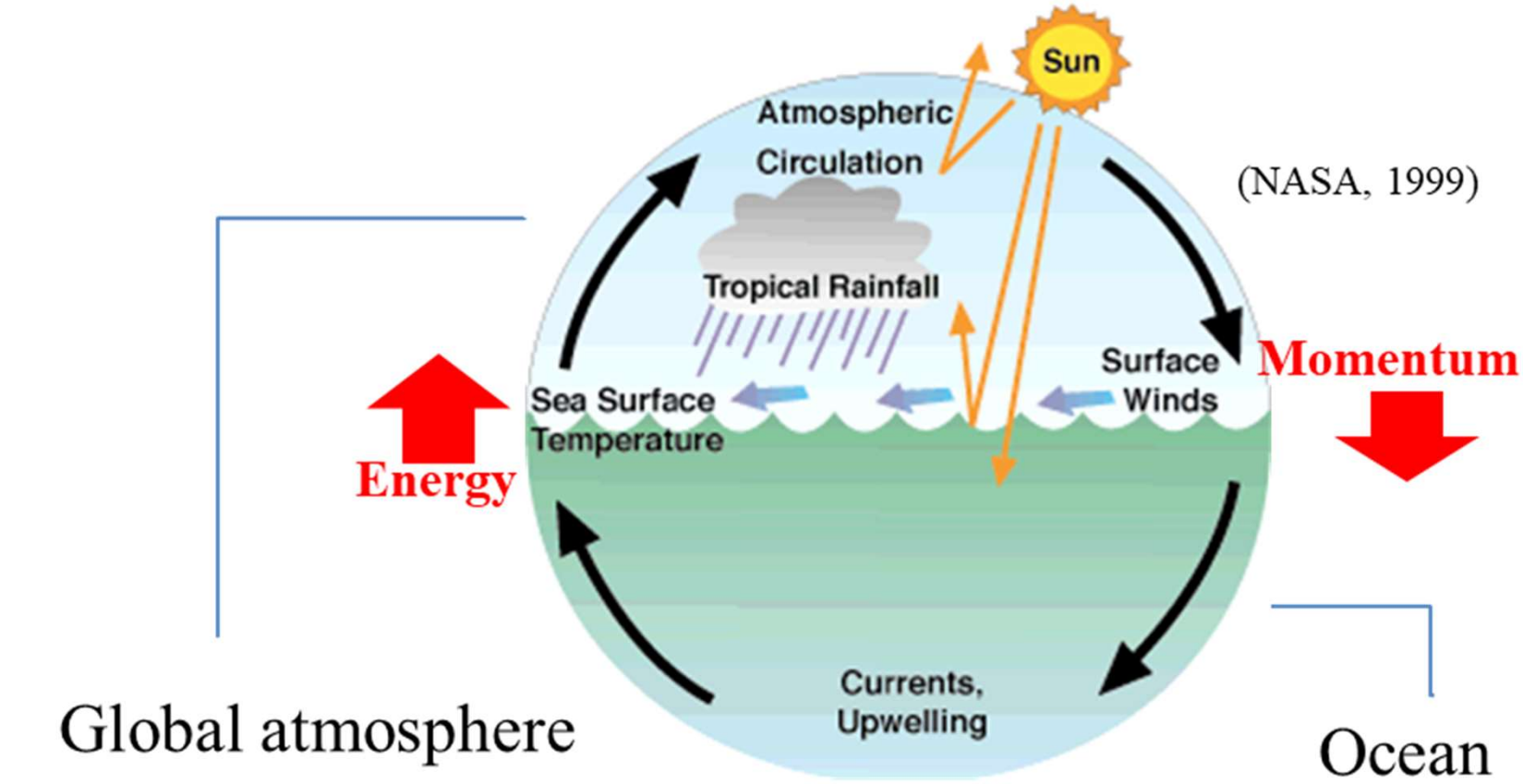

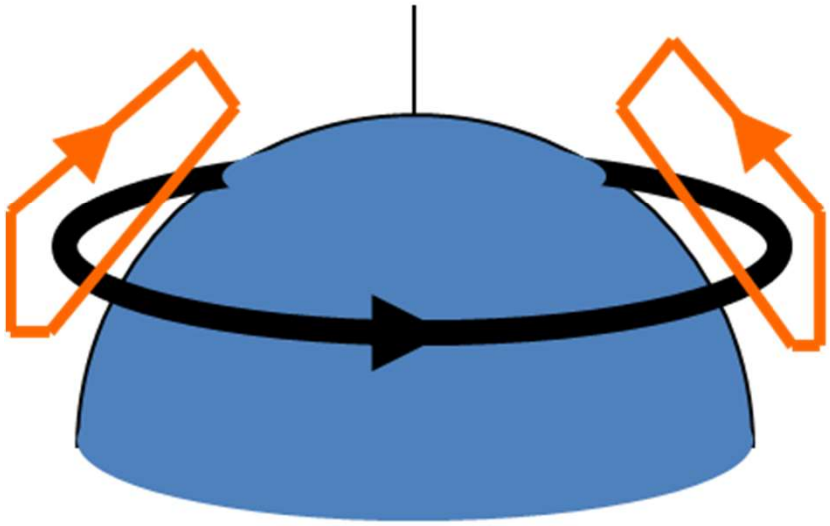

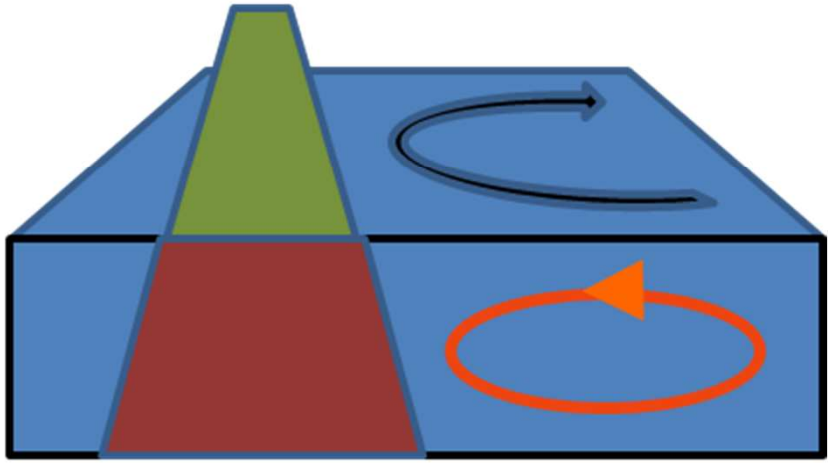

Atmosphere-ocean interaction and El Niño-southern oscillation (ENSO)

- South-American fishermen: Bad fishery in Christmas season → El Niño
- Walker (1920s) : Interannual pressure/monsoon variation → Southern oscillation
- Oceanographers, ichthyologists: Water temperature warming → plankton extinction
- Bjerknes (1969) : Atmosphere-ocean interaction → El Niño-southern oscillation (ENSO)
- Convection center/warm water shift: 1/4 equatorial circle (IMC → central Pacific)

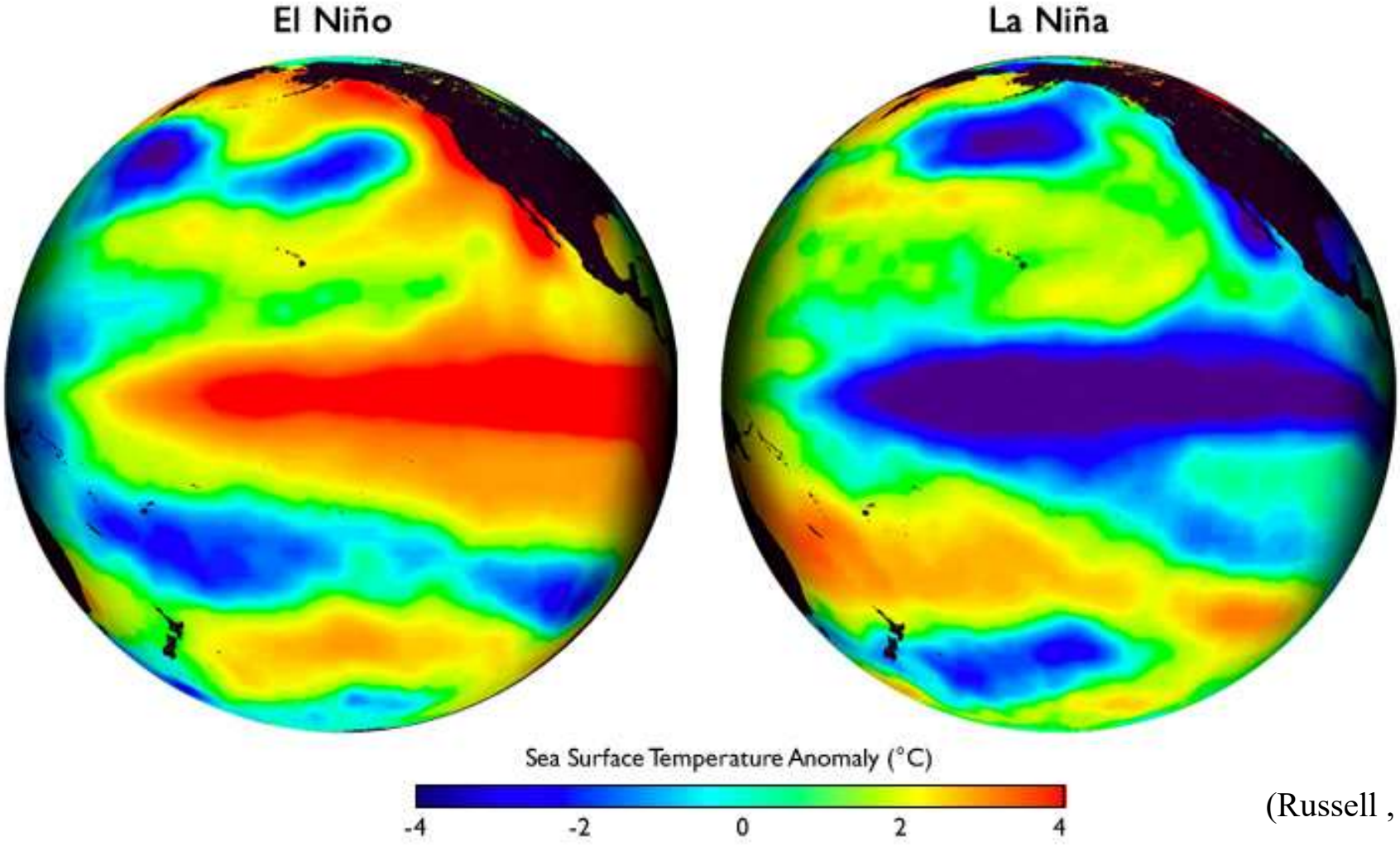

(Russell , 2004)

Strongest (1997–98) El Niño so far observed

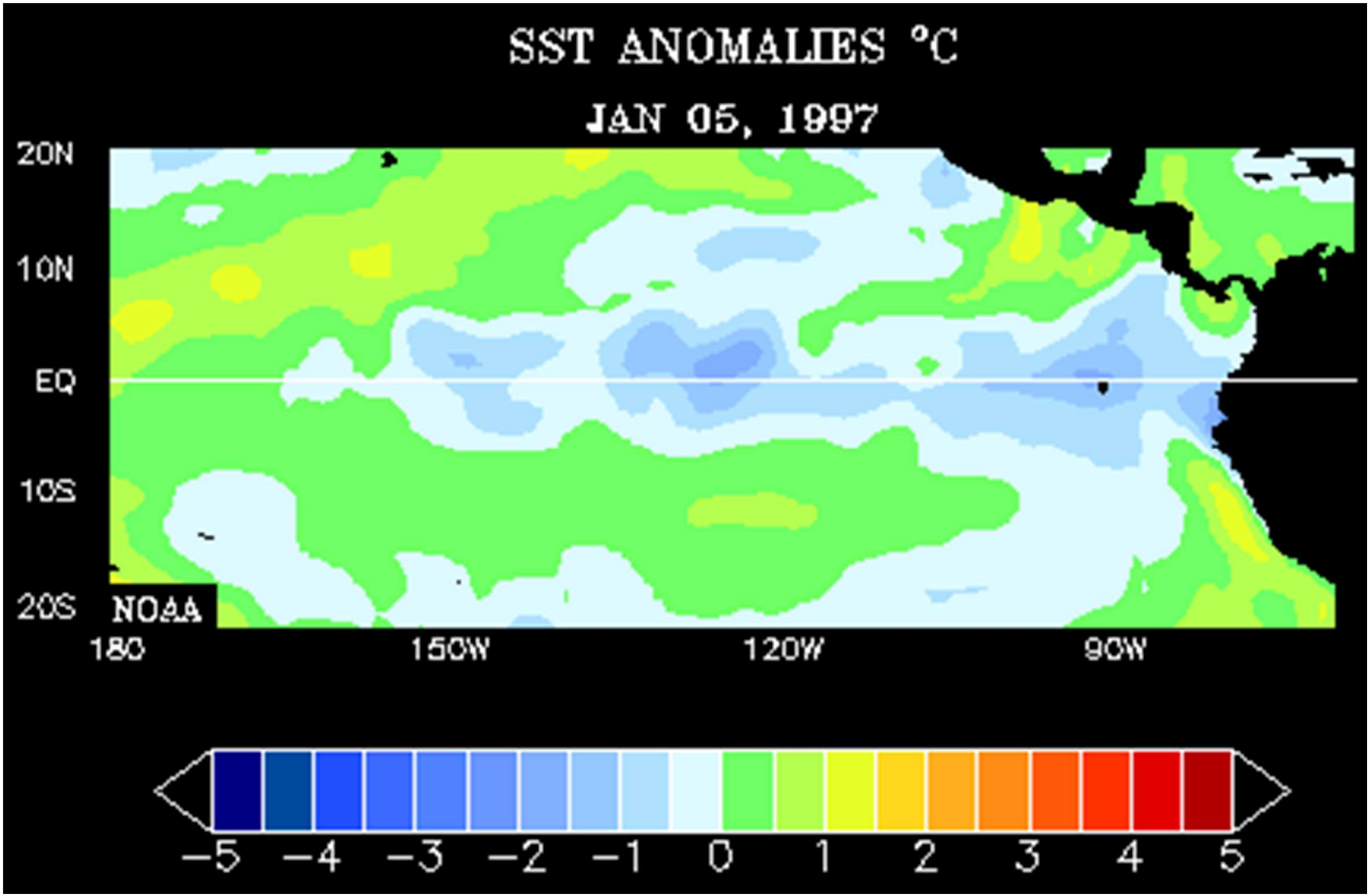

http://apollo.lsc.vsc.edu/classes/met130/notes/chapter10/graphics/sst_9798_animated.gif

Jacob Aall Bonnevie Bjerknes (1897 – 1975)

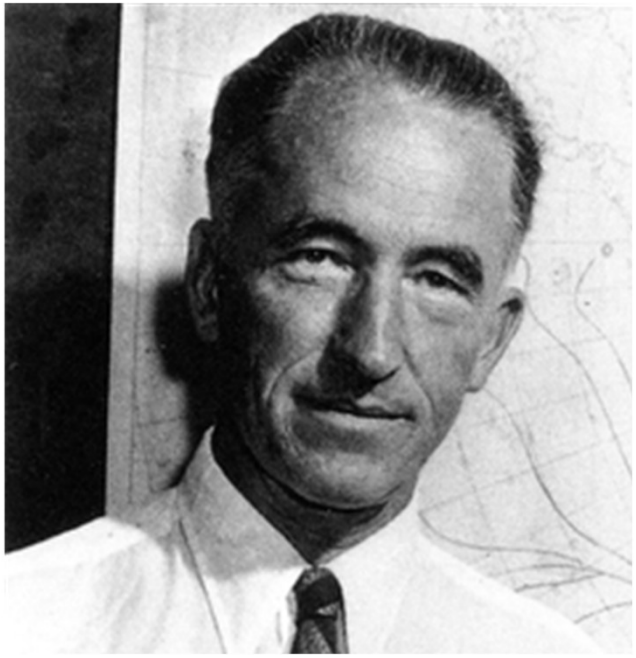

(http://docs.lib.noaa.gov/rescue/Bibliographies/Bjerknes/Bjerknes_July_2004.htm)

MONTHLY WEATHER REVIEW

VOLUME 97, NUMBER 3

http://dx.doi.org/10.1175/1520-0493(1969)097<0163:ATFTEP>2.3.CO;2

MARCH 1969

UDC 551.513:551.509.338:551.465.6(265)(267)

ATMOSPHERIC TELECONNECTIONS FROM THE EQUATORIAL PACIFIC [1]

J. BJERKNES

Department of Meteorology, University of California, Los Angeles, Calif.

ABSTRACT

The "high index" response of the northeast Pacific westerlies to big positive anomalies of equatorial sea temperature, observed in the winter of 1957–58, has been found to repeat during the major equatorial sea temperature maxima in the winters of 1963–64 and 1965–66. The 1963 positive temperature anomaly started early enough to exert the analogous effect on the atmosphere of the south Indian Ocean during its winter season.

The maxima of the sea temperature in the eastern and central equatorial Pacific occur as a result of anomalous weakening of the trade winds of the Southern Hemisphere with inherent weakening of the equatorial upwelling. These anomalies are shown to be closely tied to the "Southern Oscillation" of Sir Gilbert Walker.

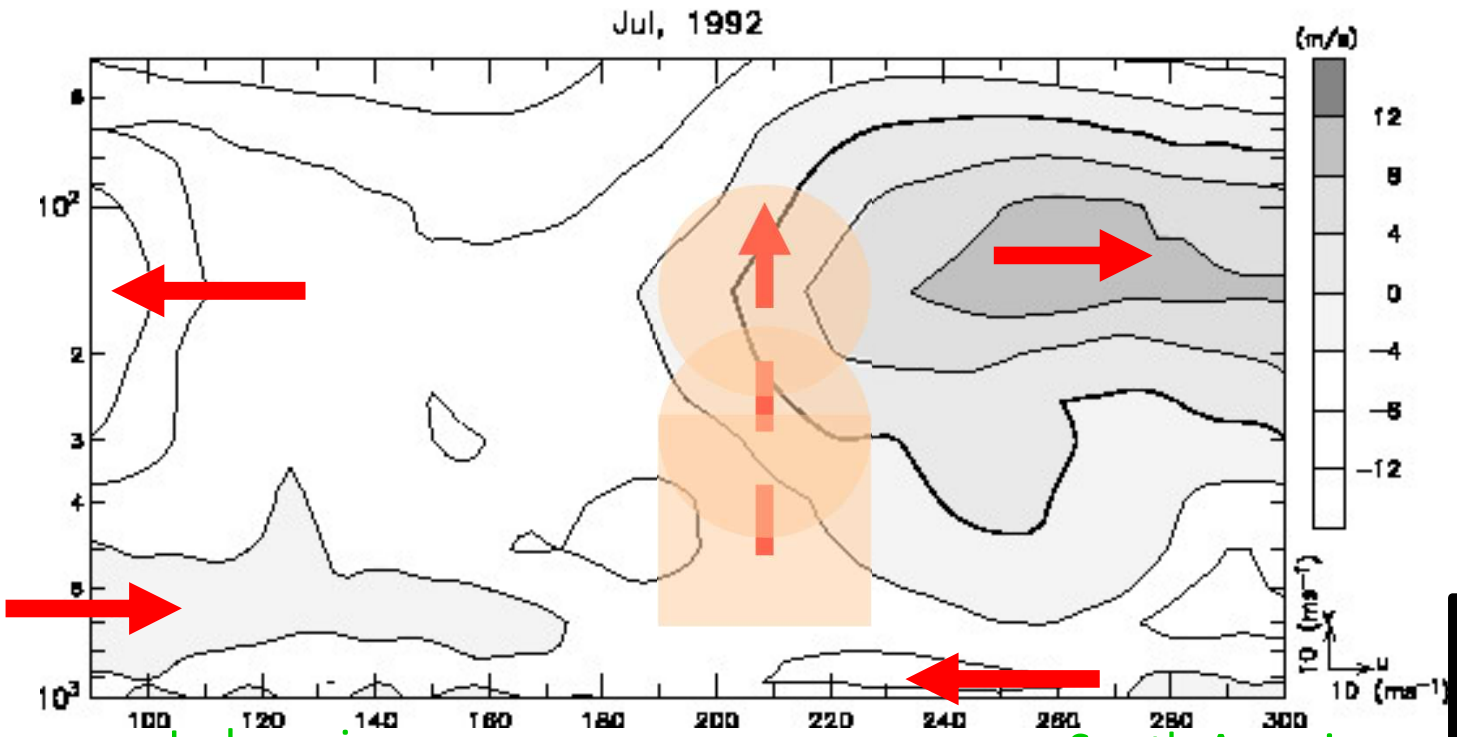

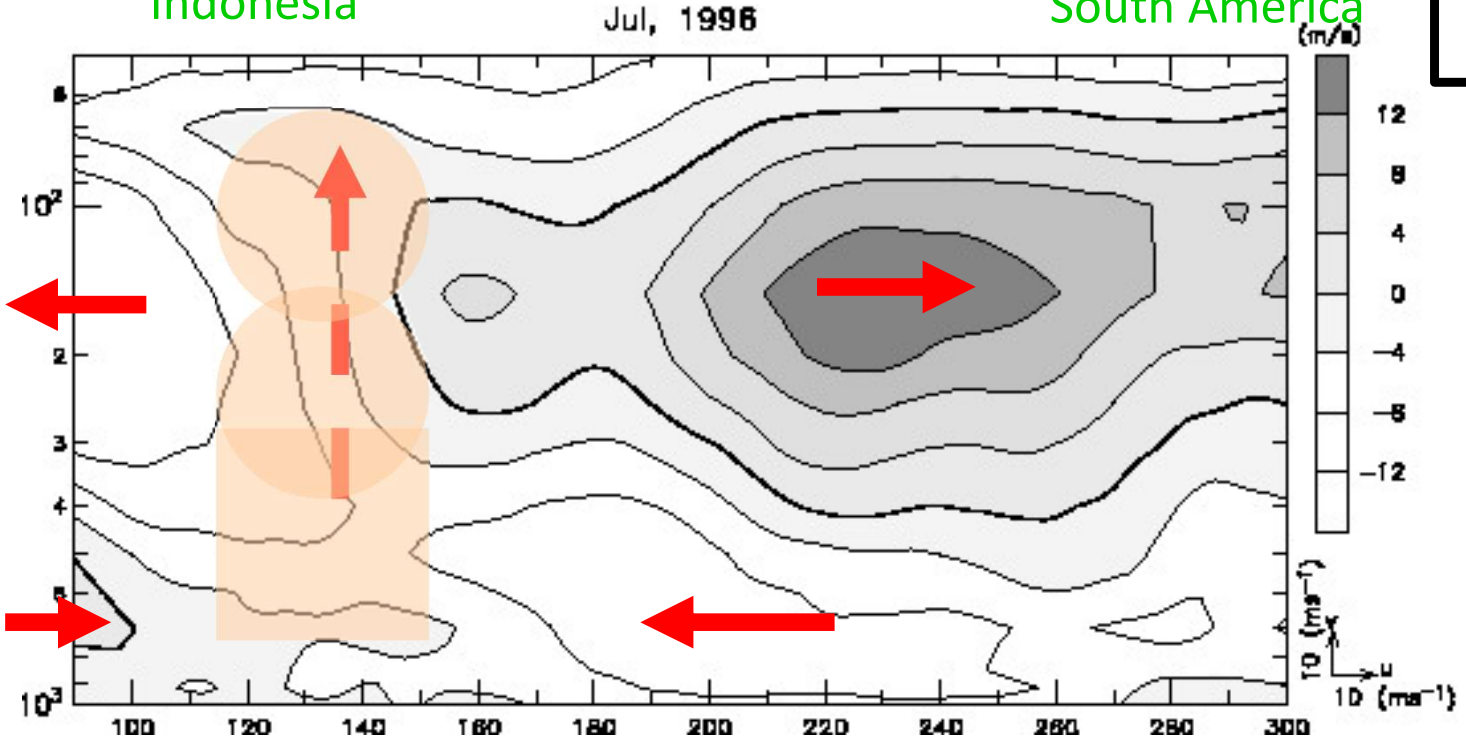

El Nino

Interannual Variation of Walker Circulation

La Nina

Note:
Based on NCEP reanalysis with almost **no Indonesian data.**

A dipole mode in the tropical Indian Ocean

N. H. Saji*, B. N. Goswami†, P. N. Vinayachandran* & T. Yamagata*‡

(1999), *Nature*

* *Institute for Global Change Research, SEAVANS N 7F, 1-2-1 Shibaura, Minato-ku, Tokyo 105 6791, Japan*
† *Center for Atmospheric and Oceanic Sciences, Indian Institute of Science, Bangalore 560 012, India*
‡ *Department of Earth and Planetary Physics, Graduate School of Science, The University of Tokyo, Tokyo 113 0033, Japan*

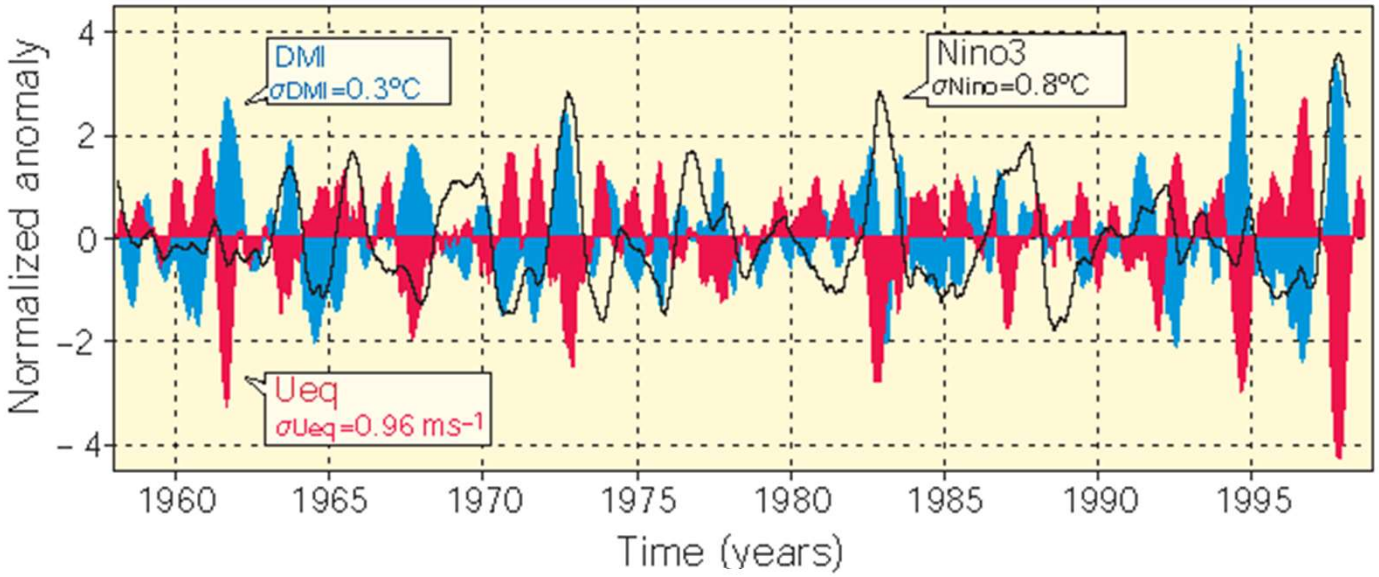

Figure 1 Dipole mode and El Niño events since 1958. Plotted in blue, the dipole mode index (DMI) exhibits a pattern of evolution distinctly different from that of the El Niño, which is represented by the Nino3 sea surface temperature (SST) anomalies (black line). On the other hand, equatorial zonal wind anomalies U_{eq} (plotted in red) coevolves with the DMI. All the three time series have been normalized by their respective standard deviations. We have removed variability with periods of 7 years or longer, based on harmonic analysis, from all the data sets used in this analysis. In addition, we have smoothed the time series using a 5-month running mean.

Figure 2 A composite dipole mode event. **a**–**d**, Evolution of composite SST and surface wind anomalies from May–June (**a**) to Nov–Dec (**d**). The statistical significance of the analysed anomalies were estimated by the two-tailed *t*-test. Anomalies of SSTs and winds exceeding 90% significance are indicated by shading and bold arrows, respectively.

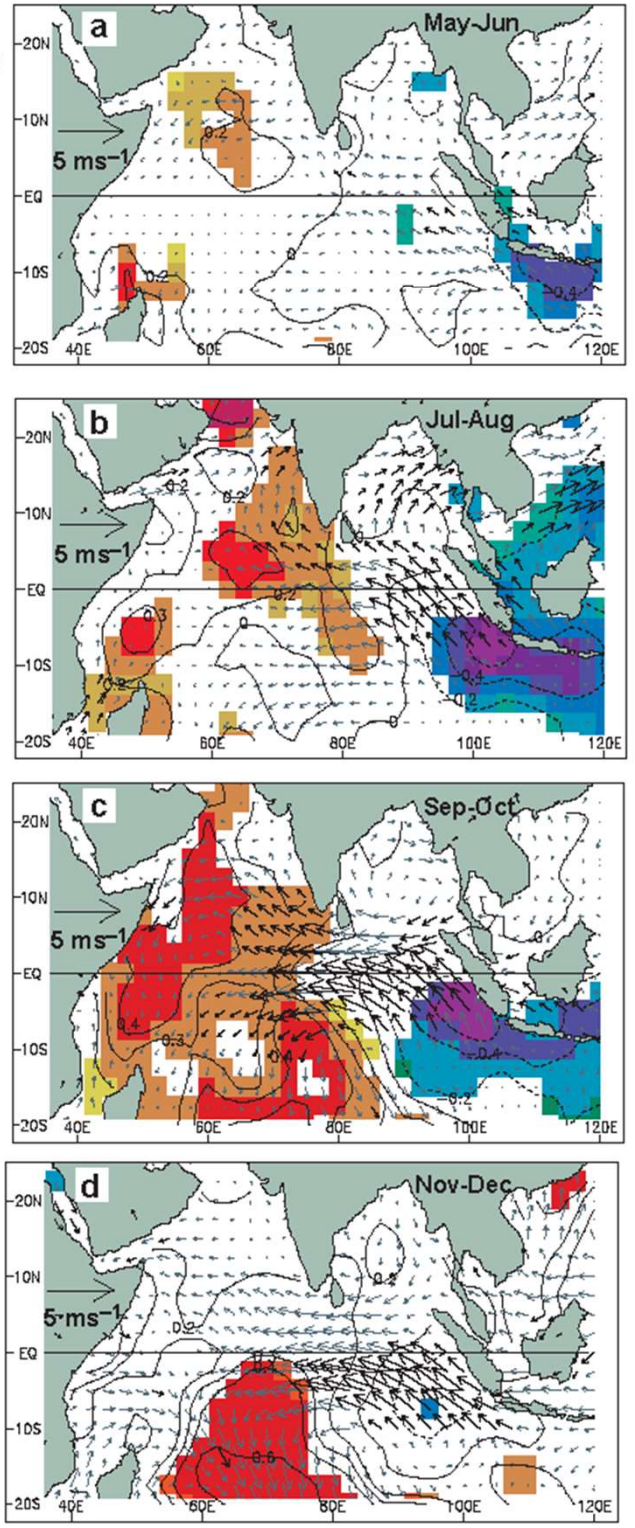

Indian Ocean dipole mode (IOD) & El Niño-southern oscillation (ENSO)

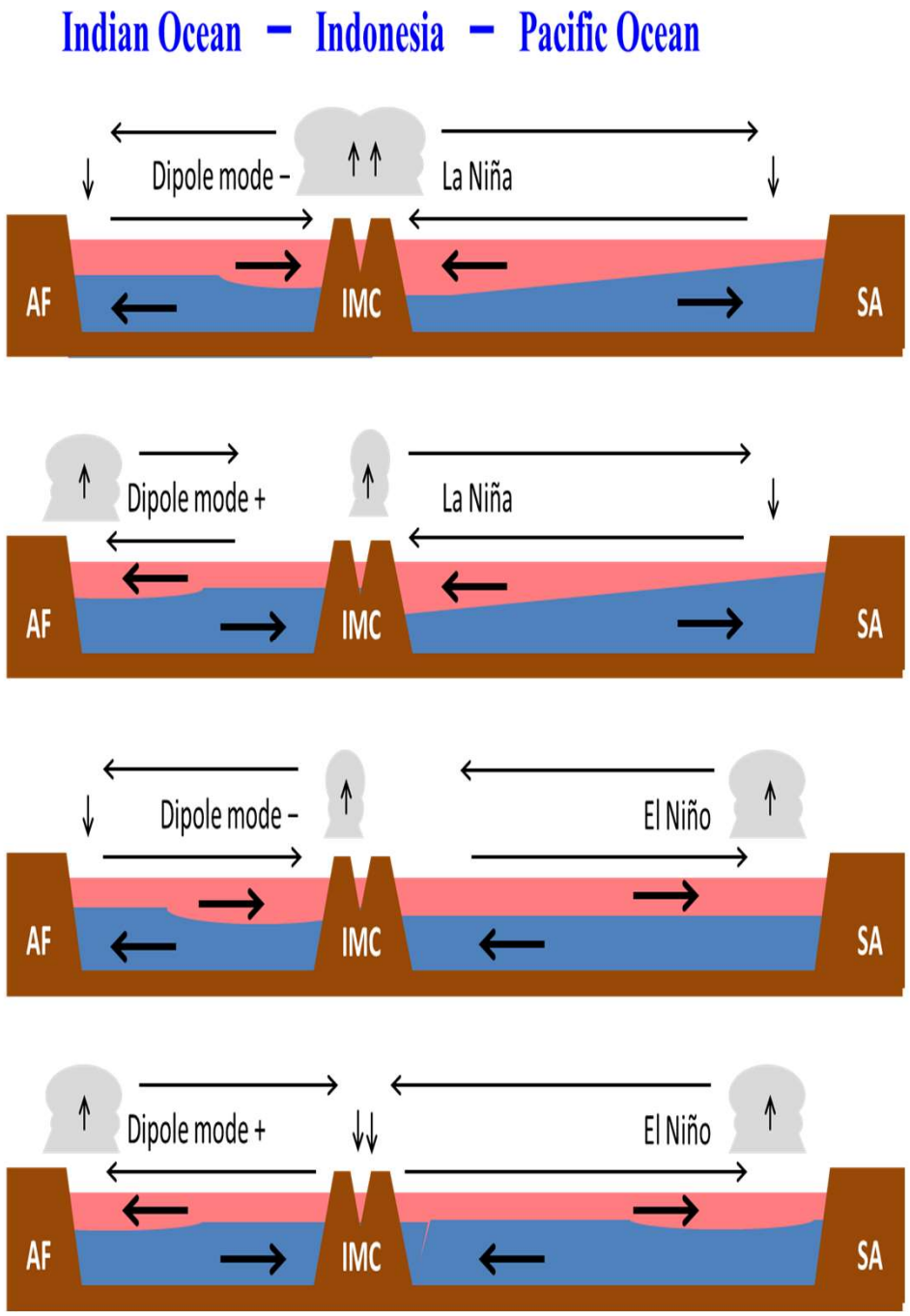

Padang monthly rainfall

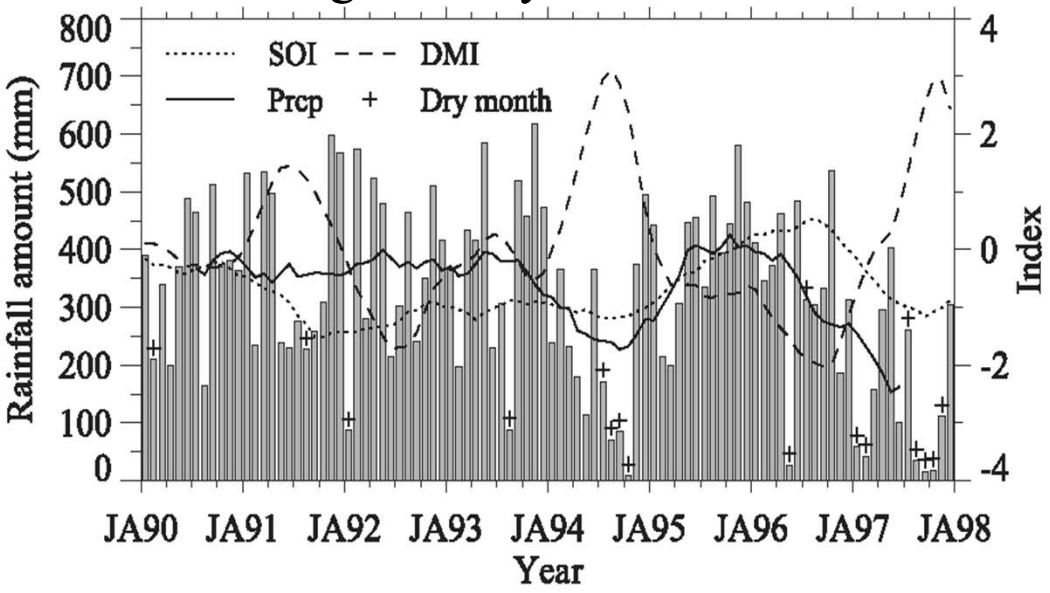

(Hamada, Yudi, Tien et al., 2008, *JMSJ*)

Jakarta (9 stations) in the dry season (ASO)

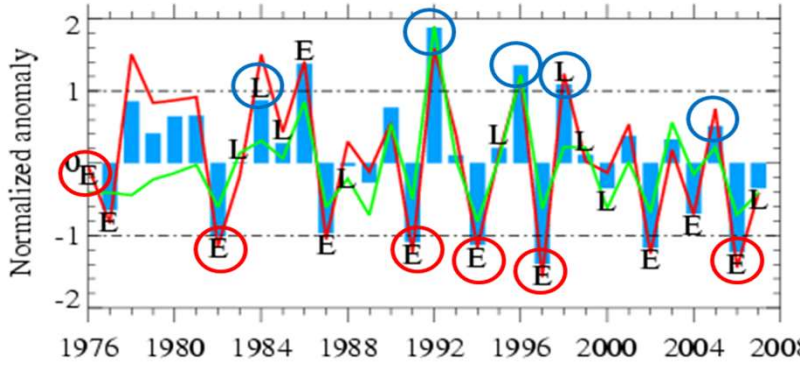

E: El Nino, : Positive IOD
L: La Nina, Negative IOD

Rainfall amount
Rainfall days
Heavy rainfall days

(Hamada, Urip, Sopia et al., 2012, *SOLA*)

El Niño and El Niño “Modoki”

SST anomaly

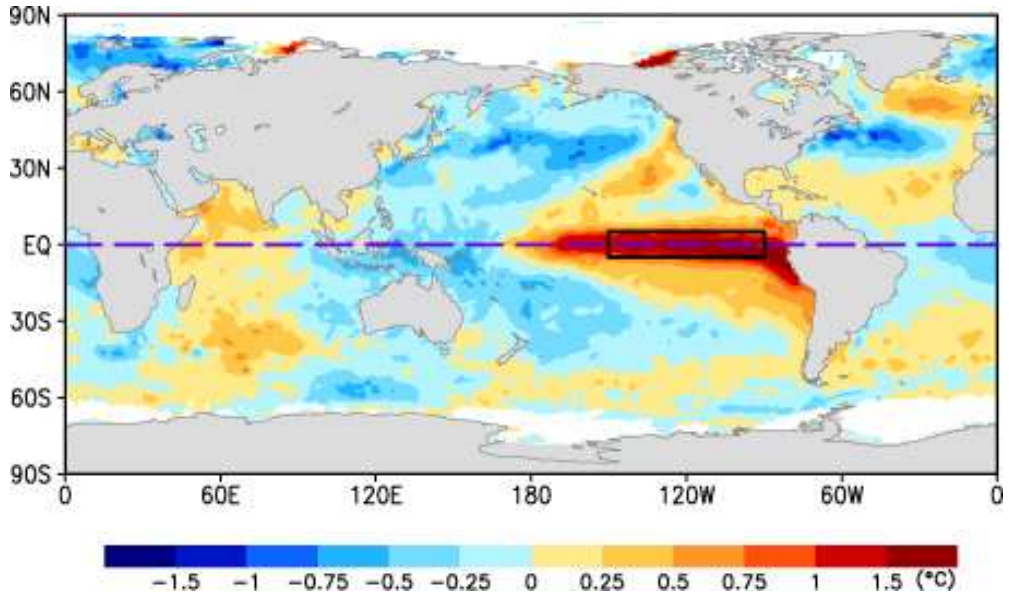

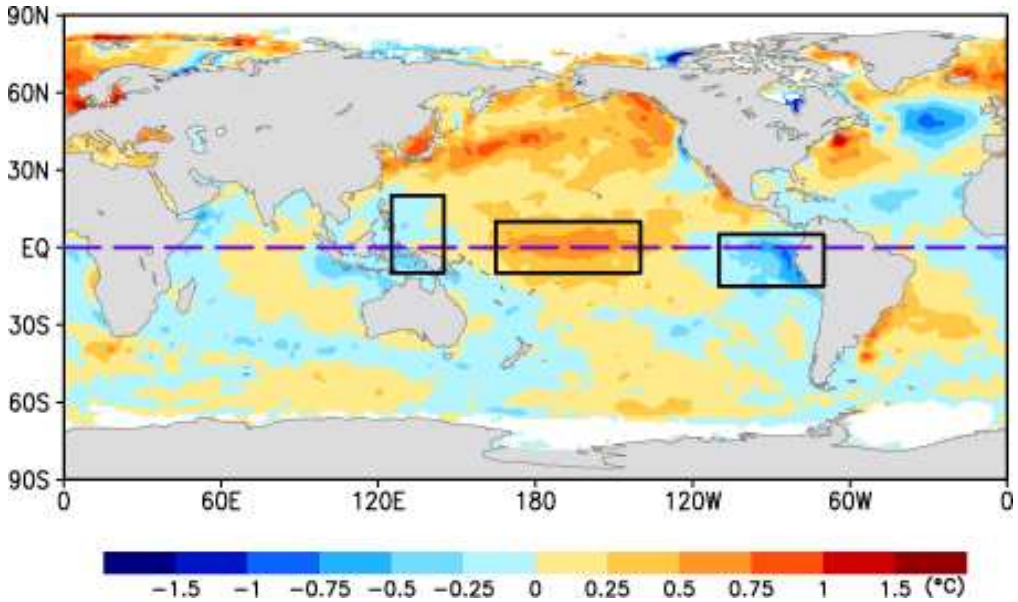

Rainfall anomaly

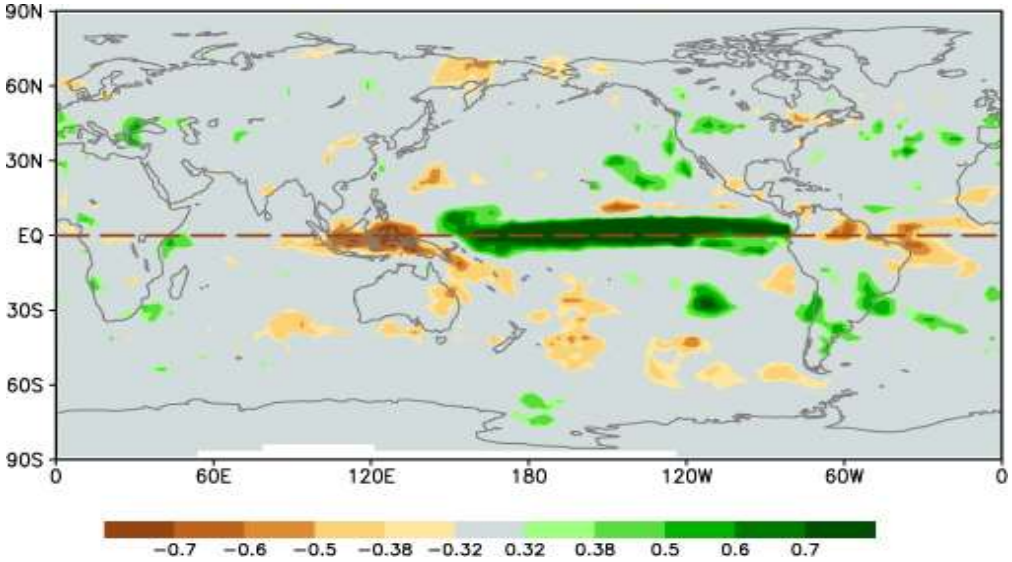

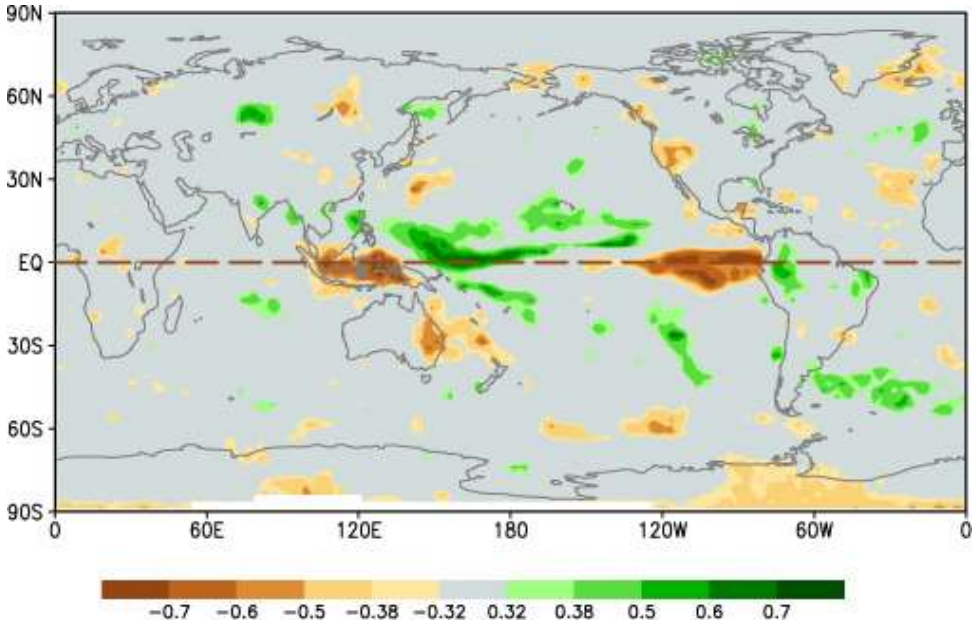

http://www.jamstec.go.jp/frcgc/research/d1/iod/enmodoki_home_s.html.en

El Niño-Southern Oscillation (ENSO)

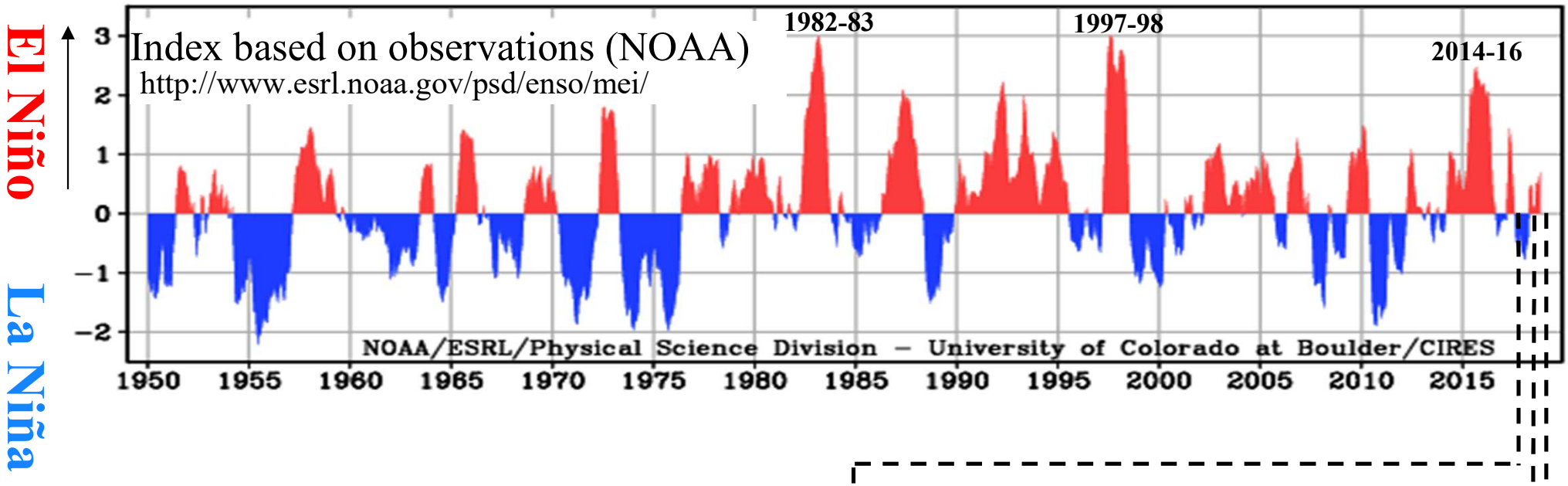

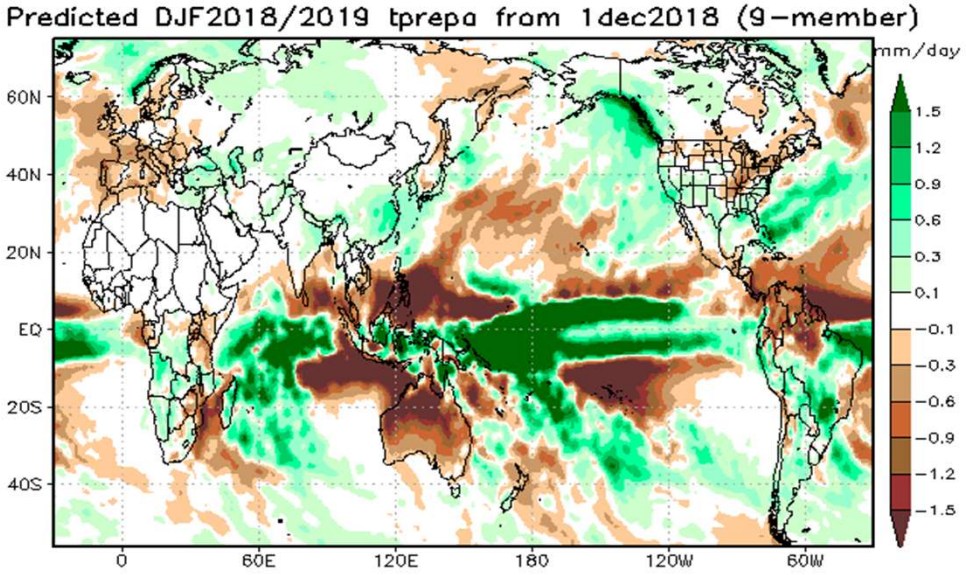

Numerical prediction (JAMSTEC/SINTEX-F)
http://www.jamstec.go.jp/frcgc/research/d1/iod/e/seasonal/outlook.html

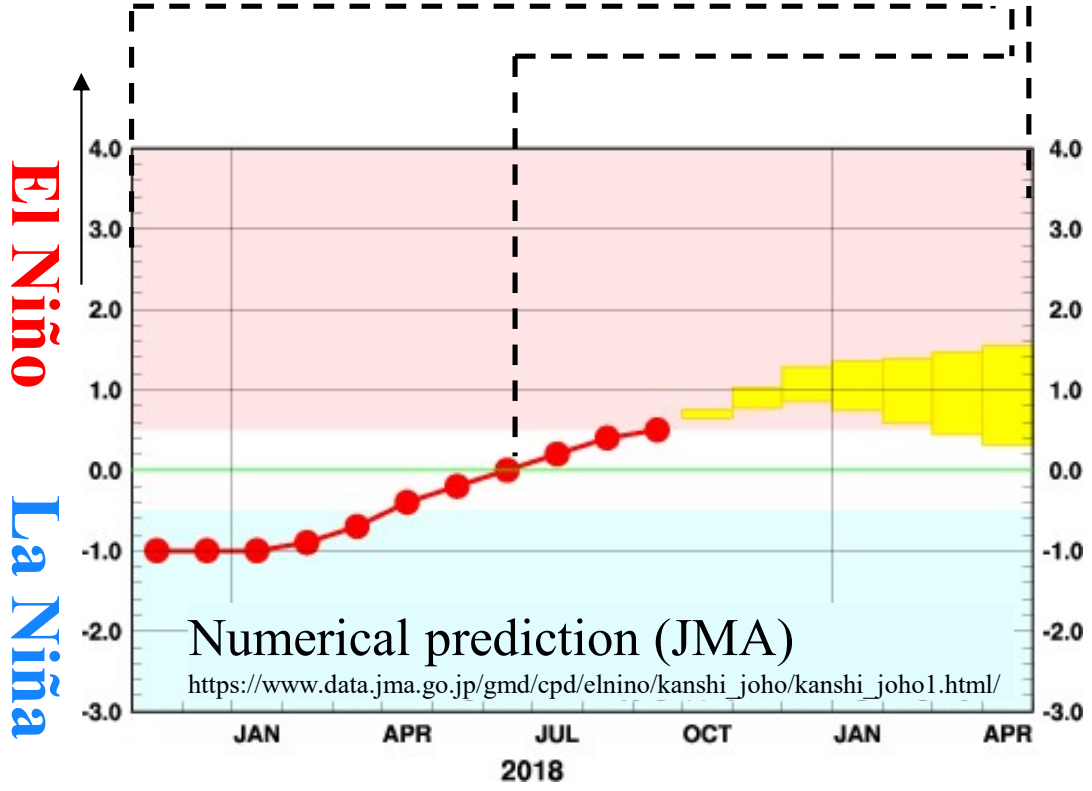

Global abnormal weather due to Rossby wave propagation forced at the equator ("Teleconnection")

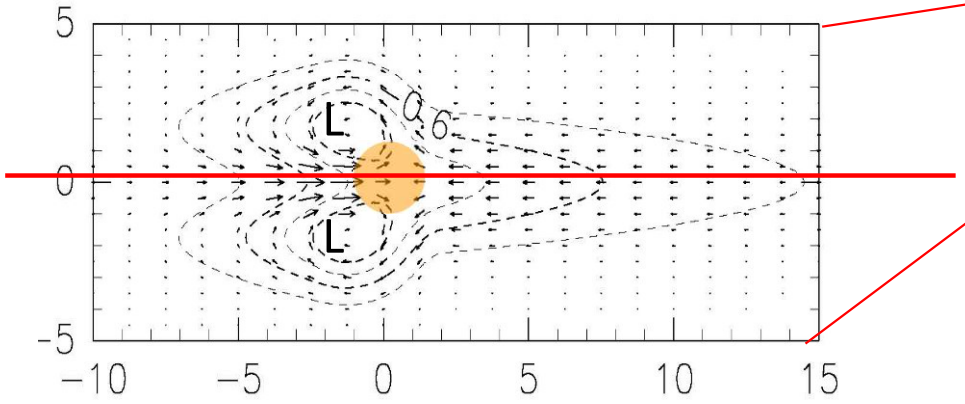

(Gill, 1966)

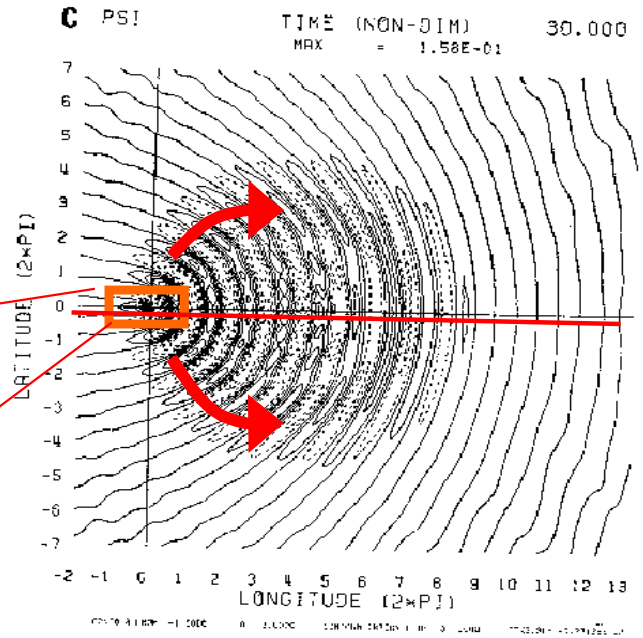

(Hayashi, 1987)

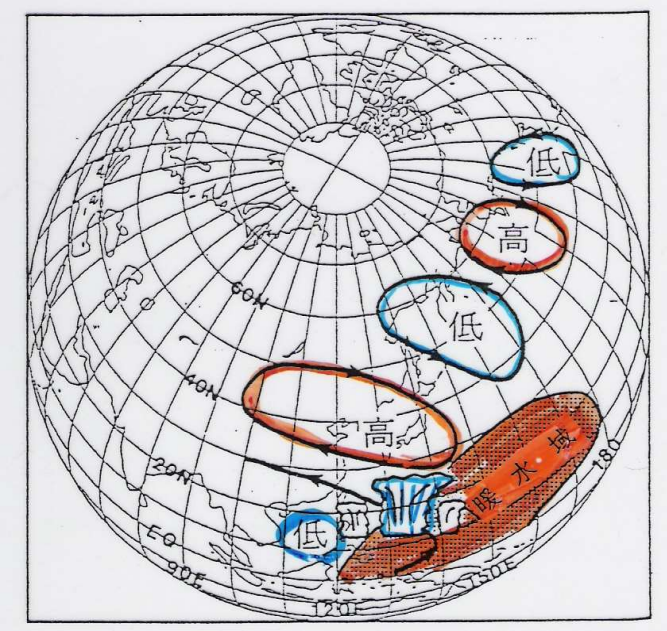

(Nitta, 1987)

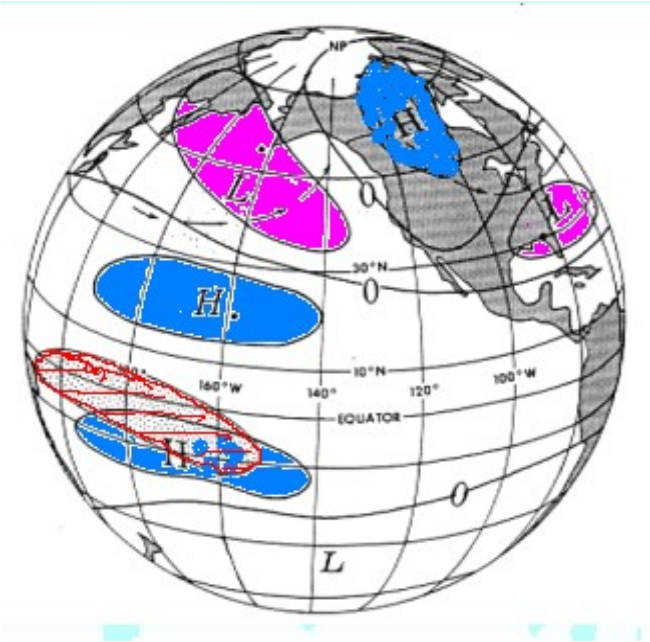

(Wallace, 1981)

Global / local effects of IOD / ENSO

IOD effects (boreal summer/autumn)

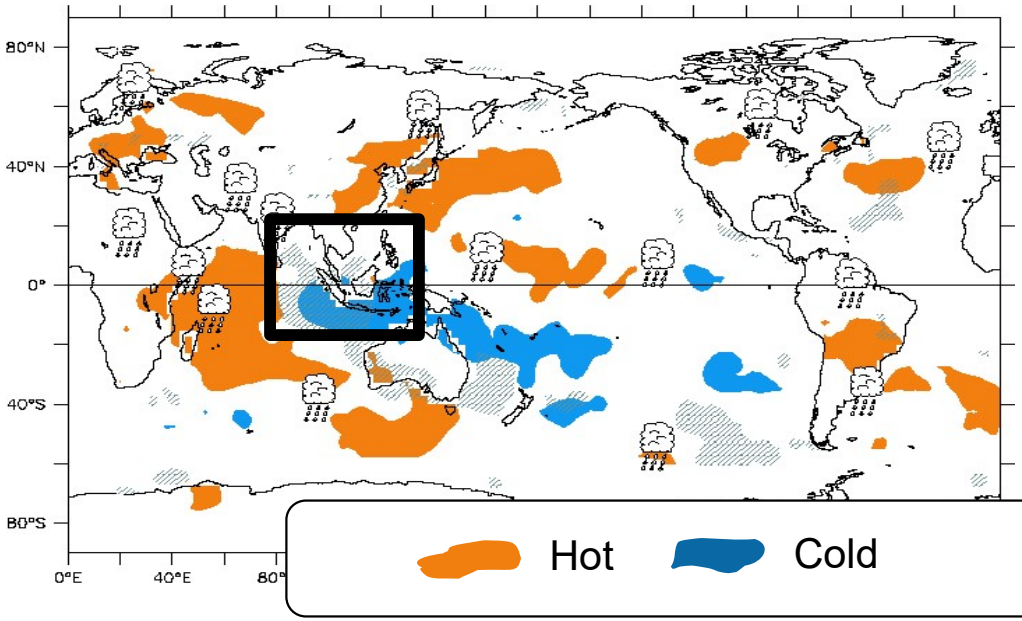

El Nino effects (boreal summer/autumn)

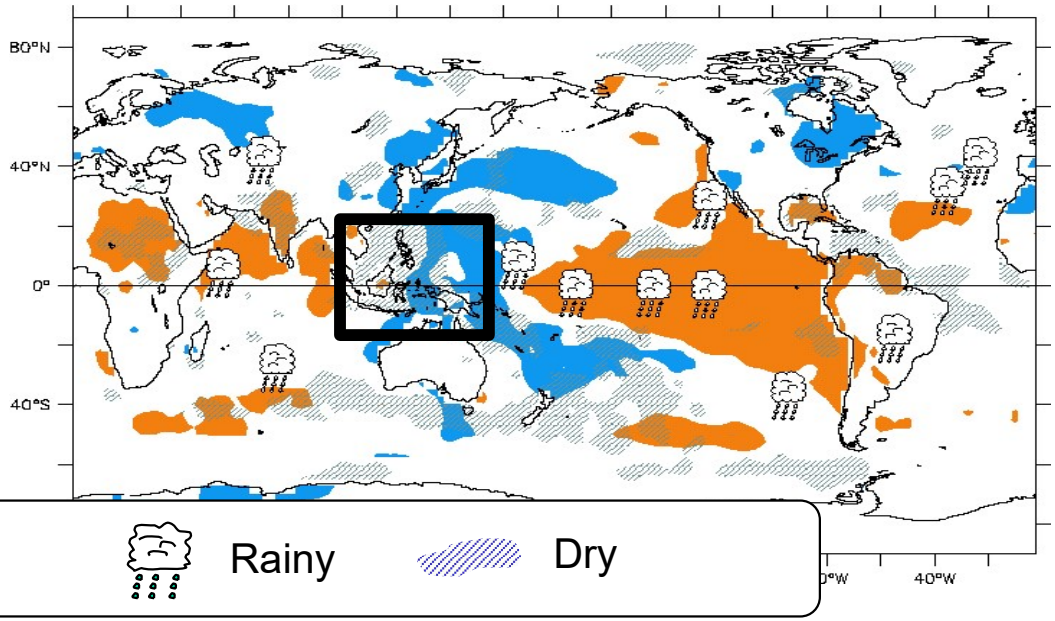

Hot Cold Rainy Dry

SST/rainfall for 2015-16 El Niño (SINTEX-F/JAMSTEC)

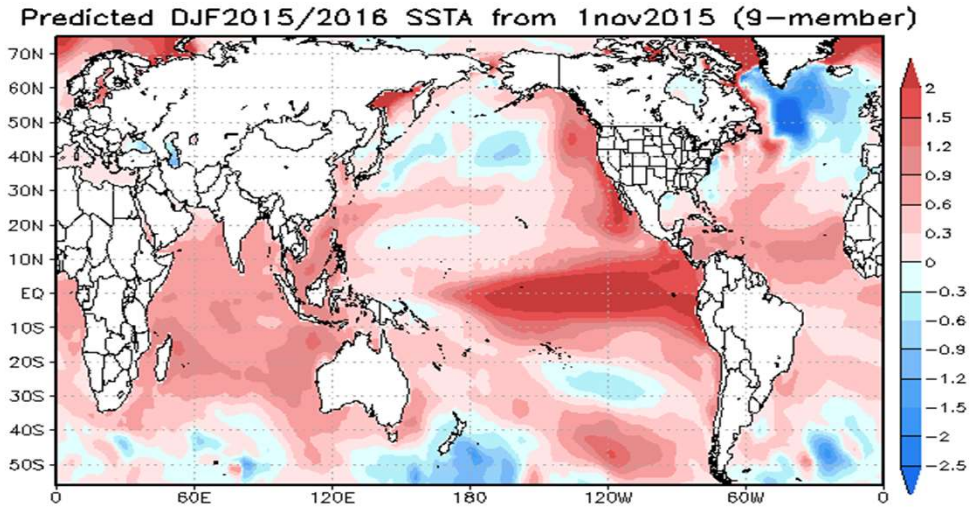

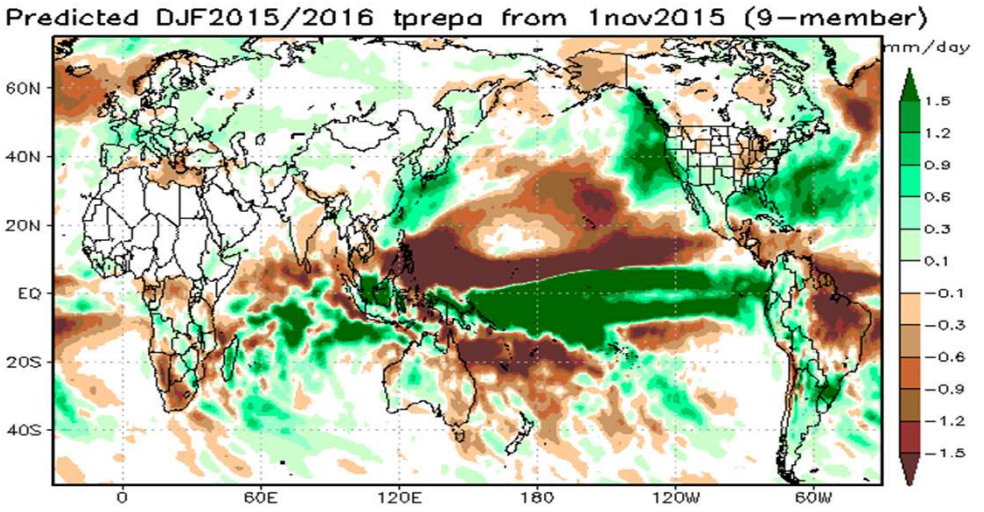

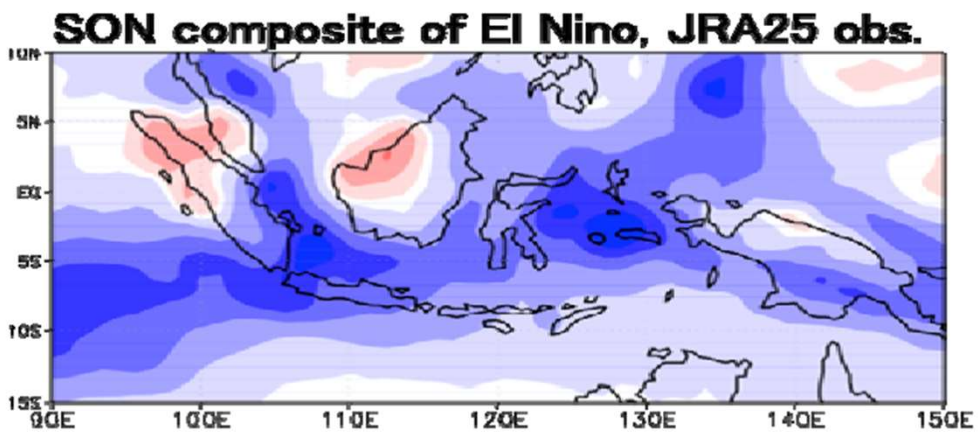

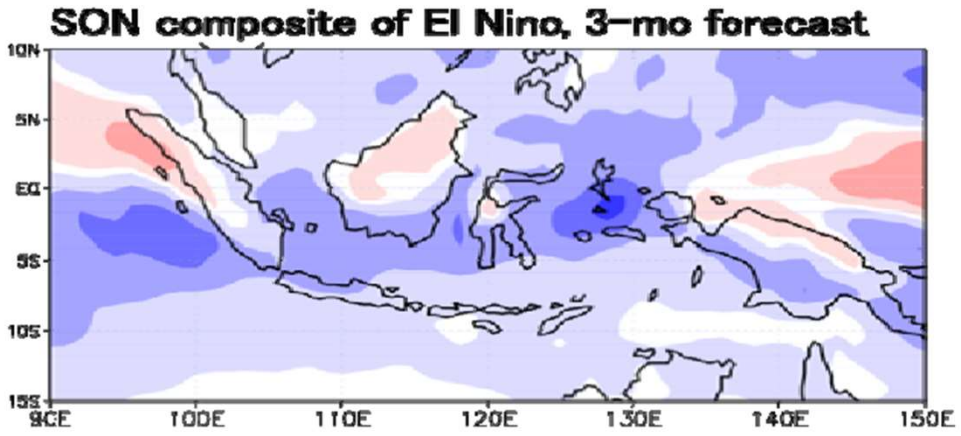

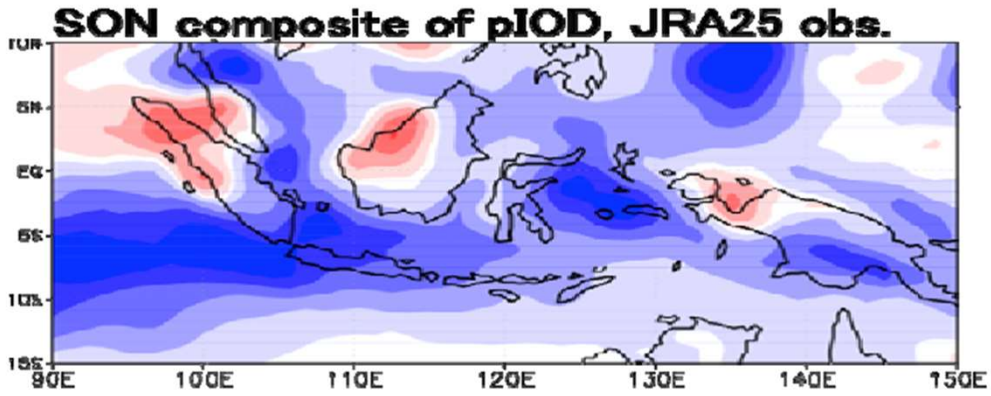

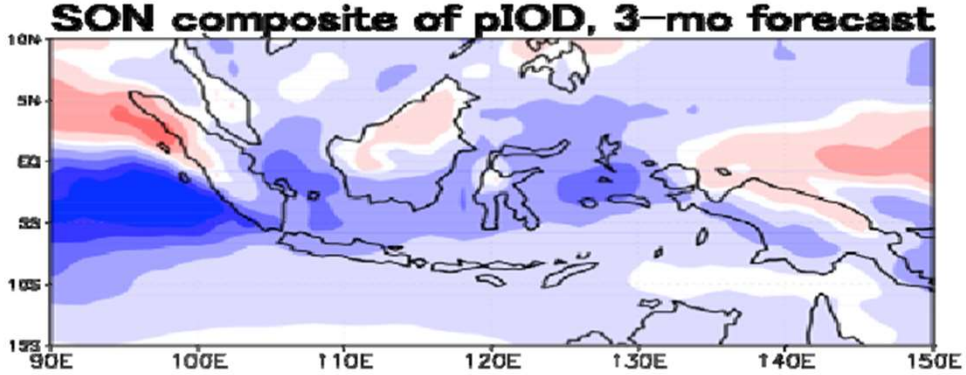

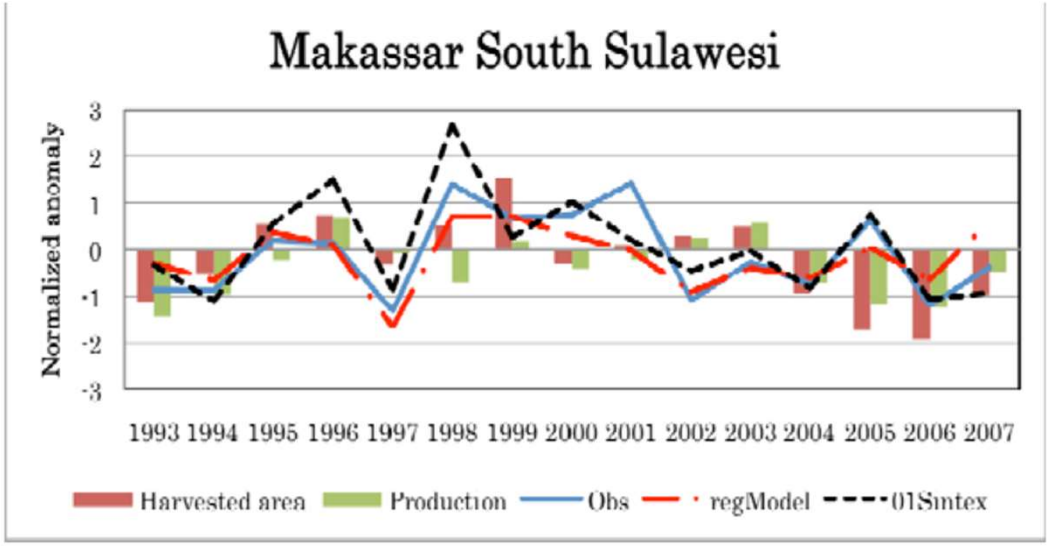

(R. Hidayat, 2013)

Forest fires - transbounbdary haze (1994, 1998, 2006, 1205)

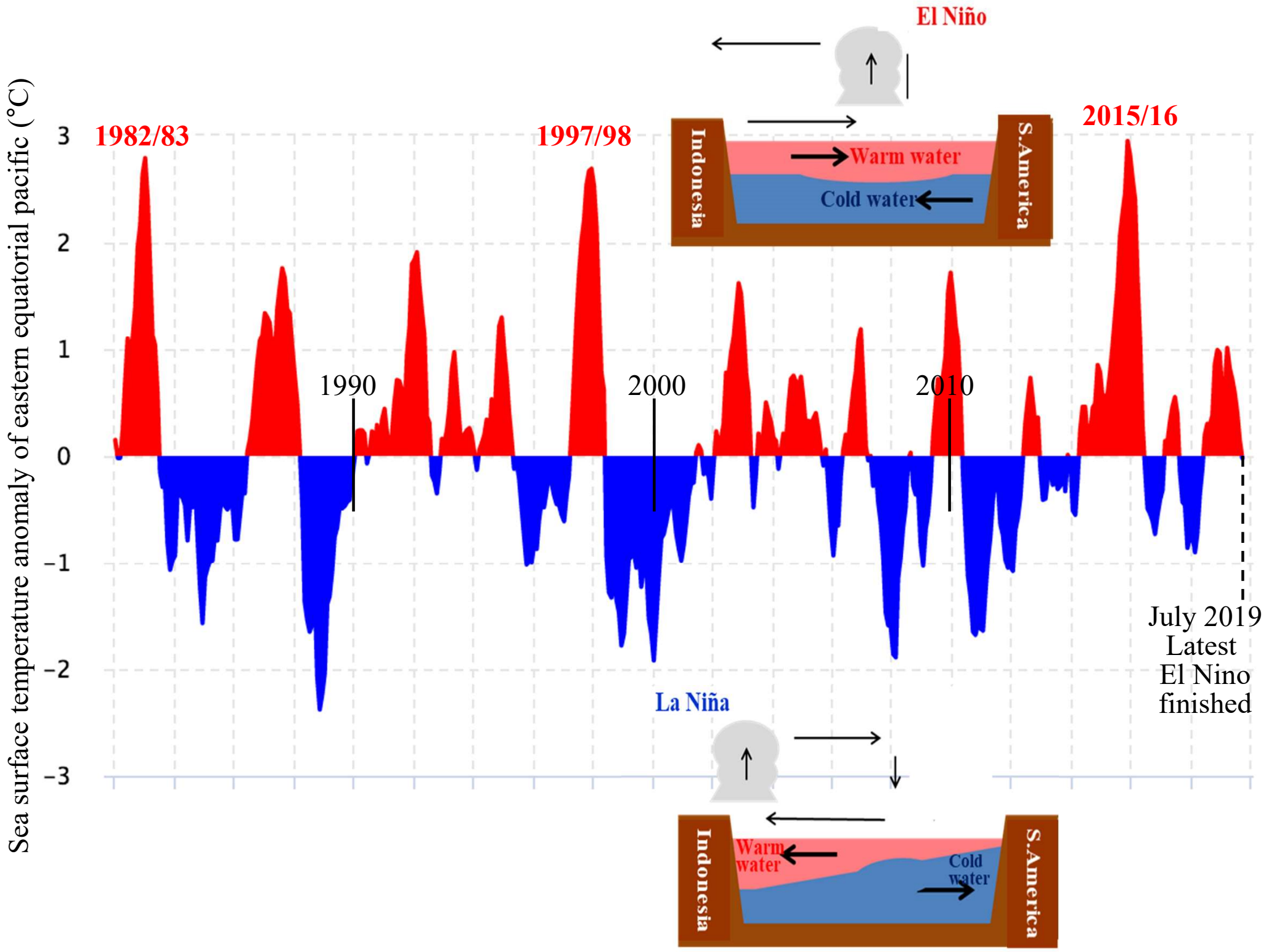
El Niño
1982/83
1997/98
2015/16
Indonesia
S.America
Warm water
Cold water
Sea surface temperature anomaly of eastern equatorial pacific (°C)
3
2
1
0
−1
−2
−3
1990
2000
2010
July 2019
Latest
El Nino
finished
La Niña
Indonesia
S.America
Warm water
Cold water

Sea surface temperature (JMA)

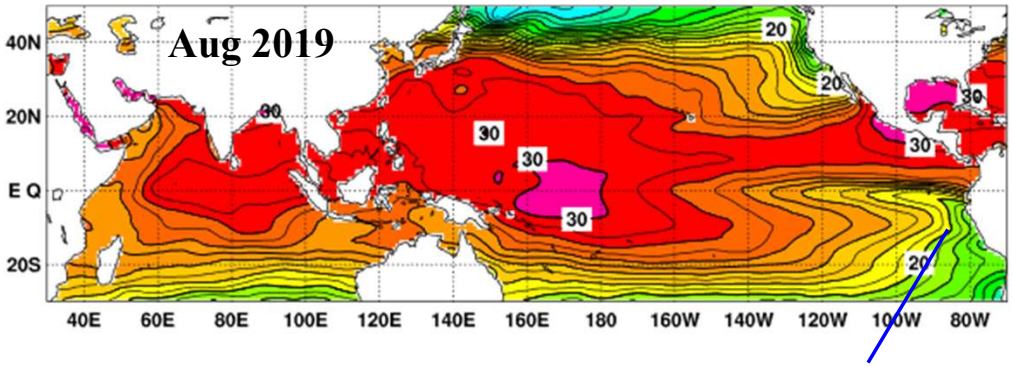

End of El Nino. Return of cold water to off Peru.

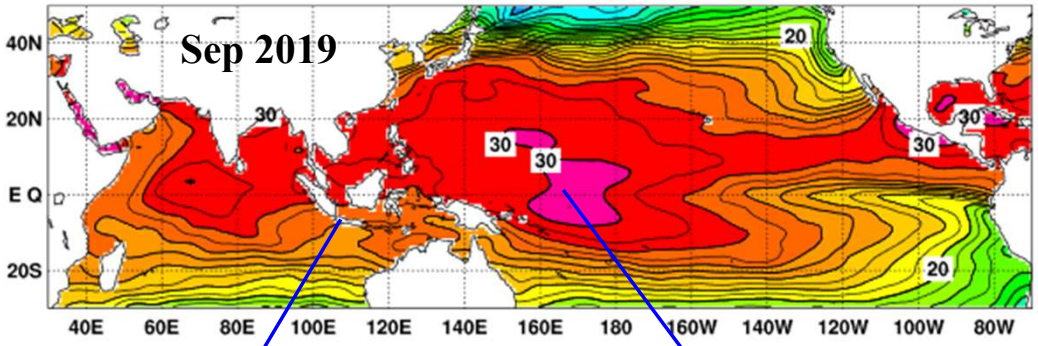

Cold eastern Indian Ocean
(Dipole mode)

No return of warm water to IMC
(El Nino *modoki*)

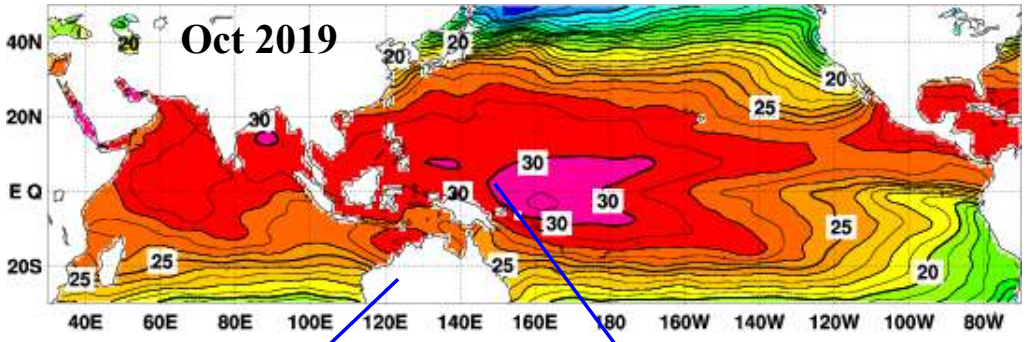

Australia going to summer

Warm water returning gradually to IMC
(Approach to normal rainy season)

CO (correlated with PM) distribution (ECMWF)

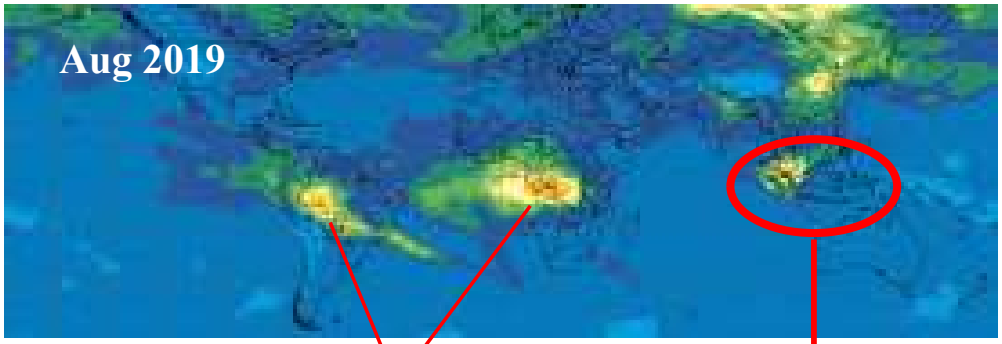

Fires in South America and
Africa weakened

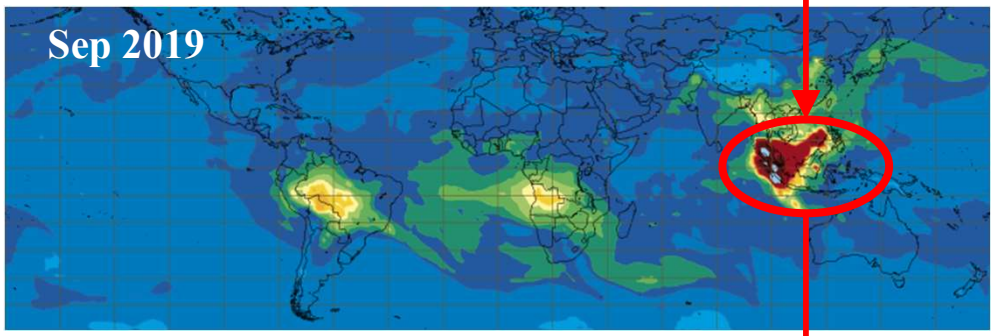

Peak of IMC fire

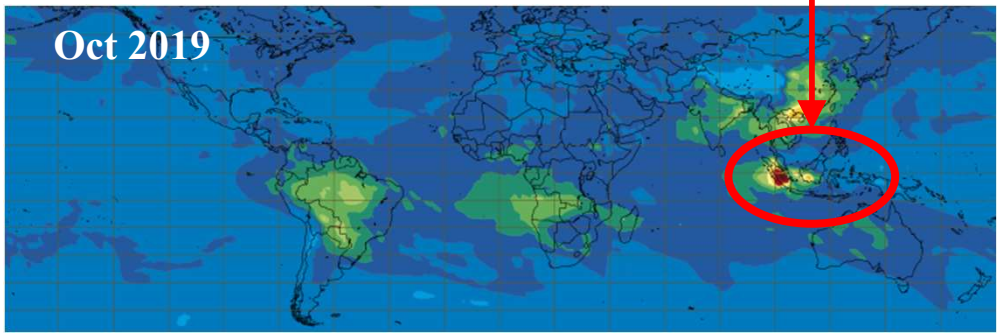

IMC fire weakned

Centennial/Millennial/Holocene global climate variations and ENSO